ANL-GenIV-057

Argonne NATIONAL LABORATORY

Generation IV Nuclear Energy System Initiative
Initial VHTR Accident Scenario Classification: Models and Data

Nuclear Engineering Division

About Argonne National Laboratory

Argonne is a U.S. Department of Energy laboratory managed by UChicago Argonne, LLC under contract DE-AC02-06CH11357. The Laboratory's main facility is outside Chicago, at 9700 South Cass Avenue, Argonne, Illinois 60439. For information about Argonne, see www.anl.gov.

Availability of This Report

This report is available, at no cost, at http://www.osti.gov/bridge. It is also available on paper to the U.S. Department of Energy and its contractors, for a processing fee, from:

U.S. Department of Energy
Office of Scientific and Technical Information
P.O. Box 62
Oak Ridge, TN 37831-0062
phone (865) 576-8401
fax (865) 576-5728
reports@adonis.osti.gov

ANL-GenIV-057

Generation IV Nuclear Energy System Initiative
Initial VHTR Accident Scenario Classification: Models and Data

by
R.B. Vilim, E.E. Feldman, W.D. Pointer, T.Y.C. Wei
Nuclear Engineering Division, Argonne National Laboratory

September 2005

work sponsored by

U. S. Department of Energy,
Office of Nuclear Energy, Science and Technology

UChicago ▶ Argonne LLC

Office of Science
U.S. DEPARTMENT OF ENERGY

A U.S. Department of Energy laboratory managed by UChicago Argonne, LLC

TABLE OF CONTENTS

TABLE OF CONTENTS (continued)

LIST OF FIGURES

LIST OF FIGURES (continued)

LIST OF TABLES

LIST OF TABLES (continued)

INITIAL VHTR ACCIDENT SCENARIO CLASSIFICATION: MODELS AND DATA

ABSTRACT

Nuclear systems codes are being prepared for use as computational tools for conducting performance/safety analyses of the Very High Temperature Reactor. The thermal-hydraulic codes are RELAP5/ATHENA for one-dimensional systems modeling and FLUENT and/or Star-CD for three-dimensional modeling. We describe a formal qualification framework, the development of Phenomena Identification and Ranking Tables (PIRTs), the initial filtering of the experiment databases, and a preliminary screening of these codes for use in the performance/safety analyses.

In the second year of this project we focused on development of PIRTS. Two events that result in maximum fuel and vessel temperatures, the Pressurized Conduction Cooldown (PCC) event and the Depressurized Conduction Cooldown (DCC) event, were selected for PIRT generation. A third event that may result in significant thermal stresses, the Load Change event, is also selected for PIRT generation. Gas reactor design experience and engineering judgment were used to identify the important phenomena in the primary system for these events. Sensitivity calculations performed with the RELAP5 code were used as an aid to rank the phenomena in order of importance with respect to the approach of plant response to safety limits.

The overall code qualification methodology was illustrated by focusing on the Reactor Cavity Cooling System (RCCS). The mixed convection mode of heat transfer and pressure drop is identified as an important phenomenon for Reactor Cavity Cooling System (RCCS) operation. Scaling studies showed that the mixed convection mode is likely to occur in the RCCS air duct during normal operation and during conduction cooldown events. The RELAP5/ATHENA code was found to not adequately treat the mixed convection regime. Readying the code will require adding models for the turbulent mixed convection regime while possibly performing new experiments for the laminar mixed convection regime. Candidate correlations for the turbulent mixed convection regime for circular channel geometry were identified in the literature. We describe the use of computational experiments to obtain correction factors for applying these circular channel results to the specialized channel geometry of the RCCS. The intent is to reduce the number of laboratory experiments required. The FLUENT and Star-CD codes contain models that in principle can handle mixed convection but no data were found to indicate that their empirical models for turbulence have been benchmarked for mixed convection conditions. Separate effects experiments were proposed for gathering the needed data.

In future work we will use the PIRTs to guide review of other components and phenomena in a similar manner as was done for the mixed convection mode in the RCCS. This is consistent with the project objective of identifying weaknesses or gaps in the code models for representing thermal-hydraulic phenomena expected to occur in the VHTR both during normal operation and upsets, identifying the models that need to be developed, and identifying the experiments that must be performed to support model development.

I. INTRODUCTION

The Very-High-Temperature Reactor (VHTR) is one of six reactor technologies chosen for further development by the Generation IV International Forum. In addition this system is the leading candidate for the Next Generation Nuclear Power (NGNP) Project in the U.S which has the goal of demonstrating the production of emissions free electricity and hydrogen by 2015. In preparation for the thermal-hydraulics and safety analyses that will be required to confirm the performance of the NGNP, work has begun on readying the computational tools that will be needed to predict the thermal-hydraulics conditions and safety margins of the reactor design.

The objective of the present multi-year project is to perform the following tasks in connection with the above nuclear systems codes and their use in safety analysis: (a) develop a formal qualification framework, (b) initial filtering of the existing databases and (c) preliminary screening of tools for use in thermal-hydraulics and safety analyses. It is expected that as an outcome of these tasks we will have 1) identified the systems codes to be used, 2) identified weaknesses or gaps in the code models for representing thermal-hydraulic phenomena expected to occur in the VHTR both during normal operation and upsets, 3) identified the models that need to be developed and the experiments that must be performed to support model development, and 4) will have identified the scaled experiments needed for validation of models. The project has been initiated within the framework of the Generation IV Nuclear Energy Systems Initiative in the area of System Design and Evaluation under the Work Package, A0802J01 “Modeling Improvement”.

The computer codes to be used in the gas reactor performance and safety analysis can be divided into two groups, one-dimensional (1-D) system type codes and multi-dimensional computational fluid dynamics (CFD) codes. The choice of one over the other in an application involves first identifying the main phenomena and from this the dimensionless numbers that characterize the phenomena and their values. The suitability of a code is then judged in part by whether models for the phenomenon exist and whether they include the dimensionless numbers in a correlation valid for the values identified. While CFD codes can in principle be equipped to model all phenomena for which the 1-D codes are suited, the substitution of the former for the latter in every application is not practical. CFD codes require more detailed problem definition input and require orders of magnitude more computational time.

Both types of codes can be reviewed using the same approach since both are conservation law based and both contain empirical models (i.e. correlations of dimensionless numbers) that are the subject of the validation. The codes differ primarily in the level of detail present in the models to describe the underlying processes and, hence, in the types of experiment datasets needed to calibrate the models. For 1-D codes, validation is achieved using integral experiments that agglomerate over more than one fundamental phenomenon. For CFD codes a separate effects experiment focuses on a single phenomenon. Once validation for fundamental phenomena is demonstrated, validation can be complemented by comparison with integral phenomena experiments. In this report

we therefore use the same methodology to evaluate the models in each type of code but distinguish between the two types of experiment datasets.

This report describes work completed to date in this project. An approach based on methods from the 1980s for light water reactor safety code qualification is developed for reviewing code model adequacy. A set of Phenomena Identification and Ranking Tables (PIRT) are generated to identify the main phenomena controlling the plant transient response for events that approach safety and design limits. Two events that result in the maximum fuel and vessel temperatures are identified and selected for PIRT generation. These are the Pressurized Conduction Cooldown (PCC) event and the Depressurized Conduction Cooldown (DCC) event. A third event that may result in significant thermal stresses is also identified and selected for PIRT generation. This is the Load Change event. The important phenomena in the primary system as indexed by transient phase and component are identified for all three events. The phenomena are then ranked as to relative importance with respect to the approach of plant response to safety and design limits. To demonstrate the concepts and show how the work will proceed in subsequent years, we step through for a single phenomenon the sequence for assessing the adequacy of the models. The case examined involves pressure drop and heat transfer in the mixed convection mode in a 1-D systems code. We use dimensional scaling to determine the presence of this phenomenon as a function of component and upset event. Where mixed convection is shown to occur, we examine the adequacy of the 1-D system code for modeling it. If a model is lacking we identify the experiments needed to support the required model development.

II. VERY HIGH TEMPERATURE REACTOR

A. Prismatic Modular Reactor

Figure 1 shows the reactor vessel for the Prismatic Modular Reactor (PMR). The flow through the reactor core (fuel) and reflectors is vertically downward where it exits into a common outlet plenum that is in line with the hot duct shown on the lower left. The flow exits the vessel through the hot duct where it is transported to the power conversion unit (PCU). The reactor coolant inlet duct is an annulus that is concentrically located around the hot duct. The inlet flow, which comes from the PCU, enters a plenum below the outlet plenum where it is transported vertically between the core barrel and the reactor vessel to a plenum in the upper part of the reactor vessel. The reactor core is annular and surrounded by reflectors on the top, bottom, and both annular sides. In the figure the core is the red region inside the dashed rectangles. Figure 2 shows a top cutaway view of the reactor vessel. As shown in Figure 2, there are three concentric rings of hexagonal fuel assemblies surrounding an inner reflector of hexagonal assemblies and surrounded by an outer reflector largely made of hexagonal assemblies. The core barrel is along the perimeter of the outer reflector. The reactor fuel is inside rods that are located in vertical holes in the hexagonal graphite core blocks. There are vertical coolant holes in the hexagonal fuel blocks.

In Figure 1 102 hexagons represent the entire core regions. Each of these hexagons represents a vertical stack of 10 fuel blocks and an assembly lower reflector below the fuel stack and an assembly upper reflector above it. Similarly, most, if not all of the hexagons that represent inner or outer reflectors, is a stack of hexagonal graphite blocks.

The reactor is to be located in a concrete silo that is below grade. This silo will be vented so that the walls of the silo will not be subjected to high pressure should a breach in the reactor pressure boundary cause high-pressure helium to enter the reactor cavity, which is the space between the reactor vessel and the inner surfaces of the silo.

Heat given off from the surface of the reactor vessel would cause the silo to heat up considerably if an effective means of heat rejection to the atmosphere were not provided. This means is the reactor cavity cooling system (RCCS). Figure 3 shows a schematic drawing of the RCCS for the proposed reactor design. Vertical intake ducts through the top of the silo transport outside air to plena (not shown) near the bottom of the silo. The air then travels upward through 292 vertical heating panels, or RCCS ducts, and ultimately out through the exhaust ducts above the silo. These 292 ducts are evenly spaced in a circle around the vessel and are 2 inches by 10 inches in exterior dimensions. The 2-inch side faces the reactor vessel and the ducts are aligned along radial lines emanating from the center of the vessel. There is 2 inches between adjacent ducts at the closest point. This system is designed so that the outside air used for removing heat is completely separated from the rest of the air inside the silo. The air inside the RCCS ducts is heated by heat transferred, mostly by radiation, from the surface of the reactor vessel. The air flow through the RCCS is driven entirely by natural convection caused by the air in the RCCS ducts being less dense than the cold air entering from outside. The RCCS not only protects the concrete walls of the silo from excessive temperatures, but also provides an essential heat removal system during the PCC and DCC transients under consideration. For these transients, once the compressors have stopped, the RCCS is part of the only path through which reactor decay heat can be rejected.

B. Pebble Bed Modular Reactor

The reference PBMR is a 400 MWth direct cycle gas reactor with a pebble core as shown in Figure 4. Reactor operating pressure is 90 bars and outlet temperature is 900^{o}C. The VHTR differs mainly in that the target reactor outlet temperature is higher at 1000^{o}C and the VHTR is to produce hydrogen in addition to electricity. The 400 MWth pebble core consists of approximately 450,000 fuel pebbles that are stacked in a graphite reflector structure. Pebbles are continuously refueled during plant operation. Central reflector pebbles are replaced by central graphite reflector column in the recent design of the 450 MWth.

As shown in the figures, the PMR and PBMR designs differ mainly in the core configuration, that is, prismatic or pebble. The basic idea of the system layout is the same for both designs. The GT-MHR design adopts an integral power conversion unit (PCU) in a vessel and a concentric hot/cold duct that connects the reactor system vessel and the

PCU system vessel, while the PBMR design adopts distributed PCU components and separated hot and cold ducts.

In the PMR core the helium coolant, within the hexagonal blocks, follows well defined one-dimensional flow paths described by the coolant channels. However, an undefined quantity of bypass flow, ranging from ~10% to ~25% of the total coolant, moves between the blocks. The bypass flow varies according to the quality of the block construction, the movement of the graphite as a function of irradiation and temperature, and the core stacking procedures. Contact heat transfer between the blocks that plays an important role in transmitting core afterheat during accidents is also affected by them. In contrast, the helium coolant moving through the PBMR core follows multi-dimensional flow paths defined by the pebble-void fraction, which varies as a function of core radius, and the individual contact points described by the pebble column. During accidents, radiation and contact heat transfer between pebbles plays an important role in transmitting core afterheat to the reactor vessel wall. Core axial power distribution in the pebble core is more apt to be top-skewed than in the prismatic core due to on-line refueling of fresh pebble from the top.

The detailed design of the reactor vessel internals is different for the PMR and the PBMR as shown in Figures 5 and 6. In the prismatic design, helium flow from the loop is mixed and redistributed in the inlet plenum and flows upward through 6 square riser ducts between core barrel and vessel wall. It is collected in the hemisphere top plenum then flows downward into the core. In order to prevent overheating at the vessel, thermal insulation is provided at the inner side of the vessel head. Helium jet discharged from the core is collected and mixed in the outlet plenum then flows out of the vessel to the PCU. In the pebble design, Helium flow from the loop is distributed in the donut-like inlet plenum and flows upward through the riser consisting of 36 circular channels inside the outer reflector. It passes through the slots at the top of the riser and is collected in the cylindrical top plenum inside the upper graphite structure. It then flows downward to the core. Helium exited from the core is collected and mixed in the outlet plenum and then flows out of the vessel to the PCU. However, considering the expected increase in vessel inlet temperature of the VHTR design, the current riser design of the prismatic vessel may not be acceptable enough to meet the design limit of the vessel wall temperature. There may have to be a modification of the riser design in order to lower the vessel wall temperature. One of the options is to have the riser channel inside the outlet reflector as in the pebble design.

The pebble-bed core slowly moves downward while the prismatic core is stationary. The cycle time through the core for an individual pebble is approximately 80 days. The transit distance is ~9.5 m.

III. METHODOLOGY

The method we apply for NGNP thermal-hydraulic code qualification is related to the best estimate plus uncertainty method developed in the late 1980's for safety analysis of

light water reactors (LWR). The Code Scaling, Applicability, and Uncertainty (CSAU) procedure [1] was used to conduct performance analyses of the Emergency Core Cooling System (ECCS) on a best-estimate basis rather than applying bounding conservatisms as had been the case previously. The method provided a systematic means for quantifying the uncertainty in the code predictions for severe loss of cooling accidents.[2] The process involves identifying the physical phenomena, selecting the key safety criterion, characterizing the phenomena in terms of scaled or dimensionless quantities, use of experiments with similar scale to assess accuracy of models in code, and finally making an estimate for the uncertainty in model prediction. The method was subsequently adapted for use in code development and improvement where the objective is ensuring the code can model the plant behavior. Since that is very nearly our objective we have borrowed from that work.

There are differences between the issues addressed for LWRs and those important for the NGNP. For the LWR the requirement was sufficient confidence in the uncertainty in the code predictions that a reliable estimate could be made for accident damage and resulting release rate. The objective of the safety analysis was protection of the public. For the NGNP, however, the passive safety characteristics of the reactor are deemed to result in no significant fuel failure and, hence, negligible risk to the public. The objective is to confirm that for even the most serious events there is no significant release. With this shown, the question of risk to plant investment produced by elevated temperatures that shorten component lifetimes becomes an issue to confirm. Reactor and safety system performance is therefore also included as an objective in this exercise.

In a gas thermal reactor the dominant thermal-hydraulic phenomenon remain essentially unchanged ranging from normal operation to the severest accidents. No coolant phase change occurs and the fuel does not melt. As a consequence there likely will be no equivalent in the NGNP to the LWR experimental programs that involved hundreds of man years of analysis effort aimed at characterization and modeling of post-accident heat removal. Instead, the conditions that accompany the most severe gas reactor accident are a perturbation on normal operation. As a consequence the code qualification process should be simpler.

The goal is to identify the model improvements needed for the computer codes so that the codes properly represent the phenomena and can be used to address safety and design issues. This task has been broken into four steps: phenomena identification and ranking, modeling and scaling analysis, code review, and experiments. In the *phenomena identification and ranking* step we transition from an upset based means of identifying phenomena to an operating regime and equipment based approach. There are countless numbers of upsets of varying severity while there are only a limited number operating regimes and plant equipment components. Operating in terms of the latter provides increased assurance that all cases have been covered. In the *modeling and scaling analysis* step, it is assumed we have a specific phenomenon occurring in a specific component. The task is to determine an appropriate model to describe the phenomenon. We do so by first performing a scaling analysis to identify the dimensionless numbers that characterize the phenomenon. We then identify models that have been correlated in

terms of these quantities and that provide a quantitative representation of the phenomenon. Should no model be identified, then we note this for consideration shortly. Assuming an acceptable model has been identified we move to the *code review* step where we examine the computer code with respect to modeling the phenomenon. If the model proves deficient we identify the model from the *modeling and scaling analysis* step, if was found, as being better suited. If no model was identified we move to the *experiment* step where we attempt to identify an existing experiment that could serve as a basis for deriving a model. If no experiment can be identified, then we indicate this as a development need. Figure 7 is schematic of this process.

IV. SENSITIVITY STUDIES

A. Background

Analytical studies can aid in evaluating and ranking the phenomena that affect the safe operation of the VHTR. Two reactor upsets that are initiated with a loss of primary flow and a reactor scram are considered. In one upset—the Pressurized Conduction Cooldown (PCC)—the reactor pressure boundary is assumed to remain intact and the pressure throughout the primary system equilibrates at 5 MPa. In the other—the Depressurized Conduction Cooldown (DCC)—the pressure boundary is breached and the pressure in the primary system decreases to atmospheric pressure.

The General Atomics direct cycle version of the VHTR is the design being studied. INL provided a RELAP5 model of the reactor under consideration, including the input for the two upset transients being considered. Among the phenomena of concern are 1) the conduction between regions of the reactor and the reflectors, 2) the heat capacitance of the graphite matrix of the core and the reflectors, and 3) the heat transfer from the inner surfaces of the cooling ducts in the reactor cavity cooling system (described in the next section) to the air flowing inside the ducts. The predictions of the model depend on values of parameters that are used in the representation of these phenomena. Therefore, for both the PCC and the DCC, key parameters in the RELAP5 model were varied to study the sensitivity of the peak fuel and reactor vessel temperatures to variations in these parameters.

B. RELAP5 Model

Figure 8 shows the RELAP5 model of the reactor cooling circuit. The helium flow originates in node 100 (at the lower left) and travels through the vessel inlet plenum (note 110) and upward through the reactor riser (node 130), located between the reactor vessel and the core barrel. The flow then goes from the riser to the core inlet plenum (node 140). The hatch regions in Figure 8 represent solid structure that conduct and store heat. The structure at the top of node 140, which is the reactor vessel upper plenum shield, does not block the flow path, but merely absorbs and conducts heat from the passing flow. There are five parallel paths that connect to the core inlet plenum. The one labeled 142 represents the inner reflector of the reactor and 145 is the outer reflector of the reactor. The solid structure in region 145 models both the outer reflector graphite material and the

core barrel. The three paths, 152, 154, and 156, represent the three concentric rings of core hexagonal assemblies.

In the model, each of the three core regions (152, 154, and 156) has 12 axial nodes. The top and bottom nodes represent the upper and lower reflector, respectively. The ten middle nodes represent the stack of ten core blocks. The inner and outer reflector regions each have 12 axial nodes. In the model the nodes in the five regions are aligned to form 12 horizontal layers. Thus, the two reflector and three core regions taken together have a total of 5 × 12, or 60 nodes. Each of the four inner regions (inner reflector and three core regions) is modeled as a number of identical concentric annuli with coolant going through the center surrounded by a multilayer solid annulus. This solid annulus is used to represent the fuel and graphite of each region. The diameter of the coolant hole in the middle is that of the coolant channel in the reactor. Each annulus represents one coolant hole and the fuel and graphite associated with it. The number of identical annuli in each of these four each regions is specified so that the amount of fuel, graphite, and coolant in each is accurately represented. In the model the solid materials of the outer reflector and the core barrel are combined into two concentric annular layers of the outer reflector region. The geometry of the core barrel is as in the reactor and the amount of graphite in the outer reflector is properly represented. The coolant channel that is attached to this region is represented with the proper hydraulic parameters, such as hydraulic diameter and flow area.

RELAP5 permits heat to be transferred from any one of these 60 annular solid surfaces to any other. This is accomplished by a 60 × 60 matrix that, in a manner analogous to radiation view factors, allows conduction from any of the 60 solid nodes to any of the other 59. The rate of heat transfer from one solid node to another is specified as a conductance, which is defined as a material conductivity divided by a conduction length. This heat conduction matrix is used to represent heat transfer in the horizontal direction from one reflector or core region to immediately adjacent ones. It is also used to approximate axial heat transfer within each of the five reflector and core regions. This is accomplished by the use of a conduction path that connects the vertical surface of a node to the same vertical surface of the node immediately above or below it.

The radial conductance between adjacent horizontal regions assumed that two solid hexagonal blocks were in perfect contact with each other. The conduction length was taken to be the distance from the center of one hexagon to the center of the other while the two were in contact along a common side. The conductivity used determining the conductance was taken to be a weighted average of the graphite matrix and fuel cross-sectional areas. No reduction in conductivity was taken for the presence of the coolant hole in the blocks. No gap or contact resistance was included where the two hexagons come together. Therefore, the resultant conductances are expected to be on the optimistically high side and in the sensitivity studies only the same or smaller values are considered.

Figure 9 shows a top view of the RELAP5 representation of the RCCS. The downcomer shown in the figure is part of the inlet path for the outside air. Heat that is radiated from

the reactor vessel, in addition to heating the RCCS ducts, also heats the downcomer and the concrete wall of the silo. In the model the concrete wall and the earth beyond it are both represented. The air flow path in the model is shown in Figure 10. The source of outside air is node 950 and the sink is node 980. The downcomer is region 960, the common plenum is node 965, and the 292 identical RCCS ducts are represented by region 970. Region 900 represents the air contained inside the reactor cavity that does not flow through the RCCS ducts.

C. Selection of Cases

For both the PCC and the DCC transients, six cases were analyzed in the sensitivity study. These cases are:

1. Base Case
   This is the model as provide by INL.

2. 50% Conduction
   This is the Base Case with the all of the heat conduction among the 60 core and reflector regions cut in half. This was accomplished by changing the values of the conductances in the 60-by-60 conduction matrix.

3. No Conduction
   This is same as case 2, but with the conductances reduced to zero.

4. 80% Graphite Heat Capacitance
   This is the Base Case with the fuel and reflector region graphite (not including any graphite in the fuel rods) reduced by 20%.

5. 80% RCCS Inner Surface Film Coefficient
   This is the Base Case with the film coefficient on the inner surfaces of the RCCS coolant ducts reduced by 20%. This was accomplished in the model by reducing the fouling factor inside the RCCS ducts from 1.0 to 0.8.

6. 50% Inner Surface Film Coefficient
   This is the Base Case with the film coefficient on the inner surfaces of the RCCS coolant ducts reduced by 50%.

The Base Case was analyzed to provide a reference with which all of the others could be compared. It was observed that peaks in fuel and reactor vessel temperature tend to occur gradually and typically within the first four days after shutdown. Therefore, all cased were designed to simulate the four days of the transient. However, as may be expected, the PCC and DCC no conduction cases produced very high temperatures, 2500 K, early in the transient. This caused property table ranges to be exceeded and the simulations to stop prematurely.

D. Results

The transient result for the PCC cases are provided in Figures 11 through 16. Figure 11 provides peak fuel temperature, Figure 12 provides peak reactor vessel temperature, and Figure 13 provides the RCCS exit coolant temperature. These three figures compare Cases 2 through 4 with the Base Case. In each of these figures the curves appear in the same order that they are shown in the legend. Case 4 is indicated by a thin brown line. Similarly, the next three figures compare Cases 5 and 6 with the Base case. The transient results of the DCC cases are provided in Figures 17 through 22 and are arranged in an analogous manner to their PCC counterparts.

Each peak fuel or vessel curve represents a temperature history at a single point in the reactor. The location of the peak fuel temperature and the location of the peak vessel temperature were obtained by surveying all candidate locations for the maximum. Then only the temperatures at these locations were plotted. Thus, if the location of the peak changes with time, higher values than those shown could be observed for all but the absolute peak. The peak vessel temperatures occur on the inner surface of the vessel because the heat source is inside the vessel. A substantial temperature gradient across the vessel wall thickness it to be expected. It is important to keep the temperature drop across the reactor vessel in mind when interpreting the results because it is the temperature on the outer surface of the vessel that determines the behavior of the RCCS. Similarly, the axial distribution along this surface is important because entire surface provides the energy that is removed by the RCCS.

Table 1 provides a summary of the peak fuel and vessel temperature for the PCC. The maximum and minimum air flow rates for the RCCS are also included in the table. These are to show that variations in RCCS air flow rate are small with each case and from case to case. Table 2 provides analogous results to Table 1, but for the DCC.

E. Discussion

The RCCS flow rates indicated in Tables 1 and 2 shows that the air flow rate varies only within a narrow range within each case and from case to case. The air inlet temperature to the RCCS was assumed to be 43º C and constant in all cases. Thus, the RCCS exit air temperature history provides an indication of the relative amount of energy being removed by the RCCS over time. This extra temperature history was included with the fuel and vessel temperature histories because it could be used to approximate, or at least judge, heat balances and also provide valuable insight into the behavior of the RCCS.

The no conduction cases were included as a bound. Previous analyses of natural convection in helium systems tend to indicate that for the PCC the system pressure should be high enough to enable a significant amount of natural circulation between the hotter central regions of the reactor and the cooler outer ones. This natural circulation potentially could transport sufficient power from the central region of the reactor to the outer region to keep the peak temperatures within acceptable bounds without radial conduction. Prior analyses have also shown that essentially no natural circulation of

helium is to be expected in the DCC and hence acceptable peak fuel temperatures are not a possibility for this no-conduction case.

The results show a strong sensitivity to conduction in both the DCC and PCC cases and having a good assessment of the radial conduction is essential to any safety case. Reducing the conduction raises the peak fuel temperature and lowers the peak vessel temperature. This occurs because the reduced conductivity causes greater thermal resistance inside the reactor while the thermal resistance on the outer surface of the reactor vessel is unchanged.

Reducing the heat capacitance of the reactor graphite raises both the peak fuel and the peak vessel temperature. This occurs because the ability of the reactor to store energy without increasing temperatures is diminished and produces higher reactor internal temperature and these high internal temperatures cause higher vessel temperatures.

The reduced RCCS film coefficient has only a very minor effect on the peak fuel temperatures of no more than about 6º C increase. But it has a larger effect on vessel temperature with an increase of about 23º C for the case studied. Halving the film coefficient should cause an approximate doubling of the film temperature rise between the mixed-mean temperature of the flowing air in the RCCS duct and the duct inner surface. This should cause a corresponding increase in the temperature on the outer surface of the RCCS duct. Since the mode of heat transfer between the this surface and the outer surface of the reactor vessel is by radiation, which correlates with a difference in the forth powers of absolute temperature of the two surfaces, the increase in the temperature on the outer surface of the vessel should be much less than the increase in the film temperature inside the RCCS duct. If steady-state or nearly state-state heat transfer were occurring when the peak fuel temperature was approached an increase in vessel temperature would results in a nearly equal increase in fuel temperature. However, a higher peak fuel temperature allows more heat to be stored as the higher peak is approached and this causes the increase in the peak fuel temperature to be diminished and therefore be considerably less than the increase in the reactor vessel temperature.

V. PHENOMENA IDENTIFICATION AND RANKING

A. Background

Safety analyses are required to support the licensing of new reactor designs, their purpose being to demonstrate that safety criteria are met for design basis events. These analyses are aided by computer code simulations of the plant response to these events. Ultimately, these simulations become part of the technical basis for licensing the reactor. A supporting requirement is that the phenomenological models within the computer code be shown to give reliable and high fidelity representations of the phenomena in the plant response to the event. A formal code qualification procedure exists to ensure this.[2] As part of this procedure and to provide a guide for the efficient allocation of resources to improve model fidelity where needed, a set of phenomena identification and ranking

tables (PIRT) are generated to identify the main phenomena controlling the plant transient response. The PIRT was originally developed in the 1980s as an aid to light water reactor safety code qualification.[2] A PIRT identifies the phenomena that are active in a transient and then ranks them as to importance. Importance is measured in terms of the influence of the phenomena on safety related response.

B. Events

The specific PIRTS to be generated depend on the design basis events. The NGNP project, however, has not yet identified the set of such events. Below we use two different approaches to generate what should be a plausible set of design basis events. Three events are then selected for PIRT generation.

B.1 Categorized By Operating Regime

One can deduce the spectrum of design basis events by considering that they are the consequence of an equipment failure or operator error. The consequence falls into one or more of seven event classes. The classes are reactivity insertion, loss of heat sink, loss of flow, overcooling, flow runup, flow blockage, and loss of coolant. For each class there is a single event that bounds the severity of conditions for all events in the class.

It is instructive to classify these single events by operating regimes or phases, though this is not a standard element of the PIRT process. Operating regimes correlate with important phenomenon. Operating regimes are deduced by examining what key features describe the thermal-hydraulic regime the reactor is operating in. This is a function of three variables: pressure, cooling mode, and heating mode. As shown in Figure 23, for these variables, respectively: the reactor is pressurized or depressurized; there is net flow through the core or there is only internal re-circulation; and the core is neutronically critical or is shutdown and producing decay heat. Table 3 gives the values of these features for all classes of duty cycle, design basis, and beyond design basis events. Table 4 rearranges this information giving the event classes in each operating regime.

B.2 Identified in Prior Safety Analyses

The second area of guidance comes from prior gas reactor work. A review in [3] of the licensing work for the Fort Saint Vrain and the AVR Reactors produced a list of transients for which safety analyses were required. The results taken from Shultz appear in Table 5.

B.3 Selection of Events for PIRT Generation

Two design basis events thought to result in the maximum fuel and vessel temperatures were selected for PIRT generation. The Pressurized Conduction Cooldown (PCC) event is initiated by a loss of the main heat transport system coolers followed by a reactor trip and the failure of the Shutdown Cooling System to start. The Depressurized Conduction Cooldown (DCC) event is initiated by a double-guillotine break of the coaxial hot-cold

pipe that connects the reactor vessel to the Power Conversion Vessel. The reactor trips and the Shutdown Cooling System fail to start. Both the PCC and DCC appear in the lists in Table 4 and 5. There are other events in Table 4 that result in more severe conditions, e.g., the events that result in depressurized condition with heat removal by conduction cooling and neutronic power generation. However, the simultaneous occurrence of initiating failures for these events is most unlikely and places the events in the beyond-design-basis category. These events are not treated in a licensing safety analysis and so there should be no need for a PIRT. The main safety criteria are 1) the maximum fuel temperature should not exceed 1600^{o} C and 2) the maximum vessel temperature should not exceed 425^{o} C for the PCC and 3) 530^{o} C for the DCC. These criteria are based on material properties. In addition for the DCC there is a limit on the radiation release to the environment during blowdown. The main source of radioactivity will be graphite dust that is dislodged during depressurization. The PIRT should identify those phenomena and components that are important to remaining within these limits.

A third event thought to result in a local hot spot was selected for PIRT generation. The Load Change is an operational transient initiated by a reduction in plant power from full power to a new steady state. The main concern is the relocation of a structure hot spot during the transient and the thermal stresses generated. The temperature field at the turbine inlet piping has been suggested as an area for concern.[4]

C. Components

The reactor is composed of a number of different regions or components as listed in Table 6. Under normal operating conditions, cold coolant enters the inlet plenum from the cold pipe where it is distributed to the risers, a series of parallel vertical channels. The flow up through the risers exits into the top plenum where it is distributed to the core. In the PMR parallel flow enters the core coolant channels and the reflector channels. The flow leaves the core and enters the outlet plenum. From the outlet plenum the flow enters the hot pipe and then progresses through the Power Conversion Unit.

The reactor conditions that develop during the conduction coodown events and the load change event are a consequence of heat generation in the core and the removal of that energy through a heat removal path. The dominant path for heat removal in any of the three events is composed of several components with each component having several phenomena that affect the overall heat removal rate. In general the main heat removal path differs for each event. For each of the three events a task is to determine the relative importance of the phenomena in each of the components in Table 6 to the removal of heat through the dominant heat removal path.

The components and phenomena of importance differ among the three events. This is illustrated by comparison of the PCC and the DCC for the PMR. In the former the top plenum, core and reflector channels, and outlet plenum form a network of thermal hydraulic circuits that function to transport heat from the interior of the core out to the colder reflector channels where heat can be more readily conducted through the vessel wall. This contrasts with the DCC event where the thermal hydraulic circuit is ineffective

because of reduced pressure. In this case heat is transported directly by conduction and radiation radial through the fuel, coolant channels, and gaps between the prismatic blocks.

D. Phenomena

Table 7 presents a list of phenomena in the VHTR and the generic issues that are thought to be important for each. The right-hand side of the table shows the components for which these phenomena are believed to be important, effecting the generation, removal, and storage of energy. One shortcoming of Table 7, however, is that it neglects the dependence of the importance of a phenomenon in a component on the transient event. The event plays an important role as illustrated above for heat removal in the PMR for PCC versus DCC. Thus, phenomena must be considered with respect to both component and transient event.

The following conventions are adopted. The *coastdown* and *conduction cooldown* phases are demarcated by the transition from *forced* to *natural convection heat transfer*. The *fluid properties* phenomenon refers to the species mix of the coolant. The mix is dependent on species transport processes including air ingress into the break, movement of air through the vessel and piping, and consumption of oxygen by oxidation of graphite. The properties associated with a particular gas species are assumed lumped into the *heat transfer* and *pressure drop* phenomena. Thus, fluid properties takes in the changing species mix associated with air ingress, movement of air into the system, and consumption of oxygen. The *flow distribution* phenomenon refers to the macroscopic paths where the coolant is going. On the other hand, the *molecular diffusion* phenomenon refers to the time evolution of a species spatial concentration. *Decay heat* is broken into three components, the normalized *axial and radial power profiles*, a time varying *scale factor*, and *the initial stored energy*. It is assumed the plant design is based on confinement, not containment. The *homogeneous chemical reaction* refers to the migration of low temperature oxygen into the bulk graphite and its reaction with the graphite. *Graphite oxidation* is a surface phenomenon where high temperature oxygen reacts with the exposed graphite. We do not consider the intermediate heat exchanger that provides heat to the hydrogen plant, the ingress of water due to a shutdown cooling system leak, or an indirect cycle arrangement of components.

E. PIRTs

The structure of the PIRT reflects the factors that determine the plant response and whether it is within safety limits. Figure 24 shows these factors which include the phases or operating regimes that the transient progresses through, the phenomena occurring in each of these in each of the plant components, and the material limits upon which the safety limit is based. The material limits reflect permissible temperature and temperature rate of change in components. The structure of the PIRT reflects these factors with table entries identifying the transient phase, plant component, and the phenomena in each phase and component. The PIRT gives a ranking of the importance of each of the phenomena for each phase of the transient with respect to safety criteria.

The phenomena were ranked as to their importance by a group of four individuals who did not confer while preparing their original rankings. The individual rankings are given in Appendix A. Each individual received the same set of tables in which to enter his ranking. There was a separate table for each of the components listed in Table 6. The left column lists the phenomena for the component and along the top row are the three events, each divided into phases. The task of each investigator was to rank those phenomena in the left column as to their importance. A phenomenon, if considered to be present during a phase, was ranked in importance as either high (H), medium (M), or low (L). The ranking reflects the degree to which the plant response as gauged by the process variable associated with a safety limit is influenced by the phenomena. For example, in rating the importance of flow distribution in the top plenum during the coastdown phase of the PCC, the rank assigned to flow distribution reflects the importance of this phenomena on the value of fuel and vessel temperature, both of which have associated safety criteria. Additionally, when ranking a phenomenon, each phase is examined to the exclusion of all others. That is, one does not look across all phases for where the phenomenon has maximal importance; rather each phase is treated in isolation of the other phases. In some cases, however, a phenomenon in one phase may have a consequence for a peak condition in a later phase (e.g., molecular diffusion of air in DCC). Then a footnote to this effect is made.

The individual investigator rankings in Appendix A were combined into a single composite set of tables. The procedure for combining rankings was as follows. The four ranking values collected from the individual investigators for the importance of a phenomenon in a component in a phase of a transient event were arithmetically averaged. High importance was assigned a 3, medium importance was assigned a 2, and low importance was assigned a 1. However, of the four values the lowest one was first discarded and the average taken with respect to the remaining three. The intent was to reflect the fact that not all investigators are equally knowledgeable about all aspects of the transient events. Removing the low value tends to reduce the likelihood that an important phenomena would be weighted low mistakenly by the least knowledgeable investigator. The average was then rounded up or down according to whether the fractional component was greater or less than 0.5. The result was then transformed back into H, M, or L given values 3, 2, or 1, respectively.

The ANL PIRTs of Appendix A were subsequently presented at an I-NERI meeting at KAERI in South Korea in May 2005. The meeting was a forum for discussing the VHTR phenomena and for compiling a single set of PIRTS that reflected the consensus opinions of three national laboratories, INL, ANL, and KAERI. A single set of PIRTs was compiled by the meeting members after all sides presented their organization PIRTs and the basis for their rankings. The resulting PIRTS are given in Appendix B.

This section presents ANL composite tables of the important phenomena for each of the three events broken down by component.

E.1 Pressurized Conduction Cooldown Event

The PCC event is initiated by a loss of the main heat transport system coolers while the plant is at the full power condition. This is followed by a reactor trip and the failure of the Shutdown Cooling System to start. With the loss of the main coolers the capability of the primary system to function as a heat engine is lost. The turbomachine coasts down until it stops at which point there is no longer forced circulation through the core. Heat removal from the core is by the Reactor Cavity Cooling System. The PCC thus has two distinct phases, (1) the coastdown phase and (2) the conduction cooldown phase. The important phenomena for each component are described below.

Inlet Plenum – The phenomena considered important in the inlet plenum appear in Table 8. The inlet plenum feeds the risers during the coastdown phase and has an impact on the distribution of flow among the risers. The proportioning of flow among the risers during coastdown will change if the inlet plenum is not large enough to preclude pressure drop around its azimuthal periphery. A non-negligible pressure drop in turn will change the flow distribution in the core. The effect is not as great for the PBR since the pebbles tend to diffuse any flow maldistribution as the coolant moves down the core. This phenomenon ceases to be a factor once coastdown is complete. At that time the inlet plenum ceases to participate hydraulically since its flow is stagnant.

Riser – The phenomena considered important in the risers appear in Table 9. The risers are a set of parallel channels that connect the inlet plenum to the top plenum. Their hydraulic characteristics will effect the re-proportioning of coolant among them during the coastdown phase of the transient. This phenomenon ceases to be a factor once coastdown is complete. At that time the risers cease to participate hydraulically since the flow is stagnant. The risers are gas filled channels distributed around the periphery of the vessel. During conduction cooldown radiation heat transfer and gas conduction may be important components in the radial flow of heat to the vessel wall. There may be internal recirculation paths established with each riser, aiding heat transfer. The possibility of no net flow but alternating up flow and down flow between the inlet and top plenums exists.

Top Plenum and Components – The phenomena considered important in the top plenum appear in Table 10. During forced circulation the top plenum distributes coolant to the core. The volume of the plenum is an important factor in the manner in which flow from the risers distributes itself during the coastdown. When coastdown is complete the top plenum connects the core and reflector channels with the outlet plenum establishing a network of parallel passages. The coolant in the hotter channels exits the core upward in buoyant plumes while flow in the cooler channels moves down discharging into the outlet plenum. The hot fluid entering the top plenum may stratify in the absence of active mixing. The heat capacity and the thermal resistance of the thermal shroud will be important factors in the temperatures seen by the vessel at the upper head. The heat transfer to the shroud will be both radiative from the top of the core and mixed and natural convection from the gas in the plenum.

Core and Reflector – The phenomena considered important in the core and reflector appear in Table 11. There are a number of important phenomena during both the coastdown and conduction cooldown phases. The fraction of coolant that bypasses the core coolant channels in the PMR is perhaps the most important phenomenon for fuel temperature. The fraction is related to core configuration and is dependent on fuel block dimensional changes over life. In the PMR fueled blocks stacked one on top of the other may have gaps between them that causes flow diversion. In the PBR flow diversion is less important because the leakage paths among fueled balls over life can be better predicted. However, the pebbles in contact with the vessel wall will have an average porosity that is greater than the bulk. This gives rise to a multi-dimensional heat distribution and bypass overcooling. The flow distribution through the PMR core is important as it affects the thermal conditions in the hot channel. Transition from coastdown to cooldown may be marked by flow stoppage in some channels as flow undergoes reversal. The PMR core contains a multi-dimensional arrangement of coolant channels within a block that may require detailed spatial to locate the local hot spot. While a porous body modeling of the fluid is not suited to the PMR, it may be adequate for the PBR. In addition the neutronic power may need to be computed on a block–by-block basis to properly resolve the radial heating profile. This profile is important for the flow distribution by natural convection in the cooldown phase. The temporal behavior of the decay heat curve is important since it affects the heat load seen by the heat removal systems. Fluid properties, particularly viscosity, are important during both coastdown and cooldown. Viscosity increases with temperature. During cooldown the coolant flowing in the hottest channel will have the greatest viscosity which will decrease cooling in that channel and increase fuel temperature. The core heat capacity is very important as it is a main mechanism for storing heat that otherwise would be removed through a heat transport path. Fuel temperatures would otherwise be greater. The gaps between blocks in the same plane and the associated gap conductance are important to radial heat transfer in the PMR. Under core configuration, the pebbles in the PBR may pile up locally at the top of core affecting the core power distribution.

Outlet Plenum and Components – The phenomena considered important in the outlet plenum appear in Table 12. During the coastdown phase the hot core coolant enters the outlet plenum. In the PMR the coolant enters as a hot jet before it diffuses within the plenum. Thermal striping on components is an issue. Thermal stripping is less an issue in the PBR since the coolant flow paths are connected laterally and since the flow amongst the balls gives rise to converging and diverging jets, both of which give rise to better mixing before the coolant exits the core into he plenum. The plenum connects the vertical coolant channels in which parallel circulation patterns develop within the core during cooldown. These patterns are a principle means for moving energy from the core interior toward to vessel wall. The inlet plenum thus plays a role in the mixing and stratification in the top plenum.

Hot/Cold Pipe – The phenomena for the hot/cold pipe appear in Table 13. The leakage of heat by conduction from the hot inner pipe to the cool outer annulus and the related performance of the insulation are the main phenomena. The hot and cold pipes in the PBR are much longer than the PMR so conduction phenomenon may be more important in the PBR. The hot-cold pipes may act as a heat pipe transporting heat away from the

vessel and radiating it to the reactor cavity. The transport may be a combination of convection and conduction.

Reactor Cavity – The phenomena considered important in the RCCS appear in Table 14. Heat removal by the RCCS during PCC is the main path for cooling the vessel. The radial temperature gradient developed across the core heat to the vessel. The transfer of heat from the vessel wall to the air ducts is mainly by radiation heat transfer. Computer code calculations with CFD models indicate that this is 90 percent of the heat transfer with convection by air in the cavity making up the balance.[5] The view factors for the reactor vessel communicating with the ducts are especially complex because the vessel geometry is circular while the duct layout is Cartesian. The impact of simplifications used in computing view factors must be quantified. In the cooldown phase the hot plumes in the vessel head raise the temperature of the vessel wall at the top such that the vessel temperature and not the fuel may be the limiting condition.

RCCS Air Duct – The phenomena considered important in the RCCS air duct appear in Table 15. The energy conducted through the duct walls from the reactor cavity is convected to the air inside the duct and is also radiated by the inner surfaces of the duct to adjacent surfaces. A buoyant head is established inside the duct as the air heated by the duct walls expands, rises, and draws air in at the duct inlet. The heat transfer and pressure loss phenomena inside the duct are dependant on the velocity profile at the wall. If local buoyancy at the wall is induced, then the heat transfer and pressure loss processes operate in the mixed rather than forced convection mode. Because of the non-circular geometry of the duct and non-uniform heat flux at the duct surface, modeling of the mixed convection region requires special treatment. Either scaled experiments are required to obtain integral data or a validated CFD code is needed to solve explicitly for the flow field in the duct interior. Recent results suggest that fluid property variation may be more important than the mode of convection.[6]

RCCS Piping and Chimney – The phenomena considered important in the RCCS appear in Table 16. The same considerations for the air duct apply here also. The effect of flow mixing in plena connecting pipes is considered to have negligible impact on fuel and vessel temperature because it is so far removed from the vessel and fuel.

Power Conversion Unit – The phenomena considered important in the PCU appear in Table 17. The role of the PCU diminishes as the turboshaft coasts down. While the time length for coastdown may be a factor that determines which phenomena are important, presently the coastdown time is not known. There is a possibility for generation of pressure waves in the PCU as a result of compressor stall.

E.2 Depressurized Conduction Cooldown Event

The DCC event is initiated by a guillotine break of the hot/cold pipe. The coolant inventory blows down, exiting through the opening in the inner hot duct and in the annular cold duct. The PCU is effectively isolated from the reactor vessel and plays no significant role in the event. The reactor trips on loss of pressure. After blowdown, air

begins to diffuse into the primary system through the site of the break. If sufficient air enters the primary system, natural circulation paths are established. The DCC has three distinct phases, (1) blowdown, (2) air ingress, and (3) natural convection.

Inlet Plenum – The phenomena considered important in the inlet plenum appear in Table 8. During the blowdown phase, depending on the relative volumes of the vessel flow passages, flow reversal may bring hot core coolant into the inlet plenum. During the air ingress phase, air will tend to enter at the bottom of the annular cold pipe. Acoustic noise will aid its diffusion into the plenum. The molecular diffusion of air is very dependent on the gas temperature in the plenum. Thus, thermal stratification and mixing in the inlet plenum must be first well understood before air ingress can be predicted reliably. Large thermal gradients in the inlet plenum will enhance or inhibit molecular diffusion of air into the plenum. The progression of the air ingress phase has a significant effect on the natural convection phase.

Riser – The phenomena considered important in the riser are shown in Table 9. During the air ingress phase the temperature distribution in the riser is important to the progression of air diffusion. Thus, the role of thermal stratification in the riser must be well understood. In the PBR the risers contain graphite and which may act as a parasitic sink for oxygen during the air ingress and natural convection phases. The shortest path to the core is, however, through the outlet plenum. Thus, the risers may have a reduced role in the progression of the air ingress phase. In the natural convection stage, depending on the gas mixture, there is a possibility for recirculation flow within the riser of alternating up and down flow in adjacent risers. This will enhance the transport of heat from the core to the vessel wall.

Top Plenum and Components – The phenomena considered important for the top plenum are shown in Table 10. The potential for graphite oxidation in the natural convection phase depends on how well air infiltrated in the previous phase.

Core and Reflector – The phenomena considered important in the core and reflector are shown in Table 11. Reaction forces during the blowdown phase can load vessel structures and loosen graphite dust previously created by mechanical friction of fuel elements. The PBR will have higher dust levels because the fuel is in motion. The blowdown will carry some of the dust and vent it into containment or confinement. The confinement must be equipped with a filter to prevent discharge of the dust to the environment. During the blowdown phase, the helium in the core is cooled by the mechanical work of decompression. This cooling term may serve to lower fuel temperature from what it would otherwise be. The ingress of air creates the potential for significant oxidation of the fuel. During the natural convection phase, the circulating gas will aid in the removal of the heat of oxidation. The degree of oxidation is related to available supply of air during the ingress phase. For confinement, the original air in the reactor cavity will be partially displaced by helium from the break. For containment, the available air is a function of the volume of the containment. The air flowrate into the vessel during the natural convection phase likely will be insufficient to significantly cool the core. It will however generate significant heat of oxidation, raising structure temperatures, as it reacts

with the graphite. The main path for air ingress is through the outlet plenum via the hot duct. The graphite structures below the fueled region of the core will react with the air and reduce the concentration of oxygen entering the fueled region of the core. Graphite oxidation will be more important in the PBR as a consequence of the greater fuel surface area and resulting higher oxidation rate.

Outlet Plenum and Components – The phenomena considered important in the outlet plenum and components are shown in Table 12. The outlet plenum lies between the site of the break and the core and is thus in the shorter of two paths that lead from the reactor cavity to the core. Consequently, during the blowdown phase, graphite dust lodged in the lower core and the outlet plenum may be swept through the outlet plenum and out the break into the confinement. During the air ingress phase, the thermal stratification in the outlet plenum will play a role in the rate of molecular diffusion of air into the core. If graphite is present in the outlet plenum, it will act as a site for oxidation and may result in reduced concentrations reaching the reactor fuel. During the natural convection phase the outlet plenum may be important to the flow patterns that are established.

Hot/Cold Pipe – The phenomena considered important in the hot/cold pipes are shown in Table 13. The double guillotine of the hot/cold pipe creates two separate paths from the reactor cavity to the core, one through the inlet plenum and one through the outlet plenum. As mentioned in [7] blowdown will be through both paths with the result that a plane of zero velocity will exist at some point, likely in the core. The reactor cavity conditions beginning with the start of the air ingress phase defines the air concentration boundary condition at the break.

Reactor Cavity – The phenomena considered important in the reactor cavity are shown in Table 14. The air in the reactor cavity before the onset of the upset will contain water vapor. Some of this water vapor will be present in the mixture of gases that enter the break site during the air ingress phase. In addition, the PBR may include a source of cooling water that might enter the reactor cavity and, during the air ingress and natural convection phases, enter the reactor vessel as water vapor through the break. During the blowdown phase, graphite dust may be discharged into the reactor cavity. If the cavity acts as a confinement, then the release of this radioactive dust into the environment through a relief valve must be considered. The dust may settle on RCCS heat transfer surface in the cavity changing their heat transfer characteristics. During the air ingress and natural convection phases, some the air in the cavity that was not displaced will move into the reactor vessel and oxidize graphite surfaces.

RCCS Air Duct – The phenomena considered important in the RCCS air duct are shown in Table 15. These are the same consideration as for the DCC. Additionally, one must also consider possible collapse of the air duct walls by pressure difference during blowdown..

RCCS Piping and Chimney – The phenomena considered important in the RCCS piping and chimney are shown in Table 16. These are the same phenomena that are important during the PCC.

Power Conversion Unit – The phenomena considered important in the power conversion unit are shown in Table 17. The power conversion unit is effectively isolated from the reactor vessel after blowdown and plays no significant role in the event.

E.3 Load Change Event

The LC event is initiated with a reduction in primary flowrate by 20 percent over a 20 second period and is then maintained at this value. The reactor is not tripped. The net reactivity is assumed to return to zero in the asymptote through natural temperature change without control rod motion. The PCC has two distinct phases, (1) the flow reduction phase followed by transition to a new equilibrium condition (2) and the new steady-state operating condition. The plant response is highly dependent on the behavior of the plant control system. Assuming the reactor inlet temperature is maintained constant and Doppler and coolant feedback are the main reactivity temperature effects, the reduction in cooling will raise the average core temperature which will reduce the core power. Whether the reactor outlet temperature increases or decreases depends on the coolant to fuel temperature rise and the coolant to Doppler reactivity feedbacks.
It is expected, however, that the core outlet temperature will change and that will lead to the movement of local hot spots. The main concern is the relocation of a structure hot spot during the transient and the thermal stresses generated. The temperature field at the turbine inlet piping has been suggested as an area for concern.[4] The important phenomena for each component are described below.

Top Plenum and Components – The phenomena considered important in the top plenum appear in Table 10. The flow will redistribute in the top plenum so that the flowrate into the PMR core channels will change.

Core and Reflector – The phenomena considered important in the core and reflector appear in Table 11. The redistribution of flow among the core channels will change the location of the core hot spot.

Outlet Plenum and Components – The phenomena considered important in the outlet plenum appear in Table 12. The importance of thermal striping will be greater for the PMR since the coolant streams exiting the PMR core have a wider temperature variation because there is less mixing as the coolant flows down the core. The coolant may exhibit a temperature gradient in the plane that is normal to the flow of coolant through the outlet plenum. This is because the coolant exiting the core is not isothermal.

Hot/Cold Pipe – The hot pipe takes coolant from the inlet plenum. The location of the hot spot in the hot pipe will change as the flow pattern in the outlet plenum changes with the flow reduction.

Power Conversion Unit – The turbomachine performance will effect the temperatures exiting the turbomachines and hence the temperatures seen by the recuperator.

VI. MODELS AND SCALING ANALYSIS

A wide body of literature deals with the problem of extending the applicability of experimental data taken under a limited set of conditions to a more general set of conditions.[8,9] Methods such as dimensional analysis and scaling analysis have important applicability in gas cooled reactor design work. They can be used as a basis for conducting tests on a small scale with a less expensive representation of a thermal-hydraulics system and then extrapolating the results to predict the behavior of the full size system. They can also be used as a basis for developing relationships among thermal-hydraulics variables that are independent of physical dimensions and material properties thus leading to wide spread applicability. Such relationships are referred to as empirical or correlated models and appear in the RELAP5/ATHENA, FLUENT, and Star-CD codes. A main task of this project is to identify such models and to review their applicability to the phenomenon the codes will be called on to represent.

There are a generic set of issues that arise whenever correlated models are to be used in a safety analysis. We describe them as they are the sort of issues that drive the code applicability studies and will need to be addressed to some degree. A first issue is, are there distortions of processes introduced by conducting tests in scaled-down mockups? A designer attempts to maintain geometric, kinematic, and dynamic similarity between physical processes occurring at full-scale and those taking place in the scaled-down model. In general, exact similitude cannot be achieved and compromises are required. For these the designer uses engineering judgment to optimize similitude for the processes of greatest importance. This may introduce scale distortions of other less important processes or may introduce spurious processes which are atypical of the full-scale facility. A second issue is, in the course of fitting an empirical correlation and parameters to obtain agreement with experimental data, are there compensating errors introduced that under certain scenarios the corresponding compensating effects produce non-conservative results? A third issue is, are there correlations that are not supported by experimental data or are based on data which do not cover the range of interest in the analysis?

In this section the task is, for each instance of phenomenon and associated phase and component listed in Tables 8 through 17, to identify the dimensionless numbers that characterize the related behavior. The general approach is to consider the field equations of conservation and transport. In particular the mass, energy, and momentum conservation equations are non-dimensionalized using an appropriately chosen set of scaling parameters. This yields dimensionless parameters as the sole parameters upon which the solution depends. Hence, if experimental data can be obtained from which one can infer the functional relationship among these dimensionless parameters, then one has an empirically correlated model for the phenomenon without regard to specific dimensions, thermal-hydraulic conditions, or material properties. In this section we describe the derivation of these models for heat transfer and fluid flow in mixed convection regime in the RCCS.

A. Integral Phenomena

We refer to those processes that consist of more than one basic heat transfer or fluid phenomenon as *integral phenomena*. We are interested in their combined behavior and so seek a model that reflects this rather than an individual model for each of the phenomenon. As a result, the model does not contain explicit reference to each of the underlying processes, only a cause and effect type reference to the overall behavior. When the underlying processes are multidimensional the model captures only the net effect and provides no details on the nature of the multidimensionality. It is up to the correlation developer to note the conditions under which this aggregated representation is valid and then up to the user to observe them.

In this subsection, we identify requirements for correlated models for description of heat transfer and pressure drop in the mixed convection regime in the RCCS under regime OR6 - *Depressurized/ Conduction Cooling/ Shutdown Decay Heat* given in Table 4. The suitability of models in RELAP5/ATHENA for predicting this phenomenon under these conditions is determined in the next section.

The heat transfer and pressure drop within the riser are treated as integral phenomenon. During depressurized conduction cooling conditions the axial component of the riser velocity field will have a two dimensional spatial dependence in the horizontal plane. As a result the local heat transfer coefficient and wall friction will vary around the circumference of the duct. Additionally, at the low flowrates both forced convection and natural convection heat transfer, so-called mixed convection heat transfer, may be present. Despite these multi-phenomenon, multi-dimensional elements, one can treat the mass, energy, and momentum balances for the air in the riser as one-dimensional. In so doing, one must derive integral correlations for heat transfer and friction that do not explicitly model local phenomenon that control these such as the boundary layer thickness and turbulence.

The dimensionless parameters that appear in correlated models for describing one-dimensional pressure drop and heat transfer rate are derived from the non-dimensionalized conservation equations. Below we present a summary of results for heat transfer and pressure drop for in laminar flow forced convection between two vertical parallel plates. The implication is that mixed convection, the combination of both forced and natural convection, will depend on the same dimensionless parameters.

A.1 Dimensionless Parameters

We consider two stationary vertical parallel plates with fluid between them. Assume x is the distance along the direction of flow and y is the distance along the normal to the plates. Assume the plates are separated by the distance $2\ y_0$.

For *pressure drop for fully developed laminar flow,* the conservation of momentum equation is [9]

$$\frac{dP}{dx} = \mu \frac{d^2 v_x}{dy^2} \tag{1}$$

where P = pressure,
μ = coolant viscosity, and
v_x = fluid velocity in direction of flow

where the coolant density, ρ, and viscosity are constant. The velocity v_x is solved for

$$v_x = \frac{3}{2} V \left[1 - \left(\frac{y}{y_0} \right)^2 \right] \tag{2}$$

and integrated to give the average velocity

$$V = -\frac{1}{3\mu} \frac{dP}{dx} y_0^2 \quad . \tag{3}$$

Now define a dimensionless variable, the friction factor

$$f = \frac{-\Delta P}{\frac{\Delta x}{y_0} \frac{1}{2} \rho V^2} \quad . \tag{4}$$

Eqs. (3) and (4) combine to give

$$f = \frac{6}{Re} \tag{5}$$

where $Re = \rho V y_0 / \mu$ is the Reynolds number.

For *heat transfer for fully developed laminar flow*, the temperature satisfies [9]

$$\rho C_p v_x \frac{\partial T}{\partial x} = k \frac{\partial^2 T}{\partial y^2} \tag{6}$$

where k is thermal conductivity, C_p is specific heat, and T is temperature and can be solved for analytically. Let the temperature of the two plates be T_0 and T_1, respectively. One defines a heat transfer coefficient

$$h = \frac{q''}{T_0 - T_m} = \frac{k\left(\frac{\partial T}{\partial y}\right)_{y=y_0}}{T_0 - T_m} \tag{7}$$

where T_m is the mixed mean fluid temperature obtained by averaging the velocity weighted temperature profile normal to the direction of flow. The above expression is rearranged and a new quantity, the Nusselt number defined,

$$Nu = \frac{h y_0}{k} = \frac{\partial\left(\frac{T - T_m}{T_0 - T_m}\right)}{\partial\left(\frac{y}{y_0}\right)} \; . \tag{8}$$

Since the temperature T exists as an analytic expression obtained by solving Eq. (6), then the right-side of Eq. (8) can be evaluated. Hence, the heat transfer coefficient is a function of the Nusselt number, a dimensionless quantity.

For *heat transfer for natural convection laminar flow*, assume that the plates have infinite extent in the x direction, that the temperature is independent of x, and that axial conduction and friction effects can be neglected. Then in the fully developed region the temperature is given by [9]

$$\frac{d^2T}{dy^2} = 0 \, . \tag{9}$$

If the temperature of the plates are T_0 and T_1, respectively, then

$$\frac{T - T_m}{T_1 - T_m} = -\frac{y}{y_0} \, . \tag{10}$$

The velocity is given by the momentum equation with a term to account for buoyant forces [9]

$$\frac{\mu \partial^2 v_x}{\partial y^2} + \rho \beta g_x (T - T_m) = 0 \; . \tag{11}$$

The above equation solved for the velocity with the temperature given by Eq. (10) and $v_x = 0$ at the face of the plates gives

$$v^* = \frac{1}{6} \, Gr \, Pr \, (y^{*3} - y^*) \tag{12}$$

where

$$v^* = \frac{v_x \rho C_p y_0}{k}\ , \qquad \text{dimensionless velocity}$$

$$Gr = \frac{g \beta y_0^3 (T_1 - T_m)}{\nu}\ , \qquad \text{Grashof number}$$

$$y^* = \frac{y}{y_0}\ . \qquad \text{dimensionless length}$$

The linear temperature profile was obtained for negligible friction. This will be the case for low GrPr as described in [9]. Thus, Eq. (12) is valid only for low GrPr.

The heat transfer coefficient is from Eq. (7) and (10) given by

$$Nu = \frac{h y_0}{k} = 1\ . \qquad (13)$$

As GrPr increases and frictional losses become important, the temperature profile given by Eq. (9) will no longer be valid. The temperature and velocity profiles will become interdependent. The velocity profile will maintain a Gr number dependence and so the heat transfer coefficient given by Eq. (8) will assume a Gr number dependence.

A.2 Regime Map

In the mixed convection region both natural convection and forced convection are present. We expect then that the correlation of pressure drop and heat transfer under mixed convection laminar flow conditions will exhibit those same dimensionless numbers derived for laminar flow above using simple conservation balances. See Table 18 for a summary of the above results. Thus, models for describing pressure drop and heat transfer in this regime should include a dependence on the quantities Re, Pr, Gr, and y* presented in Table 18. As a corollary experiments for obtaining correlations for pressure drop and heat transfer in the mixed convection regime should include Re, Pr, Gr, and y*.

It has been found that the demarcation among natural, mixed, and forced convection is given by values of a subset of these dimensionless numbers. Figure 25 is a regime map for circular tubes and shows the dependence of the regime on Re, Pr, Gr, and y*.

We investigated the likelihood that core channel flowrate or RCCS duct flowrate are in the mixed convection region during either normal or off normal operation. If so, then the 1-D system code used for accident analysis must have appropriate correlations for heat transfer and pressure drop. The correlations should include a Re, Pr, Gr, and y* dependence as described above. Important dimensions and conditions for an average core channel are given in Table 19. The calculation of Re and Gr for an average core channel both at full power and at shutdown with the shutdown circulator running under

pressurized and depressurized conditions is given in Tables 20 and 21. The dimensionless numbers for the axes of the Figure 25 regime map are shown in Table 22. Plotting the values from this table on the regime map shows that the channel condition remains solidly in the forced convection region.

For the RCCS air duct, the full power thermal-hydraulic conditions are given in Table 23. The calculation of Re and Gr at full power is given in Tables 24 and 25, respectively. From these tables we have Re = $1.4*10^4$ and $Gr*Pr*D/L \sim 10^7$ where we have taken D/L = 0.01. This point falls just inside the mixed convection region in Figure 25. During shutdown the point will move diagonally since the flowrate (Re) is positively correlated with the power (Gr). Whether the point moves down and to the left or in the opposite direction depends on the details of the transient and can be answered with a 1-D systems code simulation. In either case, the air in the duct will trace a path through the mixed convection region. Since the duct is non-circular and the heat flux is not uniform while Figure 25 is for vertical heated pipes, the exact path might be better determined from a flow regime map specific to the geometry and heating conditions.

A.3 Models

The pressure drop in a vertical round pipe in the turbulent flow regime is altered when wall heating is introduced. The heating of the fluid at the wall introduces buoyant forces which change the velocity profile and affect the pressure drop. The pressure drop can increase or decrease depending on the conditions. The correlation of Petukhov [10] expresses the friction factor of the heated case in terms of the unheated case. For conditions where Pr > 0.6, Re > 3000, $0< Gr < 10^{11}$, and L/D > 40 the heated friction factor is given by

$$f = \left[\frac{1 + 0.83\, e^2}{f_0^{-1/2} + 0.076 e^2 E^{1/4}} \right]^2 \tag{14}$$

where

$$e = \frac{10^3\, Gr}{\mathrm{Pr} \cdot \mathrm{Re}^{2.75}} \quad , \quad E = \frac{Gr}{\mathrm{Pr} \cdot \mathrm{Re}^{4}} \tag{15}$$

and the unheated friction factor is given by

$$f_0 = \left[1.82 \log_{10} (\mathrm{Re}/8) \right]^{-2}. \tag{16}$$

The heated friction factor is plotted in Figure 26 against Grashof number for different values of Reynolds number. One sees that the friction factor drops below the value of the

unheated case for initially small heating rates but then rises above for increased heating. We have also plotted the condition in the RCCS air duct at the full power condition. Figure 26 shows that the pressure drops to 0.8 of the value for the case where there is no heating, all other things being equal. After shutdown, the condition in the duct will move away from the full power point shown on Figure 26. Proper prediction of the RCCS response by safety analysis code requires then that mixed convection pressure drop in the turbulent regime be treated as a case distinct from the forced convection case.

Similarly, the heat transfer coefficient at the wall of a pipe with vertical upflow is altered when buoyant forces in the fluid appreciably change the fluid velocity profile in the pipe. A discussion of this phenomenon is given in [11]. Briefly, the buoyant forces induced in the fluid nearest the wall by heating of the exterior of the wall increase the fluid velocity near the wall over the case of no heating. Mass conservation implies that the velocity near the centerline decreases for a net flattening of the velocity profile. This is referred to as aiding flow. The opposite, cooling of the wall, gives rise to opposing flow. Both are shown schematically in Figure 27 [11]. If the flow is turbulent in the non-heated case, arguments based on Prandtl's mixing model suggest that heat transfer is reduced by heating. The effect on heat transfer coefficient is shown in Figure 28 [11]. If the flow in the unheated case is laminar, then heating gives the opposite effect. [12]

To summarize, there are two independent dimensions to heat transfer for single-phase flow. First we have the heat transfer mode which can be forced, mixed, or natural convection. Second we have the flow regime which can be laminar, turbulent, and transition between laminar and turbulent flow. One can considered a two dimensional array for heat transfer in which one dimension represents laminar, transition, and turbulent flow and the other represents free, mixed, and forced convection. One obtains a nine-region, three-by-three array. The situation for friction factor is identical.

An assumption we have made is that the flow and temperature boundary layers are fully developed. This, of course, can only be an idealization. However, flow channels in reactor applications tend to be hundreds of diameter long whereas fully developed flow is attained within tens of diameters. A further consideration, of particular importance for laminar flow, is the shape of the channel. Although, the law-of-the-wall makes behavior of turbulent flow relatively insensitive to channel shape, this is not true for laminar flow, even for the simplest of case of forced laminar flow.

B. Separate Effects

We refer to those processes that consist of only one basic heat transfer and/or fluid dynamics phenomenon as *separate effects*. The ability to accurately predict the behavior of a single separate effect is critical if we are interested in capturing the multidimensionality of underlying processes in the analysis of integral phenomena. Since the number of separate effects problems that could be identified for any system is almost unlimited and the end goal is to use the separate effects modeling capability to predict the multidimensional behavior of important integral phenomena, it is highly desirable to make use of a generic multidimensional modeling capability that is valid over some

limited range of conditions rather than developing many approaches that are highly specialized for each separate effect of interest. Like the integral effects correlations, it is up to the model developer to note the conditions under which each representation of heat transfer and/or fluid dynamics behavior and the user to observe them.

In this subsection we identify requirements for correlated models for use in the prediction of separate effects which may impact the performance of the RCCS under regime OR6 – *Depressurized/Conduction Cooling/ Shutdown Decay Heat* given in Table 4. The suitability of models available for computational fluid dynamics (CFD) analysis of the RCCS components under these conditions is discussed in the next section.

As stated in the previous subsection, the axial component of the riser velocity field will have a two dimensional spatial dependence in the horizontal plane during depressurized conduction cooling conditions. As a result, the local heat transfer coefficient and wall friction will vary circumferentially around the duct. Furthermore, the flow of fluid through the riser is driven entirely by thermally-induced density gradients, and flow rates through the duct are relatively low. Consequently, a mixture of natural and forced convection heat transfer as defined based upon the flow rate through the duct rather than the nature of the driving force may occur. Where there is a need to understand the multidimensionality of the flow field within the duct, the local separate effects phenomena that generate turbulence and trigger changes in boundary layer thickness must be modeled explicitly.

The Navier-Stokes equations, the mathematical representations that are employed in the CFD modeling of heat transfer and fluid dynamic phenomena, are derived from the basic conservation equations and provide a complete generic solution to any fluid dynamics and heat transfer problem. However, the application of the Navier-Stokes equations in their full detail is impractical for most flow fields, and especially for turbulent flow fields, so parameterized versions of the equations are typically employed. Empirical correlations are used to determine appropriate localized values for these parameters throughout the multidimensional domain. While dimensionless forms of the Navier-Stokes equations are know, dimensional forms are more commonly used since there is no need to try to reduce all important phenomena into a single dimensionless parameter. The parameterized form of the Navier-Stokes equations and the basic forms of the correlations that would typically employed for turbulent incompressible flow between two vertical parallel plates are discussed below. The implication of the formulation employed is that the features that are important to integral phenomena correlations, such heat transfer regime, are not as important to the accuracy of the correlated turbulence and boundary layer models as features that impact the growth of the boundary layer or development of turbulence, such as abrupt changes in geometry that result in a separated boundary layer.

B.1 Parameters

For any fluid flow field, the behavior of the flow field can be described exactly by the Navier-Stokes equations: [13]

$$\vec{\nabla} \cdot \vec{V} = 0 \tag{17}$$

$$\rho \frac{D\vec{V}}{Dt} = \rho \vec{g} - \vec{\nabla} p + \mu \nabla^2 \vec{V} \tag{18}$$

$$\rho c_p \frac{DT}{Dt} = k \nabla^2 T + \tau'_{ij} \frac{\partial u_i}{\partial x_j} \tag{19}$$

where $\vec{V}$ = velocity vector
ρ = density
t = time
$\vec{g}$ = gravitational acceleration vector
p = pressure
μ = dynamic viscosity
c_p = specific heat
T = temperature
k = conductivity
τ'_{ij} = viscous stress tensor
u_i = velocity component i
x_j = coordinate direction j

If Reynolds' time-averaging approach is utilized and each variable is assumed to be composed of the sum of an average-valued component and a fluctuating component, such that any variable Q is described by:

$$Q = \overline{Q} + Q' \tag{20}$$

where the bar notation indicates the time average component and the prime notation indicates the fluctuating component, then the Navier-Stokes equations can be reformulated as the Reynolds-Averaged Navier-Stokes equations:

$$\vec{\nabla} \cdot \overline{\vec{V}} = 0 \tag{21}$$

$$\rho \frac{D\overline{\vec{V}}}{Dt} = \rho \vec{g} - \vec{\nabla} \overline{p} + \vec{\nabla} \cdot \left[\mu \left(\frac{\partial u_i}{\partial x_j} + \frac{\partial u_j}{\partial x_i} \right) - \rho \overline{u'_i u'_j} \right] \tag{22}$$

$$\rho c_p \frac{D\overline{T}}{Dt} = -\frac{\partial}{\partial x_i} \left(-k \frac{\partial \overline{T}}{\partial x_i} + \rho c_p \overline{u'_i T'} \right) + \overline{\Phi} \tag{23}$$

where $\mu \left(\frac{\partial u_i}{\partial x_j} + \frac{\partial u_j}{\partial x_i} \right)$ = laminar flow stress tensor
$\rho \overline{u'_i u'_j}$ = turbulent flow stress tensor

$\overline{\Phi}$ = total dissipation $\approx \frac{\partial \overline{u}}{\partial y}\left(\mu \frac{\partial \overline{u}}{\partial y} - \rho \overline{u'v'}\right)$

μ = dynamic fluid viscosity

The turbulent stress tensor is still unknown, but the equations are now presented in a form that lends itself to the development of "turbulence conservation" equations that may be used to relate the turbulent stresses to the mean flow field and facilitate the solution of the above equation set without the need to know the turbulent stress tensor *a priori*. The most commonly used "turbulence conservation" equation is the turbulent kinetic energy equation, where the turbulent kinetic energy is defined as

$$K = \tfrac{1}{2}\overline{u_i' u_i'}. \tag{24}$$

The turbulent kinetic energy equation can be derived by forming the dot product of u_i and the *i*th momentum equation then subtracting the instantaneous mechanical energy from its time averaged value to form:

$$\begin{aligned}\frac{DK}{Dt} = &-\frac{\partial}{\partial x_i}\left[\overline{u_i'\left(\tfrac{1}{2}u_j' u_j' + \frac{p'}{\rho}\right)}\right] - \overline{u_i' u_j'}\frac{\partial \overline{u}_j}{\partial x_i} \\ &+ \frac{\partial}{\partial x_i}\left[\nu \overline{u_j'\left(\frac{\partial u_i'}{\partial x_j} + \frac{\partial u_j'}{\partial x_i}\right)}\right] - \nu \overline{\frac{\partial u_j'}{\partial x_i}\left(\frac{\partial u_i'}{\partial x_j} + \frac{\partial u_j'}{\partial x_i}\right)}\end{aligned} \tag{25}$$

where ν = kinematic viscosity = μ/ρ

Obviously, the terms of this relation are too complex to compute them from first principles and an engineering modeling approach will need to be applied.

B.2. Models

The most commonly applied modeling strategy is the two-equation high-Reynolds number K-ε model:

$$\frac{DK}{Dt} \approx \frac{\partial}{\partial x_j}\left(\frac{\nu_t}{\sigma_K}\frac{\partial K}{\partial x_j}\right) + \nu_t \frac{\partial \overline{u}_i}{\partial x_j}\left(\frac{\partial \overline{u}_i}{\partial x_j} + \frac{\partial \overline{u}_j}{\partial x_i}\right) - \varepsilon \tag{26}$$

$$\frac{D\varepsilon}{Dt} \approx \frac{\partial}{\partial x_j}\left(\frac{\nu_t}{\sigma_\varepsilon}\frac{\partial \varepsilon}{\partial x_j}\right) + C_1 \nu_t \frac{\partial \overline{u}_i}{\partial x_j}\left(\frac{\partial \overline{u}_i}{\partial x_j} + \frac{\partial \overline{u}_j}{\partial x_i}\right) - C_2 \frac{\varepsilon^2}{K} \tag{27}$$

where σ_K and σ_ε are effective Prandtl Numbers, which relate the eddy diffusion of K and ε to the momentum eddy viscosity ν_t. The eddy viscosity itself is modeled as

$$\nu_t = \frac{C_\mu K^2}{\varepsilon}. \tag{28}$$

Thus the turbulent fluctuations can be linked to the average velocity field using two equations containing five unknown constants that must be experimentally determined: C_μ, C_1, C_2, σ_K and σ_ε. The recommended values for these empirical constants for calculations in which the boundary layer remains attached to the wall are shown in Table 26.

Equations 26 and 27 are combined with the continuity, momentum and energy equations to form a complete system of equations to describe turbulent shear flow. This form of the model neglects molecular viscosity and sub-layer damping effects, so it can only be used in the outer and overlap regions of the boundary layer. The behavior in the inner sub-layer is typically modeled using a logarithmic wall function of the form:

$$K = \frac{v^{*2}}{C_\mu^{1/2}} \tag{29}$$

$$\varepsilon = \frac{v^{*3}}{\kappa y} \tag{30}$$

$$\frac{\bar{u}}{v^*} = \frac{1}{\kappa}\ln\left(\frac{v^* y}{\nu}\right) + B \tag{31}$$

where y = distance from the wall
κ = Kármán's constant $\approx$ 0.41
v^* = wall friction velocity
B = intercept from empirical data $\approx$ 5.0

This particular wall function form assumes that variations in velocity are predominantly normal to the wall, the effects of pressure gradients are negligibly small, and that a balance exists between turbulence generation and dissipation. These conditions are reasonable for turbulent incompressible flow between two vertical flat plates. Alternate forms may be applied when the flow field of interest is does not satisfy these conditions.

VII. CODE REVIEW

The nuclear safety codes are reviewed with respect to modeling requirements established in the previous section. The 1-D systems code is RELAP5/ATHENA and the CFD code is FLUENT. The selection of these codes as the thermal-hydraulic safety analysis tools for the NGNP design was made outside of this project. In this section, we review these codes below for each of the phenomenon examined in the previous section. For RELAP5/ATHENA we examine the treatment of mixed convection heat transfer and pressure drop. For FLUENT and Star-CD we review the available options for the modeling of turbulence.

A. RELAP5/ATHENA

We found in the previous section that the mixed convection flow regime may be present in the air duct of the RCCS during both normal and off-normal operation. We described instances where forced convection models applied to this regime under-predict pressure drop and over-predict heat transfer. Under these circumstances core fuel temperatures would be under-predicted. Since the RCCS has an important safety function in limiting fuel temperatures during accidents it is important that the thermal-hydraulics models in RELAP5/ATHENA include treatment of the mixed convection regime.

We reviewed RELAP5/ATHENA for the treatment of pressure drop and heat transfer in the mixed convection regime. The following appears on page 4-86 of Volume IV of the RELAP5/ATHENA manual: "There are other situations besides cooling that are *not accounted for*. These include entrance effects, laminar-turbulent transition and *mixed forced*, and free *convection"* where we have italicized text for emphasis. Correlations for Nusselt number are given in Section 4.2.2 starting on page 4-77 of Volume IV. In particular the table on page 4-80 indicates laminar and turbulent flows and natural convection, but no mixed convection. Correlations for friction factor are given in Volume I Section 3.3.8.6 starting on page 3-180 and also Volume IV Section 6.2.1.2 starting on page 6-40. No correlations are given for mixed convection.

B. FLUENT and Star-CD

Fluent and Star-CD both offer a wide variety of turbulence modeling options, ranging from the very simplistic to the highly complex, as part of their standard suite of tools. For extremely simplistic flow fields, both codes offer the ability to utilize a single equation Prandtl mixing length model for the prediction of the turbulence field. For basic compressible or incompressible flow fields with reasonably isotropic turbulence and minimal boundary-layer separation, both codes offer two-equation high and low Reynolds number K-ε models. Low Reynolds number models require a highly refined computational mesh near any wall in order to properly resolve the turbulence field all the way to the wall and can be computationally expensive in either code. High Reynolds number models require a separate wall function to resolve the turbulence field in the near wall region without the need for the highly refined computational mesh, and both codes offer a comparable selection of log-law and algebraic functions to address different surface characteristics. Both codes also offer a comparable selection of alternate K-ε type models that include additional terms to improve the accuracy of the calculation of the dissipation.

For slightly more complex flow fields in which significant regions of the boundary layer are separated from the wall, both codes offer a comparable selection of two-equation K-ω models. As with the K- ε models, the K-ω models may be used to model the turbulence field to the wall with a highly refined mesh or in conjunction with a wall function when a coarser mesh is used. For flow fields in which the turbulence is primarily anisotropic,

both codes offer a selection of higher order two-equation models that include additional non-linear terms in the dissipation equation to account for the anisotropy.

Both codes also include a comparable selection of advanced modeling options which provide additional details about the turbulence field at the expense of significantly larger computational investment. The additional information may make these modeling options more robust for flow fields which contain complex flow structures resulting from large regions of boundary layer separation, periodic vortex shedding mechanisms, impinging jet flows, or other pressure gradients normal to the surface. The only steady state modeling option among these models is the Reynolds Stress Models (RSM), which model each of the stresses in the stress tensor directly using algebraic formulations. Both codes also offer limited capability to utilize Large Eddy Simulation (LES), in which various formulations are used to model sub-grid turbulence while large turbulence structures are simulated directly, and Discrete Eddy Simulation, in which LES is employed in the far field and a K- ε or K-ω model is used near the wall to improve the accuracy of predictions in the near wall region. In the event that a suitable model is not included for a particular application, both codes offer the capability for the user to add a new model through pre-defined user subroutines.

VIII. EXPERIMENTS

A. Initial Filtering of Existing Databases

We compiled a list of experiment databases by performing a search of the open literature for phenomena cited mainly in the context of gas reactors. In the future, we will widen our search criteria to include consultation with experts. The consultation will not be limited to the nuclear field but will include the aeronautics and chemical engineering industries.

We describe here only those experiments that are centered on the RCCS. Then in subsections VII.B1 and 2 we weigh the usefulness of these experiments with respect to specific needs identified in Section V for modeling RCCS phenomenon and we comment on the need for additional experiments.

References [14] and [15] provide experimental data pertaining to the RCCS of the JAERI (Japan) HTTR reactor. Both contain benchmark problems with experimental data that was used for code validation by various reactor development organizations around the world—Japan, Russian Federation, South Africa, United States of America, and France in the case of [14]. Each report provides experimental data and the analytical results provided by various modelers. Both reports provide steady-state axial distributions of reactor vessel temperature and cooling panel temperature. (The cooling panels are the mostly vertical air-to-air or air-to-water heat exchangers that receive the heat transferred from the exterior of the reactor vessel and enable it to be transferred from the reactor cavity.)

Reference [14] provides experimental data obtained directly from the HTTR reactor at two power levels—full power (30 MWt) and 9 MWt. The cooling panels are water cooled. Reference [15] describes an experimental mockup of the HTTR in which an electric heater that has six axial segments is used in place of the reactor core. It appears that no attempt was made to preserve similitude between the mockup and the HTTR reactor plant and the mockup is approximately a fourth the size of the HTTR, but is not to scale. It appears that an adequate description of the experiment is provided. The data in Table 27 was copied from Table 4-0 of the reference. These are all steady state tests for which experimentally measured temperatures are provided graphically for the pressure vessel and the cooling panel. Based on the figure on page 12 of the reference, the control rod stand pipes are capped pipes that extend from the top of the reactor vessel and are used as conduits for the control rod drive handles.

The experimental data provided by the references is not specific with respect to geometry and conditions to the particular VHTR reactor under consideration in this report. Also these data would not be used to establish new fundamental relationships of general utility. However, there is considerable value in having measured data from facilities that have analogous systems and employ some of the same phenomena as those of the NGNP. Such data can be used very effectively by modeler and code developers to identify governing phenomena and modes of facility behavior that would otherwise have been overlooked. Of references [14] and [15], the latter appears to be the better of the two to use for such purposes. The facility for this reference is fundamentally simpler and the experiment is better described than in [14]. In both cases, it is not obvious that all of the details that one would need to do a thorough comparison with measured data are published, since the need for missing crucial details are often uncovered during the analytical process.

B. Measured Data Needs

B.1 Integral Phenomena

We noted earlier that friction factor and heat transfer in the mixed convection regime occupy a subset of the elements in a three-by-three array with convection mode and flow regime as independent variables. A good review of existing correlations that populate this matrix is given in [12]. This review identifies for heat transfer a correlation each for constant heat flux and constant wall temperature conditions for each of the nine elements in the matrix. Where buoyancy is a factor the correlation is for up-flow. For friction factor the review identifies for forced convection correlations for turbulent, laminar, and transition regime. For mixed convection up-flow it identifies correlations for turbulent flow. These turbulent mixed convection regime correlations are candidates for filling the void in RELAP5/ATHENA identified in subsection VI.A. For mixed convection up-flow in the laminar flow regime [12] cites a lack of data or correlations.

It is not clear whether the absence of friction factor data for mixed convection up-flow in the laminar flow regime is a void that needs to be filled for RELAP5/ATHENA qualification. These low Reynolds numbers in the core channels will be reached long into

a cooldown event. By that time and at these low flowrates the predominant mode of heat removal in the core may be radial conduction. Similarly, for the RCCS air duct these low Reynolds numbers might eventually be reached, but by then the primary system temperatures may have long ago peaked. In such a case, an error in the friction factor may have little consequence with respect to being able to make a reliable prediction that temperatures remain below safety criteria limits. Thus, before a recommendation can be made as to the need for performing experiments for the mixed convection laminar flow regime, whole plant simulations should be performed to determine primary system temperatures far out in time when either core channel or RCCS air duct flows might be expected to be laminar.

With length to diameter ratios in the hundreds and Reynolds numbers in the thousands for these channels one would expect predominantly one-dimensional flow without recirculation. That is, pure natural convection is not expected at anytime where not having the corresponding correlations in place might be of consequence. Again this should be checked by performing a whole plant simulation, computing dimensionless numbers, and then examining the regime map of Figure 25.

The RCCS air duct is decidedly two-dimensional in heat flux and channel shape. The error arising from applying circular tube correlations for heat transfer and friction factor must be quantified. In the event it is unacceptable, then a semi-scale experiment using the air duct geometry would be required to obtain integral data for heat transfer and friction factor.

B.2 Separate Effects

Since the turbulence models that are employed in multi-dimensional CFD simulations are generic in form and serve only to describe the relationship between the fluctuating and average components of any variable, any simulation regardless of turbulence model selection can be expected to provide some insight into the expected behavior of the flow field. Since engineering analyses are typically most interested in the characteristics of solid components under different system conditions, the accuracy of the simulation is typically judged by the ability of a model to predicted wall quantities of interest. Hence, the accuracy of the prediction of a specific separate effect is largely dependent on appropriateness of the selected turbulence model's treatment of the generation and dissipation of turbulence in the near wall region. Consequently, significantly more detailed data sets are needed for the assessment of turbulence model accuracy than for the assessment of one-dimensional correlations associated with integral phenomena.

While significant integral data exists for the mixed convection regime expected to dominate the performance of the RCCS, a comparable data set has not yet been identified for validation of multi-dimensional CFD simulations of compressible, mixed-convective flow in a vertical duct with heated boundaries that cannot be described as constant heat flux or constant temperature. In order to provide sufficient confidence of the ability of a turbulence model to adequately capture the turbulence field under such conditions, a suitable experiment must use a compressible coolant and be both heated and buoyancy-

driven. The data collected from such an experiment must include measurements of the velocity, temperature, and turbulence parameter profiles across the duct cross-section for direct comparison with predicted values. Furthermore, the complexity of the thermal boundary condition requires that the surface temperature distribution be sufficiently well described for use as a boundary condition in the benchmarking calculations. An example of the level of data detail needed for a separate effects validation of turbulence modeling capability can be found in the paper of Krauss and Meyer.[16]

C. Computational Data Needs

Engineering-scale experiments are the preferred means for acquiring data for qualifying models in a computer code. However, designing an experiment, assembling the equipment, and performing the experiment are costly and time consuming tasks. Therefore, prudence is required to limit the number of experiments to only the most essential As we describe below, one may be able to reduce the required number of experiments by relaxing the strict separation made in subsection VII.B between a 1-D code with integral experiments and a CFD code with separate effect experiments. We describe a cross over of models and data.

In the case of integral phenomena, the aggregation of spatial detail results in a model and measured data that are geometry specific. Geometric similitude allows generalization of measured data to different dimensions as long as aspect ratios are preserved. But for significant geometry changes, generalizing of results (e.g. extrapolation of results for 1-D uniform heat flux in a circular pipe to 2-D heat flux dependence in a rectangular duct) may introduce uncertainty that is not easily bounded without performing an actual experiment in the new geometry. Thus, there is an apparent need to perform geometry specific experiments in the case of the 1-D code models identified in subsection VII.B.1. This can lead to a large number of experiments.

In practice we may be able to limit the number of such experiments by replacing them with *in silico* or *computational* experiments. We use the case of a heated vertical flow channel with specialized cross sectional geometry, such as found in the air duct of the RCCS, as an example. This is a geometry perturbation on the *heated vertical circular pipe* experiment. Correction factors can be generated for obtaining the behavior of the heated flow channel with specialized cross sectional geometry from experiments and correlations for the simpler geometry described in the literature. If these correction factors for heat transfer coefficient and friction factor can be obtained from CFD calculations (i.e. numerical experiments) for the specialized geometry, then the number of required laboratory experiments is significantly reduced. This of course assumes that the CFD code has been first qualified for the relevant separate effects in this specialized geometry. These separate effects were described in subsection VII.B.2. A necessary test of the adequacy of the resulting capability is that the CFD code be able to replicate the measured integral behavior in the simpler geometry. Essentially, by this process, we are substituting computational data for measured data.

In summary, we expect the need for 1-D models of heat transfer and pressure drop in specialized flow channel geometries. These models are required for 1-D whole plant transient simulations to be performed for the safety analyses. The present demands of CFD codes make a whole plant CFD simulation impractical. These 1-D models can be obtained in a cost effective manner by the use of geometry correction factors generated by a CFD code and applied to the results of integral models obtained from experiments in a simpler flow channel geometry (i.e. circular and 1-D).

IX. CONCLUSIONS

Nuclear systems codes are being prepared for use as computational tools for conducting performance/safety analyses of the Very High Temperature Reactor. A formal qualification framework based on that used in the Light Water Reactor industry was developed. It consists of the development of Phenomena Identification and Ranking Tables (PIRTs), the initial filtering of the experiment databases, and a preliminary screening of these codes for use in the performance/safety analyses. The codes are RELAP5/ATHENA for one-dimensional systems modeling and FLUENT and/or Star-CD for three-dimensional modeling.

In the second year of this project we focused on development of PIRTS. Two accidents, the Pressurized Conduction Cooldown (PCC) event and the Depressurized Conduction Cooldown (DCC) event, which result in maximum fuel and vessel temperatures, were selected for PIRT generation. A third transient, the Load Change event, which may result in significant thermal stresses, was also selected for PIRT generation. Gas reactor design experience and engineering judgment were used to identify the important phenomena in the primary system for these transients. Sensitivity calculations performed with the RELAP5 code were used as an aid to rank the phenomena in order of importance with respect to the approach of plant response to safety limits.

The overall code qualification methodology was illustrated by focusing on the Reactor Cavity Cooling System (RCCS). The mixed convection mode of heat transfer and pressure drop was identified as an important phenomenon for RCCS operation. Scaling studies showed that the mixed convection mode is likely to occur in the RCCS air duct during normal operation and during conduction cooldown events. The RELAP5/ATHENA code was found to not adequately treat the mixed convection regime. Readying the code will require adding models for the turbulent mixed convection regime while possibly performing new experiments for the laminar mixed convection regime. Candidate correlations for the turbulent mixed convection regime for the circular channel geometry were identified in the literature. We described the use of computational experiments to obtain correction factors for applying these circular channel results to more specialized channel geometries. The intent is to reduce the number of laboratory experiments. The FLUENT and Star-CD codes contain models that in principle can handle mixed convection but no data were found to indicate that their empirical models for turbulence have been benchmarked for mixed convection conditions. Separate effects experiments were proposed for gathering the needed data.

In future work we will use the PIRTs to guide review of other components and phenomena in a similar manner as was done for the mixed convection mode in the RCCS. This is consistent with the project objective of identifying weaknesses or gaps in the code models for representing thermal-hydraulic phenomena expected to occur in the VHTR both during normal operation and upsets, identifying the models that need to be developed, and identifying the experiments that must be performed to support model development.

REFERENCES

1. B. E. Boyack, et al., "An Overview of Code Scaling, Applicability, and Uncertainty Methodology," Nuclear Engineering and Design 119 (1990), pp. 1-15.

2. B. Boyack, et al., *Quantifying Reactor Safety Margins, Application of Code Scaling, Applicability, and Uncertainty Evaluation Methodology to Large-Break, Loss-of-Coolant Accident*, NUREG/CR-5249, Nuclear Regulatory Commission, December 1989.

3. R. Schultz, "Defining the Research and Development Needs for the Next Generation Nuclear Plant: Neutronics and Thermal Hydraulics," American Nuclear Society Winter Meeting, 2004.

4. R. Schultz, personal communication, Idaho National Laboratory, February 2005.

5. C. Tzanos, personal communication, Argonne National Laboratory, March 2005.

6. C. Tzanos, personal communication, Argonne National Laboratory, April 2005.

7. R. Schultz, personal communication, Idaho National Laboratory, April 2005.

8. P. F. Peterson, "Scaling and Analysis of Mixing in Large Stratified Volumes," Int. J. Heat Mass Transfer, Vol. 37, 1994, Suppl. 1, pp. 97-106.

9. W. M. Rohsenow and H. Choi, "Heat Mass and Momentum Transfer," Prentice Hall, 1961.

10. B.S. Petukhov, "Heat Transfer in Turbulent Mixed Convection," Hemisphere Publishing, 1988.

11. T. Aicher and H. Martin, New Correlations for mixed turbulent natural and forced convection heat transfer in vertical tubes," International Journal of Heat and Mass Transfer, Vol. 40, No.15, pp. 3617-3626, 1997.

12. W. Williams, P. Hejzlar, M.J. Driscoll, W.J. Lee, and P. Saha, "Analysis of a Convection Loop for GFR Post-LOCA Decay Heat Removal form a Block-Type Core," MIT-ANL-TR-095, March 2003.

13. F.M. White, *Viscous Fluid Flow*, 2nd ed., Boston: McGraw-Hill, 1991.

14. IAEA-TECDOC—1382, *Evaluation of high temperature gas cooled reactor performance: Benchmark analysis related to initial testing of the HTTR and HTR-10*, Chapter 3, "High Temperature Engineering Test Reactor Thermal Hydraulic Benchmarks, November 2003.

15. IAEA-TECDOC—1163, *Heat Transport and Afterheat Removal for Gas Cooled Reactors under Accident Conditions*, 2000.

16. T. Krauss and L. Meyer, "Experimental investigation of turbulent transport of momentum and energy in a heated rod bundle", *Nuclear Engineering and Design, **180,** pp. 185-206 (1998).*

17. K. Kunitomi, "Thermal and Hydraulic Tests in HENDEL T_2 Supporting the Development of the Core Bottom Structure of the High Temperature Engineering Test Reactor (HTTR)," *Nuclear Engineering and Design*, Vol. 108, 1988, pp. 359-368.

18. Yoshiaki Miyamoto, et al., "Thermal and Hydraulic Test of Test Sections in the Helium Engineering Demonstration Loop," *Nuclear Engineering and Design*, Vol. 120, 1990, pp. 435-445.

19. Yoshiyuki Inagaki, et al., "Thermal-Hydraulic Characteristics of Coolant in the Core Bottom Structure of the High-Temperature Engineering Test Reactor," *Nuclear Technology*, Vol. 99, July 1992, pp. 90-103.

20. Yoshiyuki Inagaki, Tomoaki Kunugi, and Yoshiaki Miyamoto, "Thermal Mixing Test of Coolant in the Core Bottom Structure of a High Temperature Engineering Test Reactor," *Nuclear Engineering and Design*, Vol. 123, 1990, pp. 77-86.

21. Makoto Hishida, et al., "Heat Transfer Problems in a VHTR," *Heat Transfer in High Technology and Power Engineering*, Wen-Jei Yang and Yasuo Mori, editors, Hemisphere Publishing Corporation, New York, 1987, pp. 273-284.

22. M. S. Yao, Z. Y. Huang, C. W. Ma, and Y. H. Xu, "Simulating Test for Thermal Mixing in the Hot Gas Chamber of the HTR-10," *Nuclear Engineering and Design*, Vol. 218, 2002, pp. 233-240.

23. G. Damm and R.Wehrlein, "Simulation Tests for Temperature Mixing in a Core Bottom Model of the HTR-Module," *Nuclear Engineering and Design*, Vol. 137, 1992, pp. 97-105.

24. Gas Turbine-Modular Helium Reactor (GT-MHR) Conceptual Design Report, Report number 910720/1, General Atomics, July 1996.

APPENDIX A PIRTS by Individual Panel Members

A.1 Investigator Beta

Inlet Plenum*

Phenomena	HPCC		LPCC			LC	
	1	2	1	2	3	1	2
Flow Distribution	H,L		H,L			H,L	H,L
Heat Transfer (Forced Convection)	L,L		L,L			L,L	L,L
Heat Transfer (Mixed and Free Convection)					L		
Pressure Drop (Forced Convection)	L,L		L,L			L,L	L,L
Pressure Drop (Mixed and Free Convection)					L,L		
Thermal Mixing and Stratification		M,M		H,H	H,H		
Bulk CO Reaction				L,L	L,L		
Molecular Diffusion				H,H			
Pressure Waves							

* first entry is Prismatic Modular Reactor, second entry is Pebble Bed Reactor

Riser

Phenomena	HPCC		LPCC			LC	
	1	2	1	2	3	1	2
Flow Distribution	M,M		M,M	M,M		M,M	M,M
Heat Transfer (Forced Convection)	L,L		L,L			L,L	L,L
Heat Transfer (Mixed and Free Convection)					L,L		
Pressure Drop (Forced Convection)	H,M		M,M			H,M	H,M
Pressure Drop (Mixed and Free Convection)					H,M		
Radiation Heat Transfer		H,H		H,H	H,H		
Gas Conduction		H,H		H,H	H,H		
Bulk CO Reaction				L,L	L,L		
Molecular Diffusion				H,H			
Pressure Waves							

Top Plenum & Components

Phenomena	HPCC		LPCC			LC	
	1	2	1	2	3	1	2
Flow Distribution	H,M	H,M	H,M	L,L	H,M	H,M	H,M
Heat Transfer (Forced Convection)	M,M		M,M			L,L	L,L
Heat Transfer (Mixed and Free Convection)		M,M		L,L	M,M		
Pressure Drop (Forced Convection)	L,L		L,L			L,L	L,L
Pressure Drop (Mixed and Free Convection)		L,L			L,L		
Thermal Mixing and Stratification		H,M		L,L	H,M		
Hot Plumes		H,M		L,L	H,M		
Fluid Properties	L,L	L,L	L,L	L,L	L,L	L,L	L,L
Thermal Resistance/Heat Capacity of Shroud		H,H		H,H	H,H		
Bulk CO Reaction				L,L	L,L		
Molecular Diffusion				H,H			
Pressure Waves							

Core and Reflector (including Bypass)

Phenomena	HPCC		LPCC			LC	
	1	2	1	2	3	1	2
Flow Distribution	H,H	H,H	H,H	L,L	H,H	H,H	H,H
Heat Transfer (Forced Convection)	H,H		H,H			H,H	H,H
Heat Transfer (Mixed and Free Convection)		H,H		L,L	H,H		
Pressure Drop (Forced Convection)	H,H		H,H			H,H	H,H
Pressure Drop (Mixed and Free Convection)		H,H		L,L	H,H		
Decay Heat (including Power Distribution)	M,M	H,H	M,M	M,M	H,H		
Reactivity Feedback						M,M	M,M
Fuel/Reflector Conductivity	L,L	H,H	L,L	H,H	H,H	L,L	L,L
Fuel/Reflector Specific Heat	L,L	H,H	L,L	H,H	H,H	L,L	L,L
Multi-D Heat Conduction Including Contact	H,L	H,L	H,L	L,L	H,L	H,L	H,L
Gas Conduction (Including Gaps)		H,H		H,H	H,H		
Radiation Heat Transfer		H,H		H,H	H,H		
Graphite Oxidation				M,H	M,H		
Bulk CO Reaction				M,H	M,H		
Molecular Diffusion				H,H			
Fluid Properties	H,H	H,H	H,H	H,H	H,H	H,H	H,H
Core Configuration	H,M	H,M	H,M	L,L	H,M	H,M	H,M
Pressure Waves							

Outlet Plenum & Components

Phenomena	HPCC		LPCC			LC	
	1	2	1	2	3	1	2
Flow Distribution	H,H	H,H	H,H	H,H	H,H	H,H	H,H
Heat Transfer (Forced Convection)	M,M		M,M			H,H	H,H
Heat Transfer (Mixed and Free Convection)		M,M		M,M	M,M		
Pressure Drop (Forced Convection)	L,L		L,L			L,L	L,L
Pressure Drop (Mixed and Free Convection)		L,L		L,L	L,L		
Thermal Mixing and Stratification		H,M		H,M	H,M		
Jet Discharge						H,M	H,M
Thermal Striping						H,M	H,M
Bulk CO Reaction				L,L	L,L		
Molecular Diffusion				H,H			
Fluid Properties	L,L	L,L	L,L	L,L	L,L	L,L	L,L
Pressure Waves							

Hot/Cold Pipe

Phenomena	HPCC		LPCC			LC	
	1	2	1	2	3	1	2
Heat Transfer (Forced Convection)	L,L		L,L			M,M	M,M
Heat Transfer (Mixed and Free Convection)					L,L		
Pressure Drop (Forced Convection)	L,L		L,L			M,M	M,M
Pressure Drop (Mixed and Free Convection)					L,L		
Pipe/Insulator Conduction							M,M
Critical Flow			L,L				
Pressure Waves							

RCCS (Reactor Cavity Cooling System) Reactor Cavity

Phenomena	HPCC		LPCC			LC	
	1	2	1	2	3	1	2
Flow Distribution		M,M		M,M	M,M		
Heat Transfer (Mixed and Free Convection)		M,M		M,M	M,M		
Pressure Drop (Mixed and Free Convection)		L,L		L,L	L,L		
Radiation Heat Transfer		H,H		H,H	H,H		
Gas Conduction		L,L		L,L	L,L		
Conduction to Ground		L,L		L,L	L,L		
Dust from Core			M,H				
Air Purge and Gas Species Distribution			M,H	H,H	H,H		
Confinement Valve and Filter Characteristics							
Pressure Waves							

RCCS Tube (Air Duct)

Phenomena	HPCC		LPCC			LC	
	1	2	1	2	3	1	2
Heat Transfer (Forced Convection)		M,M		M,M	M,M		
Heat Transfer (Mixed and Free Convection)		H,H		H,H	H,H		
Pressure Drop (Forced Convection)		M,M		M,M	M,M		
Pressure Drop (Mixed and Free Convection)		H,H		H,H	H,H		
Radiation Heat Transfer		H,H		H,H	H,H		
Pressure Waves							

RCCS Piping and Chimney

Phenomena	HPCC		LPCC			LC	
	1	2	1	2	3	1	2
Heat Transfer (Mixed and Free Convection)		L,L		L,L	L,L		
Pressure Drop (Mixed and Free Convection)		H,H		H,H	H,H		
Flow Mixing in Piping Plenums		L,L		L,L	L,L		
Buoyancy Flow in Chimney		H,H		H,H	H,H		
Pressure Waves							

PCU (Power Conversion Unit)

Phenomena	HPCC		LPCC			LC	
	1	2	1	2	3	1	2
Turbine Performance						M,M	M,M
Turbine Valve Performance						H,H	
Heat Conduction in Thick-Walled Structure							L,L
Heat Transfer in Coolers						M,M	M,M
Pressure Drop in Coolers						M,M	M,M
Heat Transfer in Recuperator						M,M	M,M
Pressure Drop in Recuperator						M,M	M,M
Compressor Performance						M,M	M,M
Pressure Waves							

A.2 Investigator Delta

Inlet Plenum*

Phenomena	HPCC		LPCC			LC	
	1	2	1	2	3	1	2
Flow Distribution	M,M		M,M			M,M	M,M
Heat Transfer (Forced Convection)	M,M		M,M			L,L	L,L
Heat Transfer (Mixed and Free Convection)					M,M		
Pressure Drop (Forced Convection)	M,M		M,M			M,M	M,M
Pressure Drop (Mixed and Free Convection)					M,M		
Thermal Mixing and Stratification		M,M		L,L	M,M		
Bulk CO Reaction				L,L	L,L		
Molecular Diffusion							
Pressure Waves							

* first entry is Prismatic Modular Reactor, second entry is Pebble Bed Reactor

Riser

Phenomena	HPCC		LPCC			LC	
	1	2	1	2	3	1	2
Flow Distribution	M,M		M,M	M,M		M,M	M,M
Heat Transfer (Forced Convection)	M,M		M,M			M,M	M,M
Heat Transfer (Mixed and Free Convection)					M,M		
Pressure Drop (Forced Convection)	M,M		M,M			M,M	M,M
Pressure Drop (Mixed and Free Convection)							
Radiation Heat Transfer		H,H		H,H	H,H		
Gas Conduction		L,L		L,L	L,L		
Bulk CO Reaction				L,L	L,L		
Molecular Diffusion				M,M			
Pressure Waves							

Top Plenum & Components

Phenomena	HPCC		LPCC			LC	
	1	2	1	2	3	1	2
Flow Distribution	M,M	M,M	M,M	L,L	M,M	H,H	H,H
Heat Transfer (Forced Convection)	M,M		M,M			M,M	M,M
Heat Transfer (Mixed and Free Convection)		M,M		L,L	M,M		
Pressure Drop (Forced Convection)	M,M		M,M			M,M	M,M
Pressure Drop (Mixed and Free Convection)		M,M			M,M		
Thermal Mixing and Stratification		M,M		L,L	M,M		
Hot Plumes		H,H		L,L	M,M		
Fluid Properties	M,M	H,H	M,M	L,L	M,M	H,H	H,H
Thermal Resistance/Heat Capacity of Shroud		M,M		M,M	M,M		
Bulk CO Reaction				L,L	L,L		
Molecular Diffusion				M,M			
Pressure Waves							

Core and Reflector (including Bypass)

Phenomena	HPCC		LPCC			LC	
	1	2	1	2	3	1	2
Flow Distribution	H,H	H,H	H,H	L,L	M,M	H,H	H,H
Heat Transfer (Forced Convection)	H,H		H,H			H,H	H,H
Heat Transfer (Mixed and Free Convection)		H,H		L,L	M,M		
Pressure Drop (Forced Convection)	H,H		H,H			H,H	H,H
Pressure Drop (Mixed and Free Convection)		H,H		L,L	M,M		
Decay Heat (including Power Distribution)	H,H	H,H	H,H	H,H	M,M		
Reactivity Feedback						H,H	H,H
Fuel/Reflector Conductivity	H,H	H,H	H,H	H,H	H,H	H,H	H,H
Fuel/Reflector Specific Heat	H,H	H,H	H,H	H,H	H,H	H,H	L,L
Multi-D Heat Conduction Including Contact	M,M	M,M	M,M	H,M	H,M	M,M	M,M
Gas Conduction (Including Gaps)		M,M		M,M	M,M		
Radiation Heat Transfer		H,H		H,H	H,H		
Graphite Oxidation				L,L	H,H		
Bulk CO Reaction				L,L	L,L		
Molecular Diffusion							
Fluid Properties	H,H	H,H	H,H	M,M	H,H	H,H	H,H
Core Configuration	H,M	H,M	H,M			H,M	H,M
Pressure Waves							

Outlet Plenum & Components

Phenomena	HPCC		LPCC			LC	
	1	2	1	2	3	1	2
Flow Distribution	M,M	M,M	M,M	L,L	M,M	H,H	H,H
Heat Transfer (Forced Convection)	L,L		M,M			M,M	M,M
Heat Transfer (Mixed and Free Convection)		M,M		L,L	M,M		
Pressure Drop (Forced Convection)	M,M		M,M			H,H	H,H
Pressure Drop (Mixed and Free Convection)		M,M		L,L	M,M		
Thermal Mixing and Stratification		M,M		L,L	M,M		
Jet Discharge						H,H	H,H
Thermal Striping						H,H	H,H
Bulk CO Reaction				L,L	L,L		
Molecular Diffusion				L,L			
Fluid Properties	M,M	M,M	M,M	L,L	M,M	H,H	H,H
Pressure Waves							

Hot/Cold Pipe

Phenomena	HPCC		LPCC			LC	
	1	2	1	2	3	1	2
Heat Transfer (Forced Convection)	L,M		L,M			L,M	L,M
Heat Transfer (Mixed and Free Convection)					L,M		
Pressure Drop (Forced Convection)	L,M		L,M			L,M	L,M
Pressure Drop (Mixed and Free Convection)					L,M		
Pipe/Insulator Conduction							
Critical Flow							L,M
Pressure Waves			M,M				

RCCS (Reactor Cavity Cooling System) Reactor Cavity

Phenomena	HPCC		LPCC			LC	
	1	2	1	2	3	1	2
Flow Distribution		L,L		L,L	L,L		
Heat Transfer (Mixed and Free Convection)		L,L		L,L	L,L		
Pressure Drop (Mixed and Free Convection)		L,L		L,L	L,L		
Radiation Heat Transfer		H,H		H,H	H,H		
Gas Conduction		L,L		L,L	L,L		
Conduction to Ground		L,L		L,L	L,L		
Dust from Core			L,L				
Air Purge and Gas Species Distribution			L,L	M,M	M,M		
Confinement Valve and Filter Characteristics							
Pressure Waves							

RCCS Tube (Air Duct)

Phenomena	HPCC		LPCC			LC	
	1	2	1	2	3	1	2
Heat Transfer (Forced Convection)		H,H		H,H	H,H		
Heat Transfer (Mixed and Free Convection)		H,H		H,H	H,H		
Pressure Drop (Forced Convection)		H,H		H,H	H,H		
Pressure Drop (Mixed and Free Convection)		H,H		H,H	H,H		
Radiation Heat Transfer		H,H		H,H	H,H		
Pressure Waves		H,H		H,H	H,H		

RCCS Piping and Chimney

Phenomena	HPCC		LPCC			LC	
	1	2	1	2	3	1	2
Heat Transfer (Mixed and Free Convection)		H,H		H,H	H,H		
Pressure Drop (Mixed and Free Convection)		H,H		H,H	H,H		
Flow Mixing in Piping Plenums		L,L		L,L	L,L		
Buoyancy Flow in Chimney		H,H		H,H	H,H		
Pressure Waves							

PCU (Power Conversion Unit)

Phenomena	HPCC		LPCC			LC	
	1	2	1	2	3	1	2
Turbine Performance						H,H	H,H
Turbine Valve Performance						H,H	
Heat Conduction in Thick-Walled Structure						M,M	L,L
Heat Transfer in Coolers						H,H	H,H
Pressure Drop in Coolers						H,H	H,H
Heat Transfer in Recuperator						H,H	H,H
Pressure Drop in Recuperator						H,H	H,H
Compressor Performance						H,H	H,H
Pressure Waves							

A.3 Investigator Gamma

Inlet Plenum*

Phenomena	HPCC		LPCC			LC	
	1	2	1	2	3	1	2
Flow Distribution	L,L		L,L			L,L	L,L
Heat Transfer (Forced Convection)	L,L		L,L			L,L	L,L
Heat Transfer (Mixed and Free Convection)					L,L		
Pressure Drop (Forced Convection)	L,L		L,L			L,L	L,L
Pressure Drop (Mixed and Free Convection)					L,L		
Thermal Mixing and Stratification		L,L		L,L	L,L		
Bulk CO Reaction				L,L	L,L		
Molecular Diffusion				L,L			
Pressure Waves							

* first entry is Prismatic Modular Reactor, second entry is Pebble Bed Reactor

Riser

Phenomena	HPCC		LPCC			LC	
	1	2	1	2	3	1	2
Flow Distribution	L,L		L,L	L,L		L,L	L,L
Heat Transfer (Forced Convection)	L,L		L,L			L,L	L,L
Heat Transfer (Mixed and Free Convection)					L,L		
Pressure Drop (Forced Convection)	L,L		L,L			L,L	L,L
Pressure Drop (Mixed and Free Convection)					L,L		
Radiation Heat Transfer		H,H		H,H	H,H		
Gas Conduction		M,L		M,L	M,L		
Bulk CO Reaction				L,L	L,L		
Molecular Diffusion				L,L			
Pressure Waves							

Top Plenum & Components

Phenomena	HPCC		LPCC			LC	
	1	2	1	2	3	1	2
Flow Distribution	H,H	H,H	L,L	L,L	H,H	L,L	L,L
Heat Transfer (Forced Convection)	L,L		L,L			L,L	L,L
Heat Transfer (Mixed and Free Convection)		H,H		L,L	H,H		
Pressure Drop (Forced Convection)	L,L		L,L			L,L	L,L
Pressure Drop (Mixed and Free Convection)		H,H			H,H		
Thermal Mixing and Stratification		H,H		L,L	H,H		
Hot Plumes		H,H		L,L	H,H		
Fluid Properties	H,H	H,H	L,L	L,L	H,H	L,L	L,L
Thermal Resistance/Heat Capacity of Shroud		H,H		H,H	H,H		
Bulk CO Reaction				L,L	L,L		
Molecular Diffusion				L,L			
Pressure Waves							

Core and Reflector (including Bypass)

Phenomena	HPCC		LPCC			LC	
	1	2	1	2	3	1	2
Flow Distribution	H,H	H,H	H,H	L,L	M,M	H,H	H,H
Heat Transfer (Forced Convection)	M,M						
Heat Transfer (Mixed and Free Convection)		H,H					
Pressure Drop (Forced Convection)	L,L		L,L			L,L	L,L
Pressure Drop (Mixed and Free Convection)		H,H		H,H	H,H		
Decay Heat (including Power Distribution)	H,H	H,H	H,H	H,H	H,H		
Reactivity Feedback						M,M	M,M
Fuel/Reflector Conductivity	H,H	H,H	H,H	H,H	H,H	H,H	H,H
Fuel/Reflector Specific Heat	H,H	H,H	H,H	H,H	H,H	H,H	H,H
Multi-D Heat Conduction Including Contact	H,H	H,H	H,H	H,H	H,H	H,H	H,H
Gas Conduction (Including Gaps)		H,H		M,M	M,M		
Radiation Heat Transfer		H,H		H,H	H,H		
Graphite Oxidation				L,L	H,H		
Bulk CO Reaction				L,L	H,H		
Molecular Diffusion				M,M			
Fluid Properties	H,H	H,H	H,H	H,H	H,H	H,H	H,H
Core Configuration	H,H	H,H					
Pressure Waves							

Outlet Plenum & Components

Phenomena	HPCC		LPCC			LC	
	1	2	1	2	3	1	2
Flow Distribution	L,L	L,L	L,L	L,L	L,L	H,H	H,H
Heat Transfer (Forced Convection)	L,L		L,L			H,H	H,H
Heat Transfer (Mixed and Free Convection)		L,L		L,L	L,L		
Pressure Drop (Forced Convection)	L,L		L,L			L,L	L,L
Pressure Drop (Mixed and Free Convection)		L,L		L,L	L,L		
Thermal Mixing and Stratification		L,L		L,L	L,L		
Jet Discharge						H,H	H,H
Thermal Striping						H,H	H,H
Bulk CO Reaction				L,L	L,L		
Molecular Diffusion				H,H			
Fluid Properties	L,L	L,L	L,L	L,L	L,L	L,L	L,L
Pressure Waves							

Hot/Cold Pipe

Phenomena	HPCC		LPCC			LC	
	1	2	1	2	3	1	2
Heat Transfer (Forced Convection)	L,L		L,L			L,L	L,L
Heat Transfer (Mixed and Free Convection)					L,L		
Pressure Drop (Forced Convection)	L,L		L,L			L,L	L,L
Pressure Drop (Mixed and Free Convection)					L,L		
Pipe/Insulator Conduction							L,L
Critical Flow			L,L				
Pressure Waves							

RCCS (Reactor Cavity Cooling System) Reactor Cavity

Phenomena	HPCC		LPCC			LC	
	1	2	1	2	3	1	2
Flow Distribution		L,L		L,L	L,L		
Heat Transfer (Mixed and Free Convection)		L,L		L,L	L,L		
Pressure Drop (Mixed and Free Convection)		L,L		L,L	L,L		
Radiation Heat Transfer		H,H		H,H	H,H		
Gas Conduction		L,L		L,L	L,L		
Conduction to Ground		L,L		L,L	L,L		
Dust from Core			M,H				
Air Purge and Gas Species Distribution			L,L	L,L	L,L		
Confinement Valve and Filter Characteristics							
Pressure Waves							

RCCS Tube (Air Duct)

Phenomena	HPCC		LPCC			LC	
	1	2	1	2	3	1	2
Heat Transfer (Forced Convection)		H,H		H,H	H,H		
Heat Transfer (Mixed and Free Convection)		H,H		H,H	H,H		
Pressure Drop (Forced Convection)		H,H		H,H	H,H		
Pressure Drop (Mixed and Free Convection)		H,H		H,H	H,H		
Radiation Heat Transfer		H,H		H,H	H,H		
Pressure Waves							

RCCS Piping and Chimney

Phenomena	HPCC		LPCC			LC	
	1	2	1	2	3	1	2
Heat Transfer (Mixed and Free Convection)		L,L		L,L	L,L		
Pressure Drop (Mixed and Free Convection)		H,H		H,H	H,H		
Flow Mixing in Piping Plenums		M,M		M,M	M,M		
Buoyancy Flow in Chimney		H,H		H,H	H,H		
Pressure Waves							

PCU (Power Conversion Unit)

Phenomena	HPCC		LPCC			LC	
	1	2	1	2	3	1	2
Turbine Performance						L,L	L,L
Turbine Valve Performance						L,L	
Heat Conduction in Thick-Walled Structure							L,L
Heat Transfer in Coolers						L,L	L,L
Pressure Drop in Coolers						L,L	L,L
Heat Transfer in Recuperator						L,L	L,L
Pressure Drop in Recuperator						L,L	L,L
Compressor Performance						L,L	L,L
Pressure Waves							

A.4 Investigator Kappa

Inlet Plenum*

Phenomena	HPCC		LPCC			LC	
	1	2	1	2	3	1	2
Flow Distribution	H,L		H,L			L,L	L,L
Heat Transfer (Forced Convection)	L,L		L,L			L,L	L,L
Heat Transfer (Mixed and Free Convection)					L,L		
Pressure Drop (Forced Convection)	L,L		L,L			L,L	L,L
Pressure Drop (Mixed and Free Convection)					L,L		
Thermal Mixing and Stratification		M,M		H,H	H,H		
Bulk CO Reaction				L,L	L,L		
Molecular Diffusion				H,H[a]			
Pressure Waves							

* first entry is Prismatic Modular Reactor, second entry is Pebble Bed Reactor

[a] what happens in this phase with respect to molecular diffusion strongly impacts next phase

Riser

Phenomena	HPCC		LPCC			LC	
	1	2	1	2	3	1	2
Flow Distribution	L,L		L,L	L,L		L,L	L,L
Heat Transfer (Forced Convection)	L,L		L,L			L,L	L,L
Heat Transfer (Mixed and Free Convection)					L,L		
Pressure Drop (Forced Convection)	H,M		L,L			H,M	H,M
Pressure Drop (Mixed and Free Convection)							
Radiation Heat Transfer		H,H		H,H	H,H		
Gas Conduction		M,M		M,M	M,M		
Bulk CO Reaction				L,L	L,L		
Molecular Diffusion				H,H			
Pressure Waves							

Top Plenum & Components

Phenomena	HPCC		LPCC			LC	
	1	2	1	2	3	1	2
Flow Distribution	M,M	M,M	M,M	L,L	M,M	M,M	M,M
Heat Transfer (Forced Convection)	L,L		L,L			L,L	L,L
Heat Transfer (Mixed and Free Convection)		L,L		L,L	L,L		
Pressure Drop (Forced Convection)	L,L		L,L			L,L	L,L
Pressure Drop (Mixed and Free Convection)		L,L			L,L		
Thermal Mixing and Stratification		H,M		L,L	H,H		
Hot Plumes		H,H		L,L	H,H		
Fluid Properties	L,L	L,L	L,L	L,L	L,L	L,L	L,L
Thermal Resistance/Heat Capacity of Shroud		H,H		L,L	M,M		
Bulk CO Reaction				L,L	L,L		
Molecular Diffusion				H,H			
Pressure Waves							

Core and Reflector (including Bypass)

Phenomena	HPCC		LPCC			LC	
	1	2	1	2	3	1	2
Flow Distribution	H,H	H,H	M,M	L,L	H,H	H,H	H,H
Heat Transfer (Forced Convection)	H,H	H,H	M,M			M,M	M,M
Heat Transfer (Mixed and Free Convection)		H,H		L,L	M,M		
Pressure Drop (Forced Convection)	H,H	H,H	H,H			M,M	M,M
Pressure Drop (Mixed and Free Convection)		M,M		L,L	M,M		
Decay Heat (including Power Distribution)	H,H	H,H	L,L	H,H	L,L		
Reactivity Feedback						L,L	L,L
Fuel/Reflector Conductivity	L,L	L,L	L,L	H,H	L,L	L,L	L,L
Fuel/Reflector Specific Heat	M,M	H,H	L,L	H,H	M,M	L,L	L,L
Multi-D Heat Conduction Including Contact	L,L	L,L	L,L	H,M	M,M	L,L	L,L
Gas Conduction (Including Gaps)		L,L		H,H	M,M		
Radiation Heat Transfer		L,L		H,H	L,L		
Graphite Oxidation				M,H	M,H		
Bulk CO Reaction				M,H	M,H		
Molecular Diffusion				H,H			
Fluid Properties	H,H	H,H	L,L	L,L	H,H	L,L	L,L
Core Configuration	H,M	H,M	H,M	L,L	H,M	L,L	L,L
Pressure Waves							

Outlet Plenum & Components

Phenomena	HPCC		LPCC			LC	
	1	2	1	2	3	1	2
Flow Distribution	M,M	M,M	M,M	M,M	M,M	H,H	H,H
Heat Transfer (Forced Convection)	M,M		M,M			H,H	H,H
Heat Transfer (Mixed and Free Convection)		M,M		M,M			
Pressure Drop (Forced Convection)	L,L		L,L			L,L	L,L
Pressure Drop (Mixed and Free Convection)		H,H		L,L	M,M		
Thermal Mixing and Stratification		H,M		H,M	H,M		
Jet Discharge						H,M	H,M
Thermal Striping						H,M	H,M
Bulk CO Reaction				L,L	L,L		
Molecular Diffusion				H,H			
Fluid Properties	L,L	L,L	L,L	L,L	L,L	L,L	L,L
Pressure Waves							

Hot/Cold Pipe

Phenomena	HPCC		LPCC			LC	
	1	2	1	2	3	1	2
Heat Transfer (Forced Convection)	L,L		L,L			M,M	M.M
Heat Transfer (Mixed and Free Convection)					L,L	M,M	M.M
Pressure Drop (Forced Convection)	L,L		L,L				
Pressure Drop (Mixed and Free Convection)					L,L		
Pipe/Insulator Conduction							M,M
Critical Flow		L,L					
Pressure Waves							

RCCS (Reactor Cavity Cooling System) Reactor Cavity

Phenomena	HPCC		LPCC			LC	
	1	2	1	2	3	1	2
Flow Distribution		L,L		L,L	L,L		
Heat Transfer (Mixed and Free Convection)		L,L		L,L	L,L		
Pressure Drop (Mixed and Free Convection)		L,L		L,L	L,L		
Radiation Heat Transfer		H,H		H,H	H,H		
Gas Conduction		L,L		L,L	L,L		
Conduction to Ground		L,L		L,L	L,L		
Dust from Core			M,H				
Air Purge and Gas Species Distribution			L,L	L,M	L,M		
Confinement Valve and Filter Characteristics							
Pressure Waves							

RCCS Tube (Air Duct)

Phenomena	HPCC		LPCC			LC	
	1	2	1	2	3	1	2
Heat Transfer (Forced Convection)		H,H		H,H	H,H		
Heat Transfer (Mixed and Free Convection)		H,H		H,H	H,H		
Pressure Drop (Forced Convection)		H,H		H,H	H,H		
Pressure Drop (Mixed and Free Convection)		H,H		H,H	H,H		
Radiation Heat Transfer		H,H		H,H	H,H		
Pressure Waves							

RCCS Piping and Chimney

Phenomena	HPCC		LPCC			LC	
	1	2	1	2	3	1	2
Heat Transfer (Mixed and Free Convection)		L,L		L,L	L,L		
Pressure Drop (Mixed and Free Convection)		H,H		H,H	H,H		
Flow Mixing in Piping Plenums		L,L		L,L	L,L		
Buoyancy Flow in Chimney		H,H		H,H	H,H		
Pressure Waves							

PCU (Power Conversion Unit)

Phenomena	HPCC		LPCC			LC	
	1	2	1	2	3	1	2
Turbine Performance						M,M	M,M
Turbine Valve Performance						M,M	
Heat Conduction in Thick-Walled Structure							H,H
Heat Transfer in Coolers						M,M	M,M
Pressure Drop in Coolers						M,M	M,M
Heat Transfer in Recuperator						M,M	M,M
Pressure Drop in Recuperator						M,M	M,M
Compressor Performance						M,M	M,M
Pressure Waves							

APPENDIX B Combined INL/ANL/KAERI PIRTs

Inlet Plenum PIRT

Phenomena	HPCC		LPCC			LC	
	1	2	1	2	3	1	2
flow distribution	H		H			H	H
heat transfer (forced convection)	M		M				
heat transfer (mixed and free convection)					M		
pressure drop (forced convection)	M		M			H	H
pressure drop (mixed and free convection)					M		
bulk CO reaction				M			
molecular diffusion				M			
thermal mixing and stratification				M			
graphite oxidation (PBR)				M			
Fluid properties (gas mixture)				M			

Riser PIRT

Phenomena	HPCC		LPCC			LC	
	1	2	1	2	3	1	2
flow distribution	H	M	M				
heat transfer (forced convection)	M		M				
heat transfer (mixed and free convection)		M			M		
pressure drop (forced convection)	H		H			H	H
pressure drop (mixed and free convection)		M			M		
radiation heat transfer		H		H	H		
gas conduction		M		M	M		
bulk CO reaction				M	o		
molecular diffusion				M			
graphite oxidation (PBR)				M			
Fluid properties (gas mixture)							

Top Plenum and Components PIRT

Phenomena	HPCC		LPCC			LC	
	1	2	1	2	3	1	2
flow distribution	H	M	M		M	H	H
heat transfer (forced convection)	M		M				
heat transfer (mixed and free convection)		M		M	M		
pressure drop (forced convection)	M		M			H	H
pressure drop (mixed and free convection)		M			M		
thermal mixing and stratification		H/M		M	H		
hot plumes		H			H		
Fluid properties (G.M)			M	M			
thermal resistance/heat capacity of shroud		H			H		
bulk CO reaction				M			
molecular diffusion				M			
Graphite oxidation (PBR)							

Core and Reflector PIRT

Phenomena	HPCC		LPCC			LC	
	1	2	1	2	3	1	2
flow distribution	H	H	H	*	H	H	H
heat transfer (forced convection)	H		H			H	H
heat transfer (mixed and free convection)		H		M	H		
pressure drop (forced convection)	M		H			H	H
pressure drop (mixed and free convection)		H		M	H		
Initial stored energy	H		H				
power distribution	H	H	H	H	H	H	H
decay heat(including power distribution)	H	H	H	H	H		
reactivity feedback						H	M
fuel/reflector conductivity	M	H	H	H	H	M	M
fuel/reflector specific heat	M	H	H	H	H	M	M
multi-D heat conduction including contact	H	H	H	H	H	M	M
gas conduction (including gaps)		M		M	M		
radiation heat transfer		H		H	H		
graphite oxidation				M	H		
bulk CO reaction				M	H		
molecular diffusion				M			
fluid properties (gas mixture)				H	H		
Core material distribution (configuration)	H	H	H	H	H		

* Flow distribution in LPCC-II can be replaced with fluid properties (gas mixture)

Outlet Plenum and Components

Phenomena	HPCC		LPCC			LC	
	1	2	1	2	3	1	2
flow distribution	H	H	M		H	H	H
heat transfer (forced convection)	M		M			H	H
heat transfer (mixed and free convection)		M		M	M		
pressure drop (forced convection)	M		H			H	H
pressure drop (mixed and free convection)		M		M	M		
thermal mixing and stratification		H		H	H		
jet discharge						H	H
thermal striping						H	H
bulk CO reaction				M	M		
molecular diffusion				H			
Fluid properties (gas mixture)				H	H		
Graphite oxidation (PBR)				H	H		

Hot/Cold Pipe PIRT

Phenomena	HPCC		LPCC			LC	
	1	2	1	2	3	1	2
heat transfer (forced convection)	M		M			H	H
heat transfer (mixed and free convection)					M		
pressure drop (forced convection)	M		H				
pressure drop (mixed and free convection)					M		
Pipe/insulator conduction							M
critical flow			H				
bulk CO reaction							
fluid properties / gas mixture				H	H		

Reactor Cavity PIRT

Phenomena	HPCC		LPCC			LC	
	1	2	1	2	3	1	2
flow distribution		H		H	H		
heat transfer (mixed and free convection)		H		H	H		
pressure drop (mixed and free convection)		M		M	M		
radiation heat transfer		H		H	H		
gas conduction		M		M	M		
conduction to ground		M		M	M		
dust from core			H				
air purge and gas species distribution			H	H	H		
Fluid properties (gas mixture)			H	H	H		

RCCS Air Duct PIRT

Phenomena	HPCC		LPCC			LC	
	1	2	1	2	3	1	2
heat transfer (forced convection)		H		H	H		
heat transfer (mixed and free convection)		H		H	H		
pressure drop (forced convection)		H		H	H		
pressure drop (mixed and free convection)		H		H	H		
Radiation heat transfer		H		H	H		
Fluid properties (humidity)		M		M	M		

RCCS Piping and Chimney PIRT

Phenomena	HPCC		LPCC			LC	
	1	2	1	2	3	1	2
heat transfer (mixed and free convection)		M		M	M		
pressure drop (mixed and free convection)		H		H	H		
Flow mixing in piping plenums		M		M	M		
Buoyancy flow in chimney		H		H	H		
Fluid properties (humidity)		M		M	M		

Power Conversion Unit PIRT

Phenomena	HPCC		LPCC			LC	
	1	2	1	2	3	1	2
turbine performance	H					H	H
turbine valve performance	H					H	H
recuperator performance	*					H	H
coolers performance						H	H
Compressor performance	H					H	H

APPENDIX C Bibliography by Subject

Analysis and Experimental Needs of Generation IV Reactors

1. T. A. Taiwo and H. S. Khalil, *Assessment of Analysis Capabilities for Generation IV System Design*, Nuclear Engineering Division, Argonne National Laboratory, September 23, 2003.

2. Minutes of Workshop on Thermal-Hydraulic and Safety Analysis Tools for Generation IV Nuclear Energy Systems, Idaho National Engineering and Environmental Laboratory, Idaho Falls, Idaho, March 18-19, 2003.

3. L. J. Siefken, E. A. Harvego, E. W. Coryell, and C. B. Davis, "Transient Analysis Needs for Generation IV Reactor Concepts," Proceedings of 10th International Conference on Nuclear Energy, Arlington, VA, April 14-18, 2002, ICONE10-22641, pp. 1-18.

4. Donald M. McEligot, et al., "Thermalhydraulics Studies for Improved Safety and Efficiency of Gas-Cooled Fast-Breeder Reactors (GFRs) and Advanced HTGRs," Nuclear Energy Research Initiative Proposal Program Announcement LAB-NE-2002-1, submitted April 17, 2002.

5. Email from Khalil to Taiwo, January 7, 2004, with INEEL work package on NGNP "design and evaluation methods" mentioned and scope of work to be done briefly described.

6. Finis H. Southworth, "Very High Temperature Gas Cooled Reactor System (VHTR, Thermal-Hydraulic Analyses and Assessment Needs," slide presentation, Thermal-Hydraulic and Safety Analysis Tools for Generation IV Nuclear Energy Systems, Idaho National Engineering and Environmental Laboratory, Idaho Falls, Idaho, March 18-19, 2003.

7. Richard R. Schultz, Walter L. Weaver, Abderrafi M. Ougouag, and William A. Wieselquist, "Validating & Verifying a New Thermal-Hydraulic Analysis Tool," Proceedings of 10th International Conference on Nuclear Energy, Arlington, VA, April 14-18, 2002, ICONE10-22446, pp. 1-8.

8. Donald M. McEligot, et al., "Fundamental Thermal Fluid Physics of High Temperature Flows in Advanced Reactor Systems," INEEL/EXT-2002-1613, Nuclear Energy Research Initiative, Final Report, Project No. 99-254, Reporting Period: (September 1999-October 2002), December 31, 2002.

VHTR and GT-MHR

9. Paul D. Bayless, "VHTR Thermal-Hydraulic Scoping Analysis Using RELAP55-3D/ATHENA," Global 2003, New Orleans, LA, November 16-20, 2003.

10. Philip E. MacDonald et al., *NGNP Point Design—Results of the Initial Neutronics and Thermal-Hydraulic Assessments During FY-03*, INEEL/EXT-03-00870 Rev. 1, Idaho National Engineering and Environmental Laboratory, Idaho Falls, Idaho, September 2003.

11. Finis Southworth, Franck Carre, and Philip Hildebrandt, "Generation IV Gas Cooled Reactor Concepts," *Transactions of the American Nuclear Socie*ty, Vol. 85, November 11-15, 2001, Reno, Nevada, pp. 66-67.

12. *Gas Turbine-Modular Helium Reactor (GT-MHR) Conceptual Design Description Report*, 910720, Revision 1, GA Project No. 7658, General Atomics, July 1996.

13. M. P. La Bar and W. A. Simon, "International Cooperation in Developing the GT-MHR," Technical Committee Meeting on High Temperature Gas Cooled Reactor Technology Development, IAEA-TECDOC—988, Johannesburg, South Africa, November 13-15, 1996.

14. J. H. Gittus, "The ESKOM Pebble Bed Modular Reactor," *Nuclear Energy*, Vol. 38, No. 4, August 1999, pp. 215-221.

HTGR and MHTGR

15. *Proceedings of the Third Japan—U.S. Seminar on HTGR Safety Technology,* NUREG/CP-0045, BNL-NUREG-51674, Vol. 1, Brookhaven National Laboratory, June 2-3, 1982. (See in particular, S. Mitake, et al., "Study of the Experimental VHTR Safety with Analysis for a Hypothetical Rapid Depressurization Accident," pp. 117-129.)

16. P. M. Williams, T. L. King, and J. N. Wilson, *Draft Preparation Safety Evaluation Report for the Modular High-Temperature Gas-Cooled Reactor*, NUREG-1338, March 1989.

17. DOE, *Evaluation of the Gas Turbine Modular Helium Reactor*, DOE-GT-MHR-100002, February 1994.

Specific Codes

18. Syd Ball, "The ORNL 'GRSAC' Code for Gas Reactor Simulation – Thermal Hydraulics, and Severe Accidents," slide presentation, Gen-4 T/H Workshop – INEEL, March 18-19, 2003, Idaho Falls, Idaho.

19. Richard R. Schultz, Richard A. Riemke, Cliff B. Davis, and Greg Nurnberg, "Comparison: RELAP55-3D© Systems Analysis Code & Fluent CFD Code Momentum Equation Formulations," Proceedings of 11th International Conference on Nuclear Energy, Tokyo, Japan, April 20-23, 2003, ICONE11-36585., pp. 1-9.

20. Richard R. Schultz and Walter L. Weaver, "Using the RELAP55-3D© Advanced Systems Analysis Code with Commercial and Advanced CFD Software," Proceedings of 11th International Conference on Nuclear Energy, Tokyo, Japan, April 20-23, 2003, ICONE11-36545, pp. 1-7.

21. Gary Johnsen and Cliff Davis, "RELAP55-3D/ATHENA Capabilities for Analyzing Generation IV Reactors," slide presentation, Thermal-Hydraulic and Safety Analysis Tools for Generation IV Nuclear Energy Systems, Idaho National Engineering and Environmental Laboratory, Idaho Falls, Idaho, March 18-19, 2003.

22. K. Fischer, H. Holzbauer, and L. Wolf, "Battelle-Europe Verifications and Extensions of the Gothic Code," *Proceedings of the Fifth International Topical Meeting of Reactor Thermal Hydraulics*, NURETH-5, sponsored by the Thermal Hydraulics Division of and Idaho Section of the American Nuclear Society, September 21-24, 1992, Little America Hotel, Salt Lake City, UT, USA.

Reactor Cavity Cooling System

23. *450 MWt Reactor Cavity Cooling System System Design Description*, DOE-HTGR-90016, Revision 0, Bechtel National, Inc., November 1993.

24. J. C. Conklin, *Modeling and Performance of the MHTGR Reactor Cavity Cooling System*, NUREG/CR-5514, ORNL/TM-11451, R1, R7, R8, April 1990.

25. A. Woaye-Hune and S. Ehster, "Calculation of Decay Heat Removal Transient by Passive Means for a Direct Cycle Modular HTR," *Proceedings of the Conference on High Temperature Reactors*, Petten, NL, April 22-24, 2002.

Experiments in HDR Facility (Hydrogen Distribution in LWR)

26. Luis A. Valencia, "Hydrogen Distribution Test Under Severe Accident Conditions at the Large-Scale HDR-Facility," *Nuclear Engineering and Design*, Vol. 140, (1993), pp. 51-60.

27. P. N. Smith and P. Ellicott, "A UK Analysis of Light Gas Distribution Experiment E11.2 in the HDR Facility," *Nuclear Engineering and Design*, Vol. 140, (1993), pp. 61-68.

28. I. M. Coe and D. B. Utton, "The Use of the COMPACT Code for Calculation of Long Term Environmental Effects as a Result of High Temperature Discharges into Confined Areas," *Nuclear Engineering and Design*, Vol. 140, (1993), pp. 69-78.

Scaling of Large Stratified Volumes

29. P. F. Peterson, "Scaling and Analysis of Mixing in Large Stratified Volumes," Int. J. Heat Mass Transfer, Vol. 37, 1994, Suppl. 1, pp. 97-106.

30. P. F. Peterson, V. E. Schrock, R. Greif, "Scaling for Integral Simulation of Mixing in Large, Stratified Volumes," *Nuclear Engineering and Design*, Vol. 186, 1998, pp. 213-224.

31. ANL Intra-Laboratory Memo, W. A. Bezalla to T. Y. C. Wei, "Scaling Considerations of BMC Experiments," November 1, 1995.

32. ANL Intra-Laboratory Memo, Y. W. Shin to T. Y. C. Wei, "Scaling and Similitude Studies of HDR Tests and SBWR Reference Accidents," November 2, 1995.

Code Scaling, Applicability, and Uncertainty Methodology

33. B. Boyack, et al., *Quantifying Reactor Safety Margins, Application of Code Scaling, Applicability, and Uncertainty Evaluation Methodology to Large-Break, Loss-of-Coolant Accident*, NUREG/CR-5249, Nuclear Regulatory Commission, December 1989.

34. B. E. Boyack, et al., "An Overview of Code Scaling, Applicability, and Uncertainty Methodology," Nuclear Engineering and Design 119 (1990), pp. 1-15.

35. G. E. Wilson, et al., "Characterization of Important Contributors to Uncertainty," Nuclear Engineering and Design 119 (1990), pp. 17-31.

36. W. Wulff, et al., "Assessment and Ranging of Parameters," Nuclear Engineering and Design 119 (1990), pp. 33-65.

37. G. S. Lellouche, et al., "Uncertainty Evaluation of LBLOCA Analysis Based on TRAC-PF1/MOD 1," Nuclear Engineering and Design 119 (1990), pp. 67-95.

38. N. Zuber, et al., "Evaluation of Scale-Up Capabilities of Best Estimate Codes," *Nuclear Engineering and Design* 119 (1990), pp. 97-107.

39. I. Catton, et al., "A Physically Based Method of Estimating PWR Large Break Loss of Coolant Accident PCT," *Nuclear Engineering and Design* 119 (1990), pp. 109-117.

40. F. F. Cadek, L. E. Hochreiter, and M. Y. Young, Best Estimate Approach for Effective Plant Operation and Improved Economy, Electric Power Research Institute Workshop on Appendix "K" Relief Using Best Estimate Methods: The Revised LOCA/ECCS Rule, Cambridge, Massachusetts (August 11-12, 1988).

41. Andrej Prosek and Borut Mavko, "Evaluting Code Uncertainty-I: Using The CSAU Method for Uncertainty Analysis of a Two-Loop PWR SBLOCA," *Nuclear Technology*, Vol. 126, May 1999.

42. *An Integrated Structure and Scaling Methodology for Severe Accident Technical Issue Resolution*, NUREG/CR-5809, EGG-2659, R4, November 1991.

Phenomena Identification and Ranking Table and Analytical Hierarchy Process

43. R. A. Shaw, et al., *Development of a Phenomena Identification and Ranking Table (PIRT) for Thermal-Hydraulic Phenomena During a PWR Large-Break LOCA*, NUREG/CR-5074, EGG-2527, R4, Idaho National Engineering Laboratory, November 1988.

44. T. Saaty, *Decision-making For Leaders*, Belmont California, Lifetime Learning Publications, Wadsworth Inc., 1982.

45. Thomas L. Saaty and Kevin P. Kearns, *Analytical Planning, The Organization of Systems*, Pergamon Press, New York, 1985.

46. Thomas L. Saaty, *The Analytical Hierarchy Process*, McGraw-Hill, New York, 1980.

Thermal Striping and Fluctuations Due to Mixing

47. E. E. Feldman, L. K. Chang, and M. J. Lee, "Thermal Striping of Rod—Thermoelastic Solutions for Sinusoidal Fluid Temperatures," ASME Pressure Vessel Conference, San Diego, California, June 23-27, 1991.

48. M. J. Lee, L. K. Chang, and E. E. Feldman, "Plastic Analysis of A Circular Rod Subjected to Sinusoidal Thermal Cycling," ASME Pressure Vessel Conference, San Diego, California, June 23-27, 1991.

49. A. Nordgren, "Thermal Fluctuations in Mixing Tees (Experiences, Measurements, Predictions and Fixes)," *Transactions of the 7th International Conference on Structural Mechanics in Reactor Technology*, 1983, Vol . D. , pp. 7-14.

Materials and Material Codes

50. Bill Corwin, "Materials for Gen IV Reactors," slides presentation, UNLV Workshop on High-Temperature Heat Exchangers, Las Vegas, April 17, 2003.

51. K. Natesan, A,. Purohit, and S. W. Tam, *Material Behavior in HTGR Environments*, NUREG/CR-6824, ANL-02/37, by ANL for US NRC, July 2003.

52. V. N. Shah, S. Majumdar, and K. Natesan, *Review and Assessment of Codes and Procedures for HTGR Components*, NUREG/CP-6816, ANL-02/36, by ANL for US NRC, June 2003.

Experimental Data from Gas Reactor and Component Mockups

53. Makoto Hishida, et al., "Heat Transfer Problems in a VHTR," *Heat Transfer in High Technology and Power Engineering*, Wen-Jei Yang and Yasuo Mori, editors, Hemisphere Publishing Corporation, New York, 1987, pp. 273-284.

54. IAEA-TECDOC—1382, *Evaluation of high temperature gas cooled reactor performance: Benchmark analysis related to initial testing of the HTTR and HTR-10*, Chapter 3, "High Temperature Engineering Test Reactor Thermal Hydraulic Benchmarks", 2000.

55. Y. Shiina and M. Hishida, "Heat Transfer in the Upper Part of the HTTR Pressure Vessel During Loss of Forced Cooling," Specialists Meeting on Decay Heat Removal and Heat Transfer Under Normal and Accident Conditions in Gas Cooled Reactors, IAEA-TECDOC—757, Juelich, Germany, July 6-8, 1992, pp. 125-130.

56. IAEA-TECDOC—1163, *Heat Transport and Afterheat Removal for Gas Cooled Reactors under Accident Conditions*.

57. Yoshiaki Miyamoto, et al., "Thermal and Hydraulic Test of Test Sections in the Helium Engineering Demonstration Loop," *Nuclear Engineering and Design*, Vol. 120, 1990, pp. 435-445.

Air Ingress

58. Motoo Fumizawa, et al., "Numerical Analysis of Buoyancy-Driven Exchange Flow with Regard to an HTTR Air Ingress Accident," *Nuclear Technology*, Vol. 110, May 1995, pp. 263-272.

59. M. Hishida, et al., "Research on Air Ingress Accidents of the HTTR," *Nuclear Engineering and Design*, Vol. 144, 1993, pp. 317-325.

Commercial CFD Codes in General

60. C. J. Freitas, "Perspective: Selected Benchmarks from Commercial CFD Codes," *Transactions of the ASME, Journal of Fluid Mechanics*, Vol. 117, June 1995, pp. 208-218.

Outlet Plenum

61. N. Tauveron, "Thermal Fluctuations in the Lower Plenum of an High Temperature Reactor," *Nuclear Engineering and Design*, Vol. 222, 2003, pp. 125-137.

62. G. Damm and R.Wehrlein, "Simulation Tests for Temperature Mixing in a Core Bottom Model of the HTR-Module," *Nuclear Engineering and Design*, Vol. 137, 1992, pp. 97-105.

63. Yoshiyuki Inagaki, Tomoaki Kunugi, and Yoshiaki Miyamoto, "Thermal Mixing Test of Coolant in the Core Bottom Structure of a High Temperature Engineering Test Reactor," *Nuclear Engineering and Design*, Vol. 123, 1990, pp. 77-86.

64. K. Kunitomi, "Thermal and Hydraulic Tests in HENDEL T_2 Supporting the Development of the Core Bottom Structure of the High Temperature Engineering Test Reactor (HTTR)," *Nuclear Engineering and Design*, Vol. 108, 1988, pp. 359-368.

65. M. S. Yao, Z. Y. Huang, C. W. Ma, and Y. H. Xu, "Simulating Test for Thermal Mixing in the Hot Gas Chamber of the HTR-10," *Nuclear Engineering and Design*, Vol. 218, 2002, pp. 233-240.

66. Yoshiyuki Inagaki, et al., "Thermal-Hydraulic Characteristics of Coolant in the Core Bottom Structure of the High-Temperature Engineering Test Reactor," *Nuclear Technology*, Vol. 99, July 1992, pp. 90-103.

67. N. Tauveron, M. Elmo, O. Cionti, T. Chataing, "Thermal Hydraulic Simulations of High Temperature Reactors", *Proceedings of the Conference on High Temperature Reactors*, Petten, NL, April 22-24, 2002.

Natural, Mixed, and Forced Convection

68. G. Fu, "Heat Transfer and Friction Factor Behavior in the Mixed Convection Regime for Air Up-Flow in a Heated Vertical Pipe," Heat Transfer—Minneapolis 1991, AIChe Symposium Series, Vol. 87, No. 283, American Institute of Chemical Engineers, New York, 1991, pp. 326-335.

69. G. Fu, N. E. Todreas, P. Hejzlar, and M. J. Driscoll, "Heat Transfer Correlation for Reactor Riser in Mixed Convection Air Flow," *Transactions of the ASME, Journal of Heat Transfer*, Vol. 116, May 1994, pp. 489-492.

70. Wesley Williams, Pavel Hejzlar, Michael Driscoll, Won Jae Lee, and Pradip Saha, *Analysis of a Convection Loop for GFR Post-LOCA Decay Heat Removal from a Block-Type Core*, MIT-ANP-TR-095, Program for Advanced Nuclear Power Studies, Nuclear Engineering Department, Massachusetts Institute of Technology, Cambridge, MA.

71. Sadik Kakaç, Ramesh K. Shak, and Win Aung, *Handbook of Single-Phase Convective Heat Transfer*, John Wiley and Sons, New York, 1987.

72. Simon Ostrach, "Natural Convection Heat Transfer in Cavities and Cells," *Heat Transfer 1982, Proceedings of the Seventh International Heat Transfer Conference*, München, Fed. Rep. of Germany, Ed. U. Grigull, et al., Hemisphere Publishing Corporation, New York, 1982, pp.365-379.

APPENDIX D Outlet Plenum Experiments

Similar to the database screening work reported in Section VIII some initial work was also performed on screening experiments for the outlet plenum mixing phenomena. This work is documented here. Table D.1 identifies the experiments while Table D.2 shows the range of conditions and important nondimensional parameters for these experiments. The references shown in Table D.1 are identified in the section References.

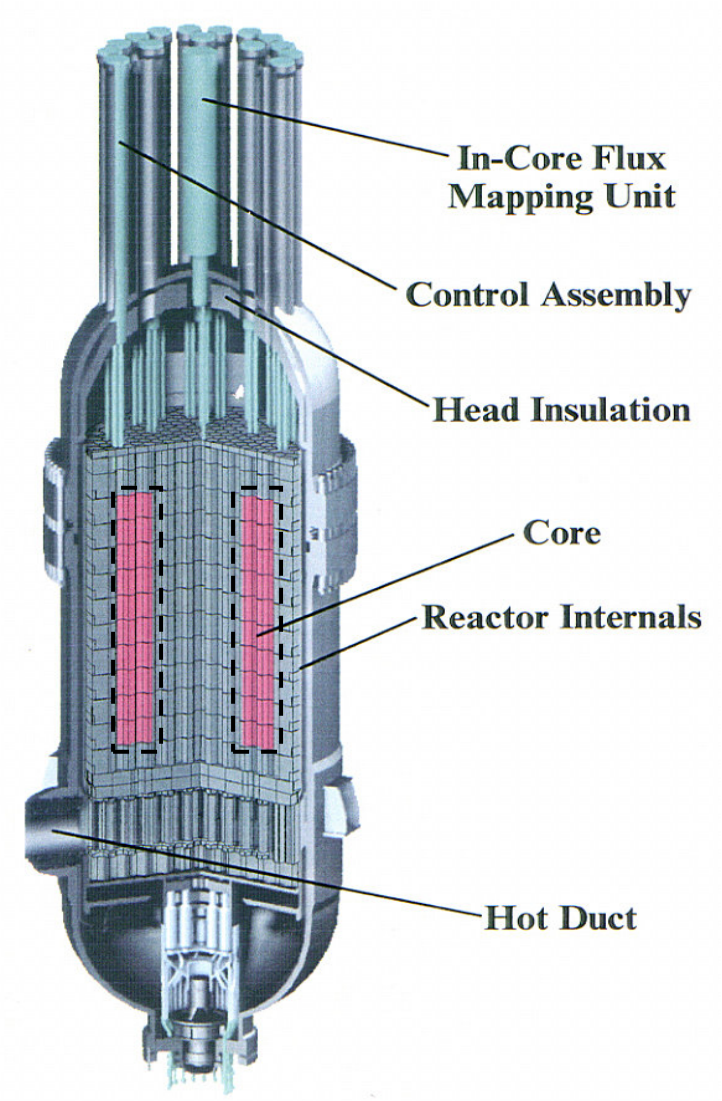

Figure 1. General Atomics
Design of VHTR Reactor

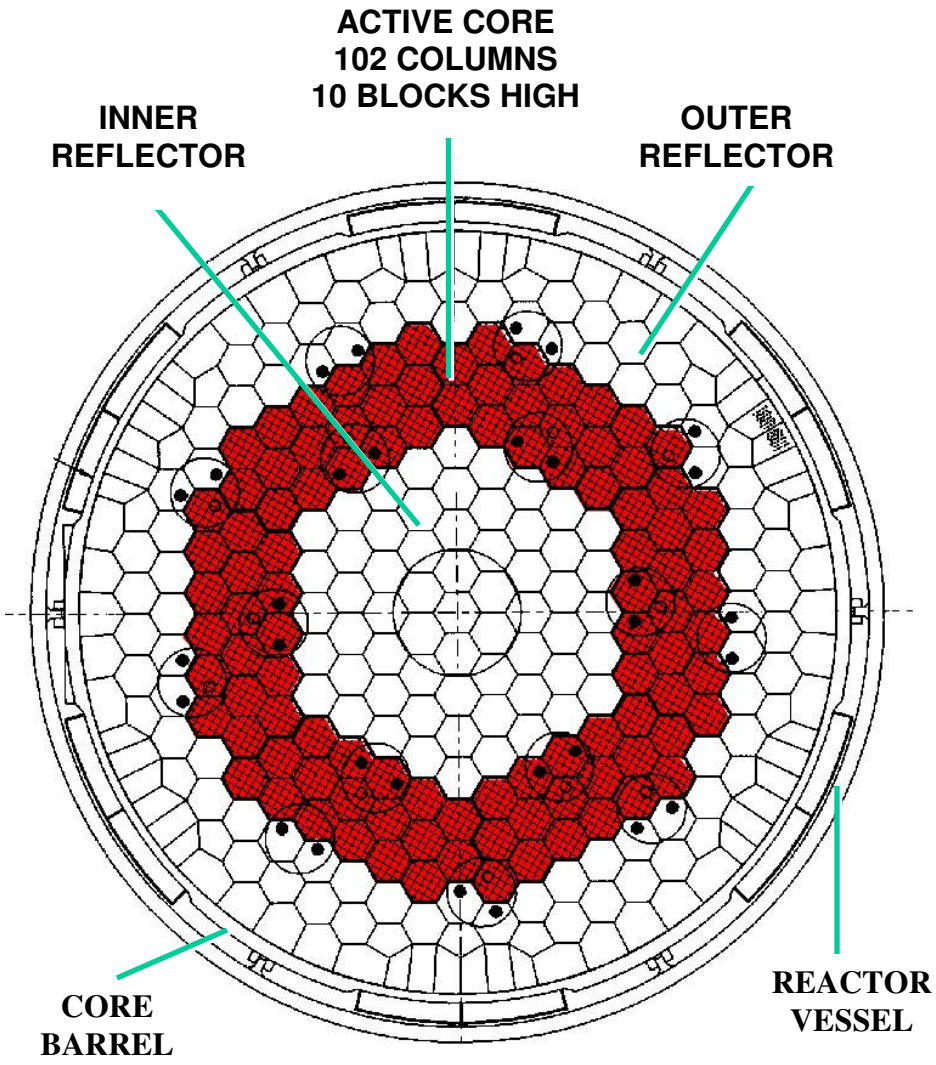

Figure 2. Top Cutaway View of Reactor Vessel

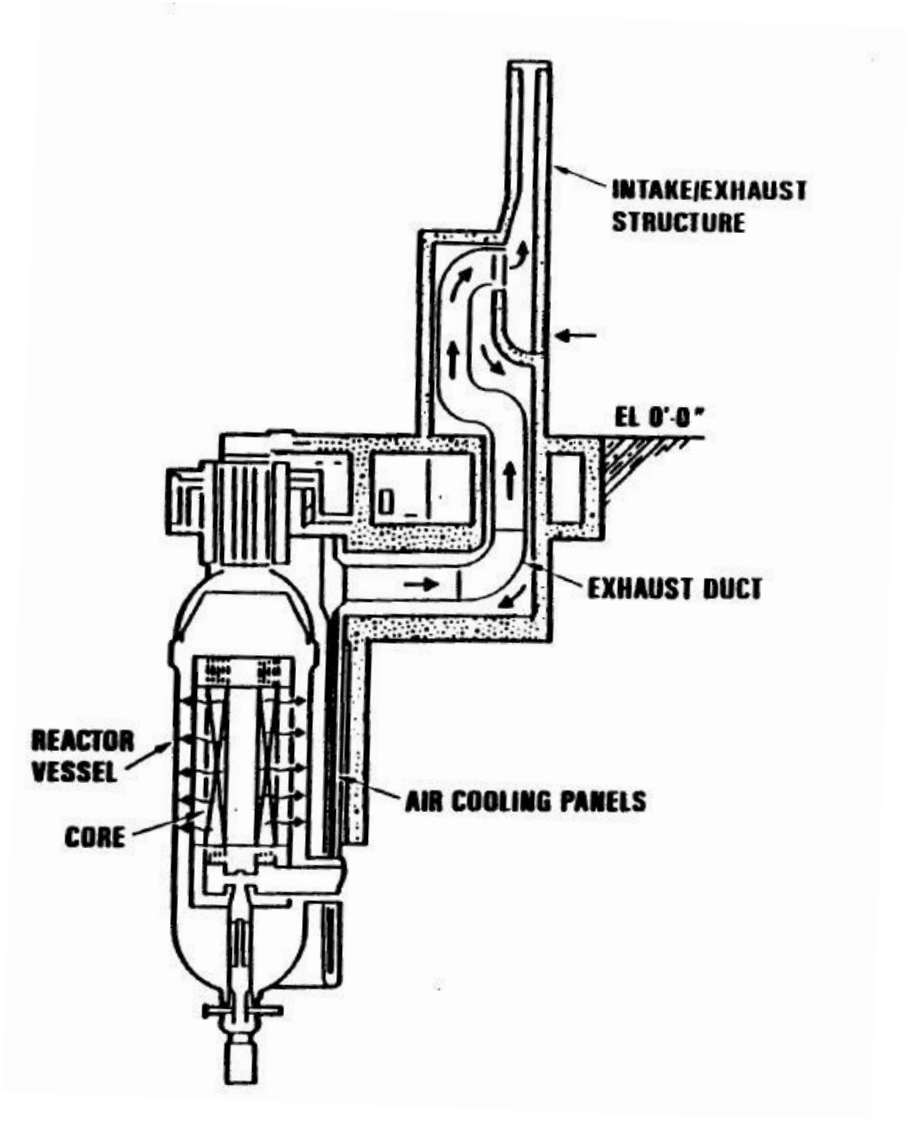

Figure 3. Reactor Cavity Cooling System (RCCS)

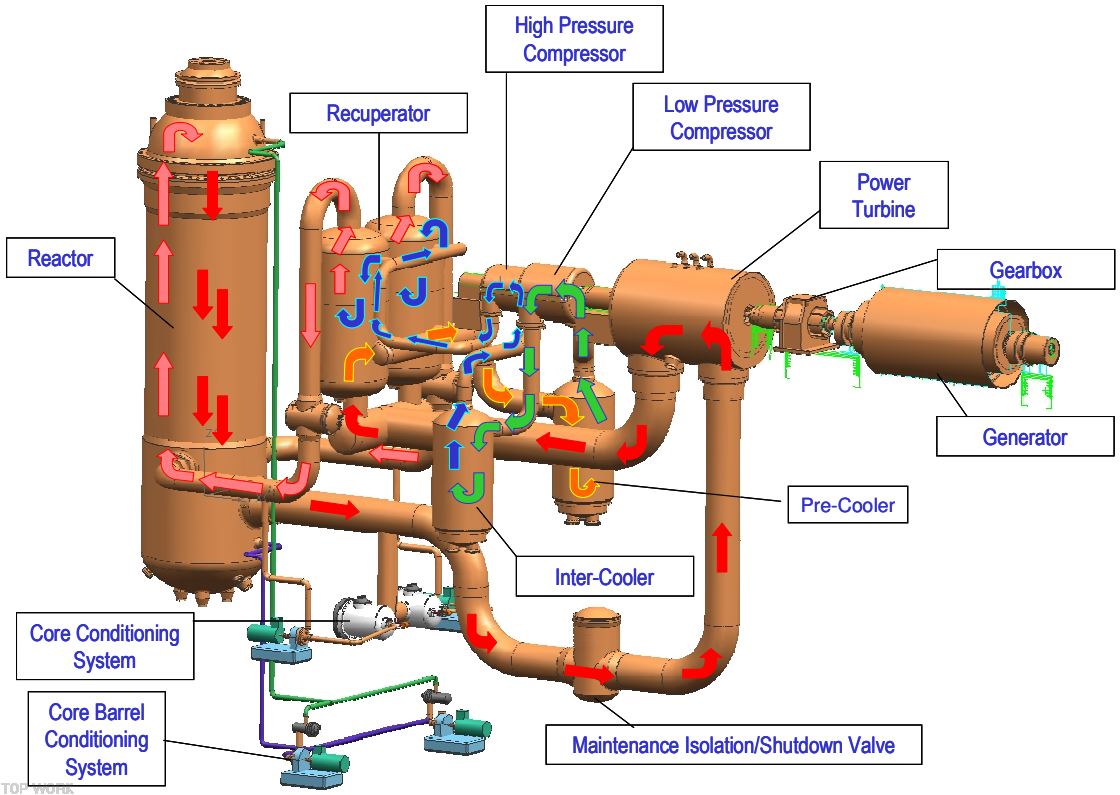

a) System Design Configuration and Helium Flow Path

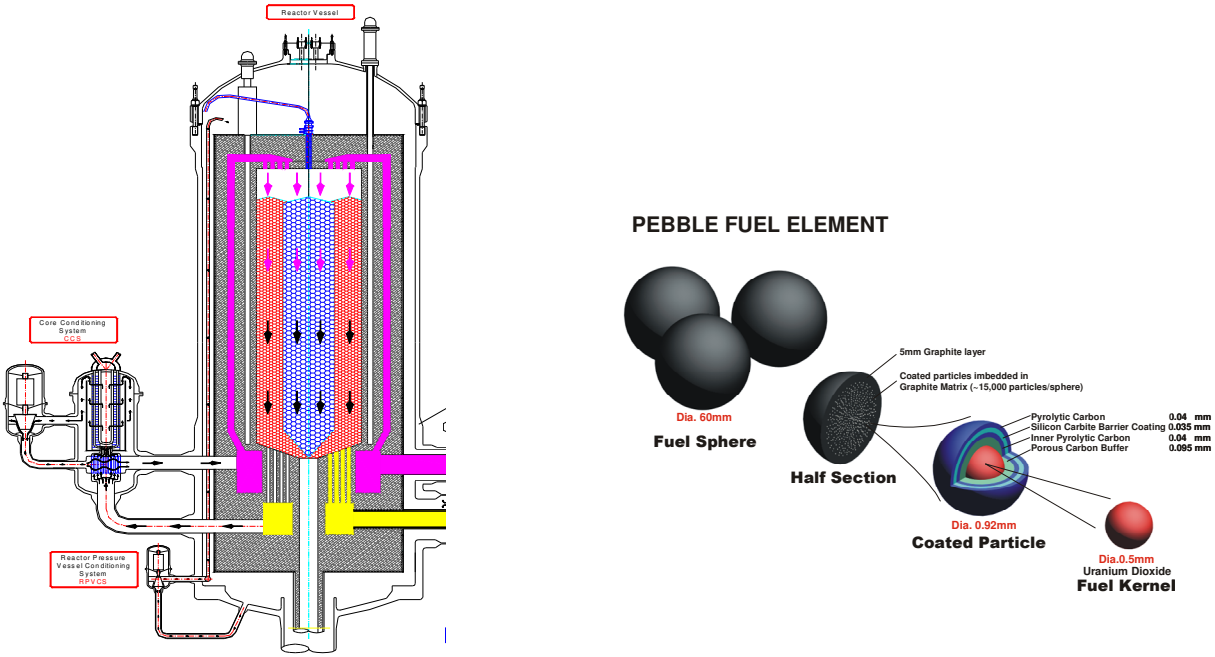

b) Pebble Core and Reactor Vessel Configuration

Figure 4. PBMR Design

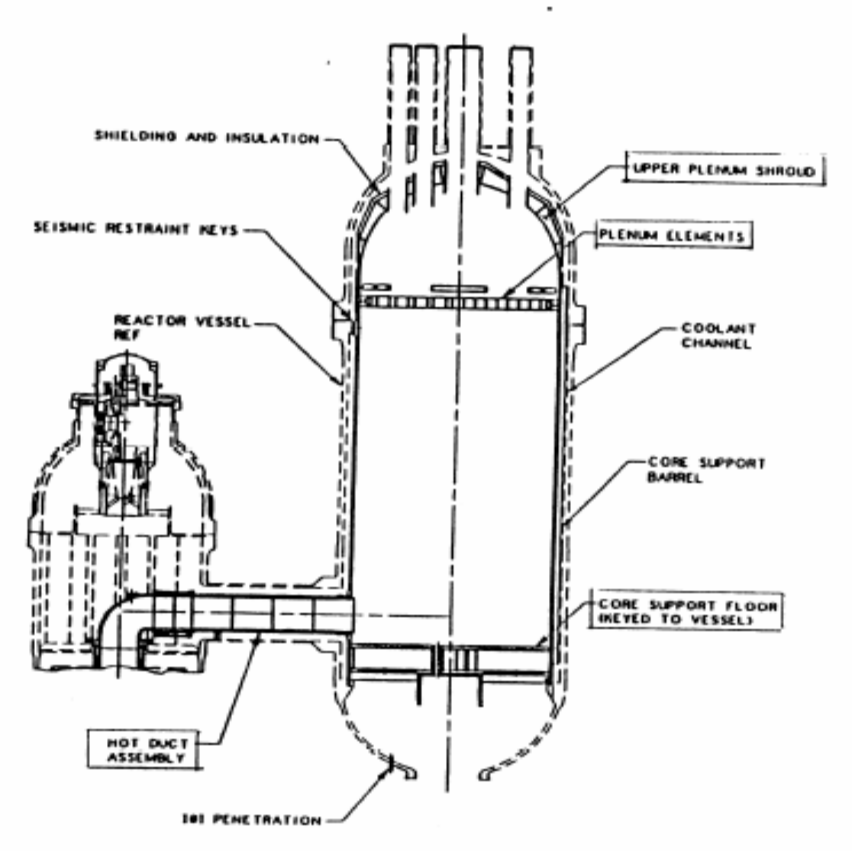

a) Vessel Metallic Structures

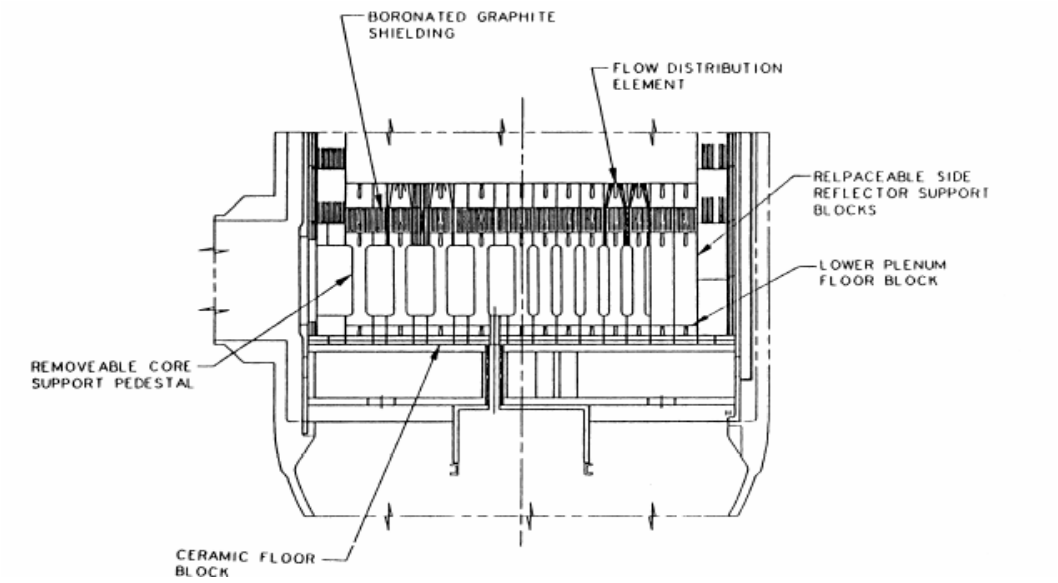

b) Vessel Outlet Plenum

Figure 5. Prismatic Reactor Vessel Internals

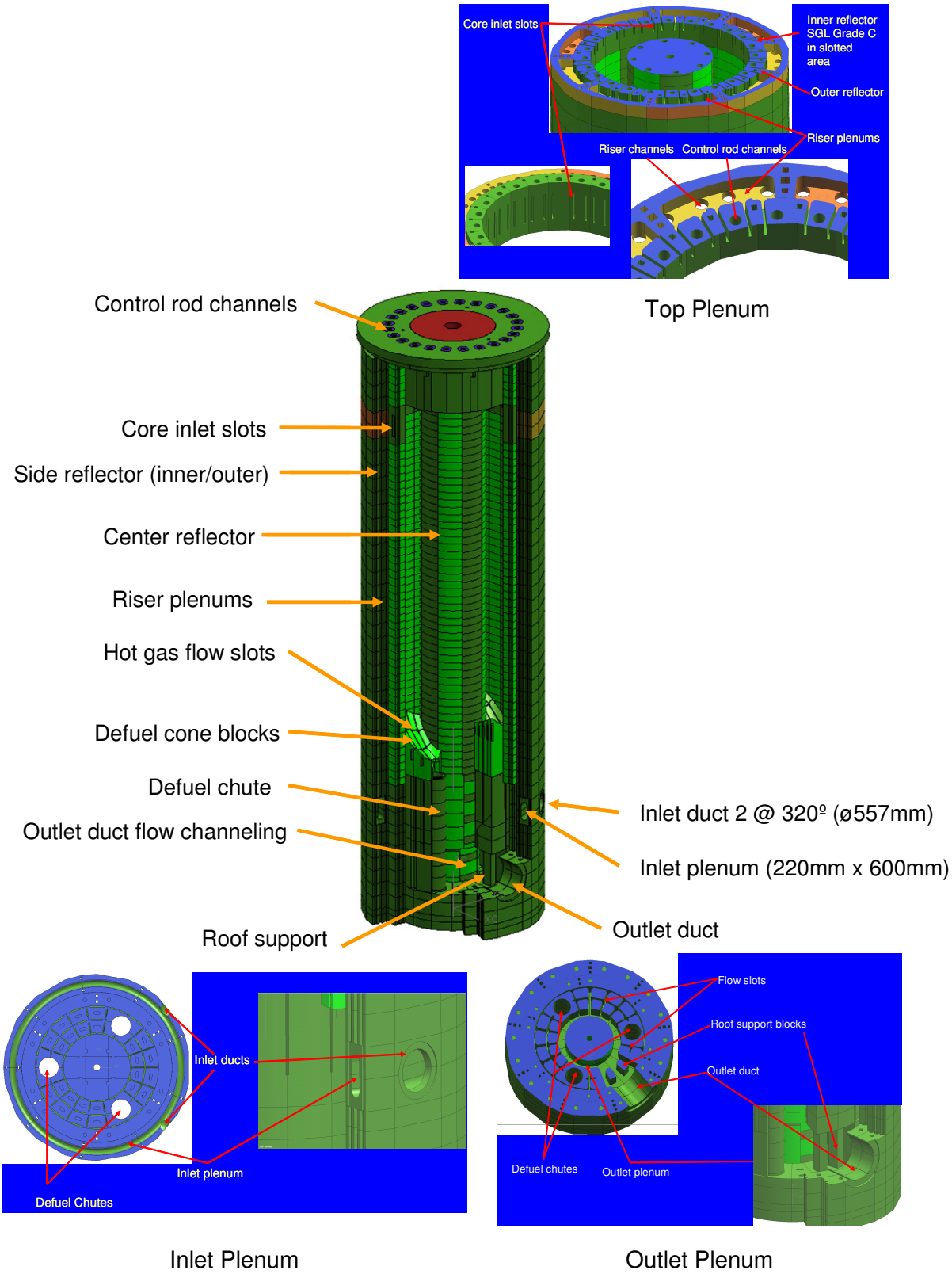

Figure 6. Pebble Reactor Vessel Internals

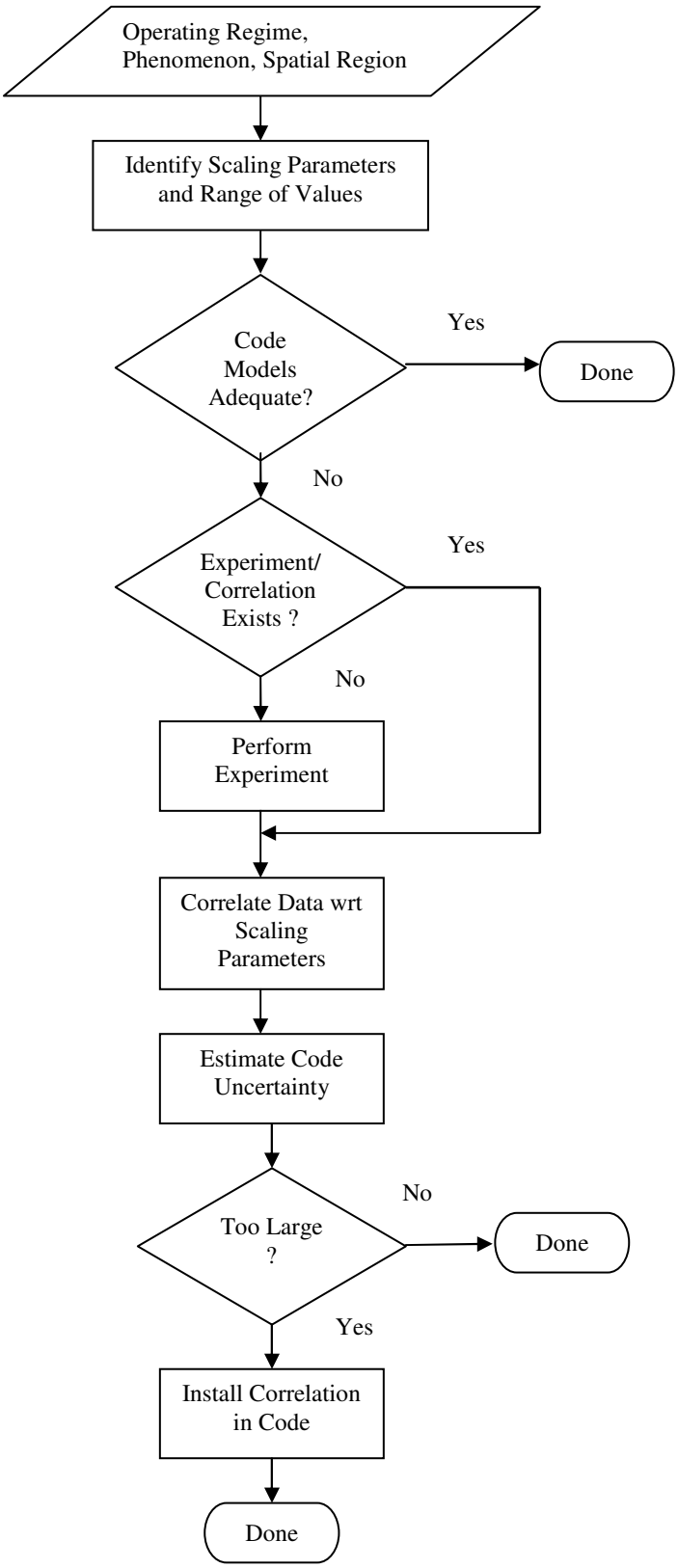

Figure 7. Code Evaluation/Improvement Process

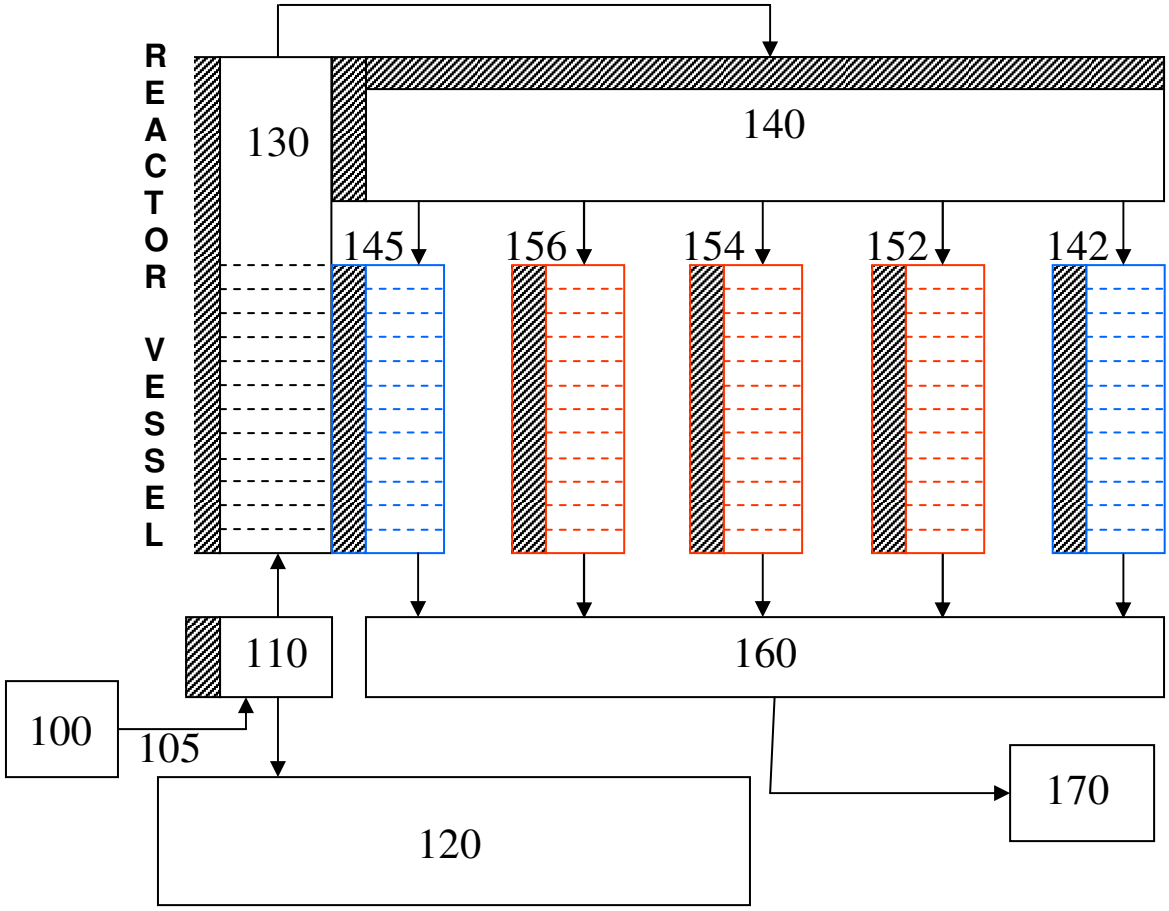

Figure 8. VHTR Vessel Hydraulic Nodalization

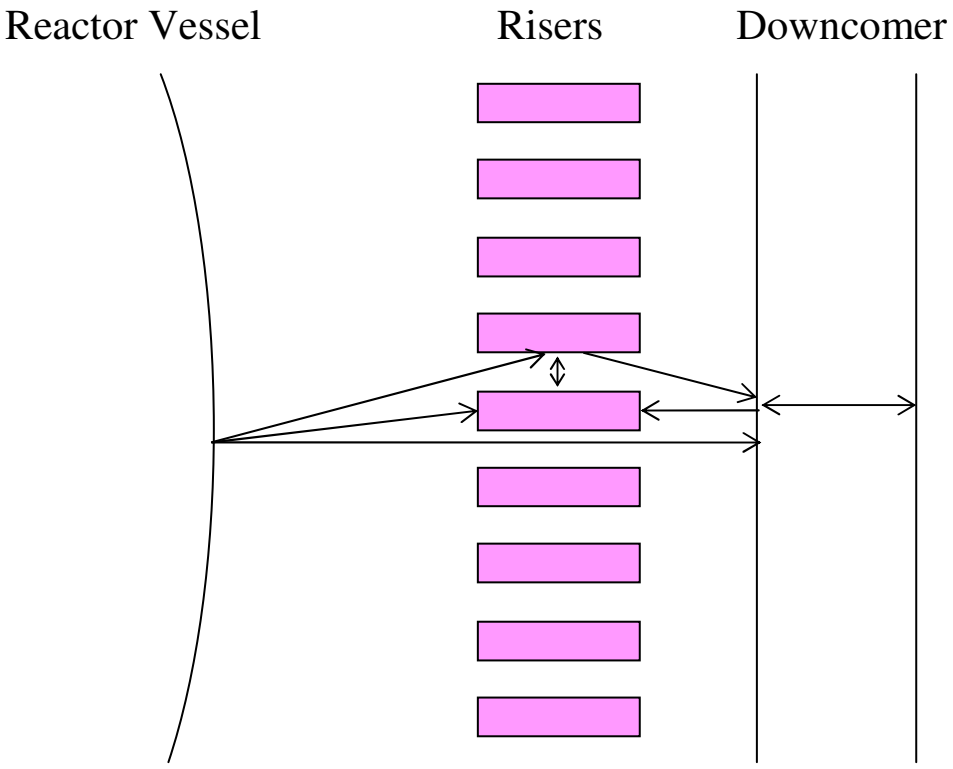

Figure 9. Reactor Cavity Radiation Model

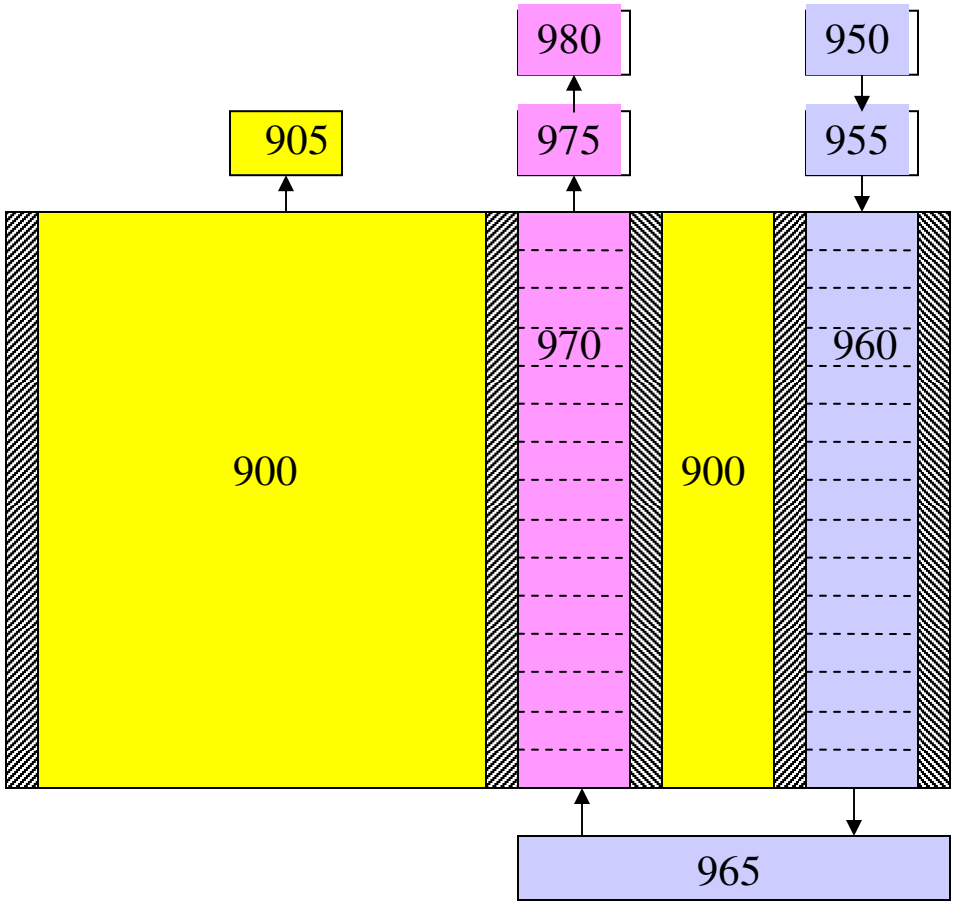

Figure 10. VHTR Reactor Cavity Nodalization

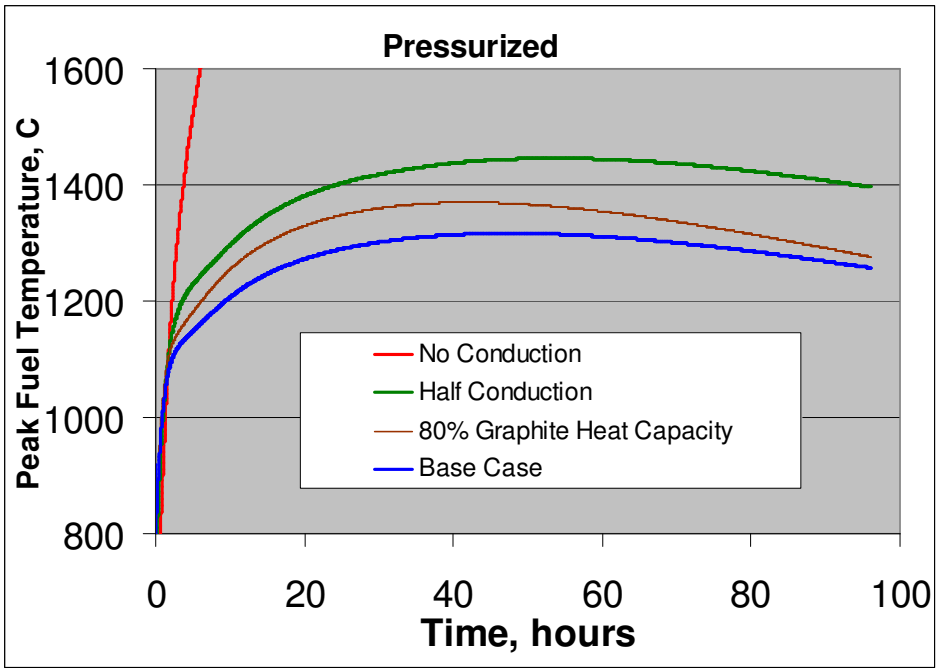

Figure 11. Effect of Core and Reflector Conductivity and Graphite Heat Capacity on Peak Fuel Temperature for Pressurized Conduction Cooldown

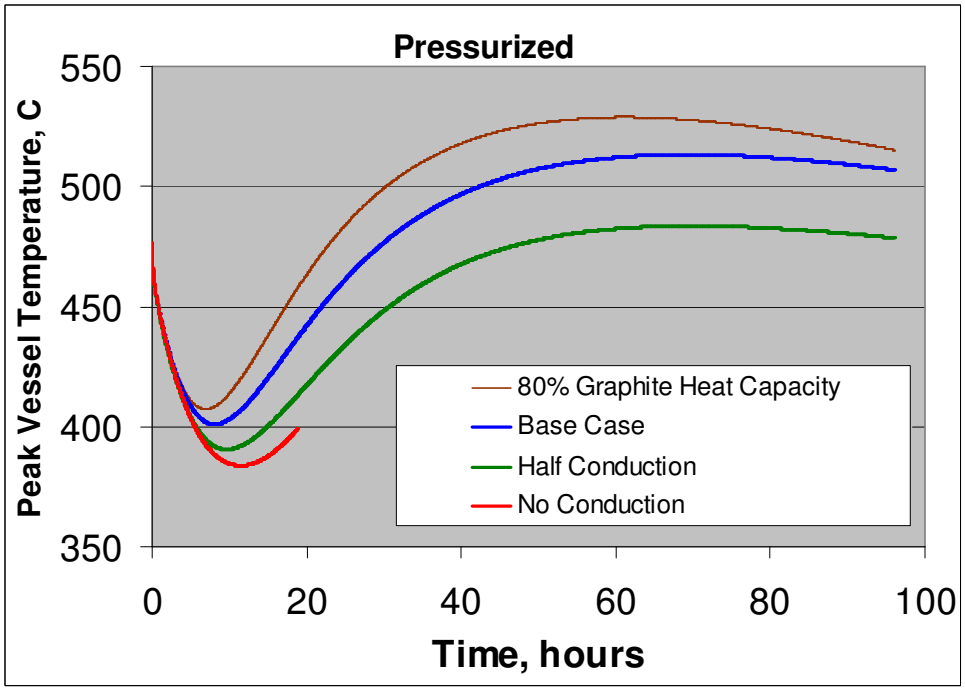

Figure 12. Effect of Core and Reflector Conductivity and Graphite Heat Capacity on Peak Reactor Vessel Temperature for Pressurized Conduction Cooldown

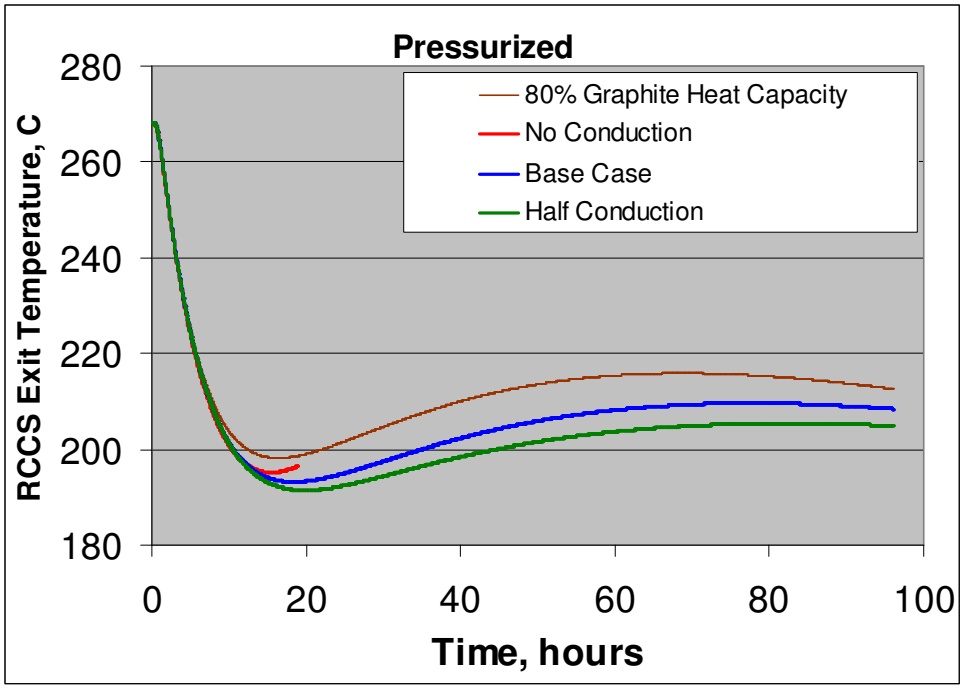

Figure 13. Effect of Core and Reflector Conductivity and Graphite Heat Capacity on RCCS Exit Coolant Temperature for Pressurized Conduction Cooldown

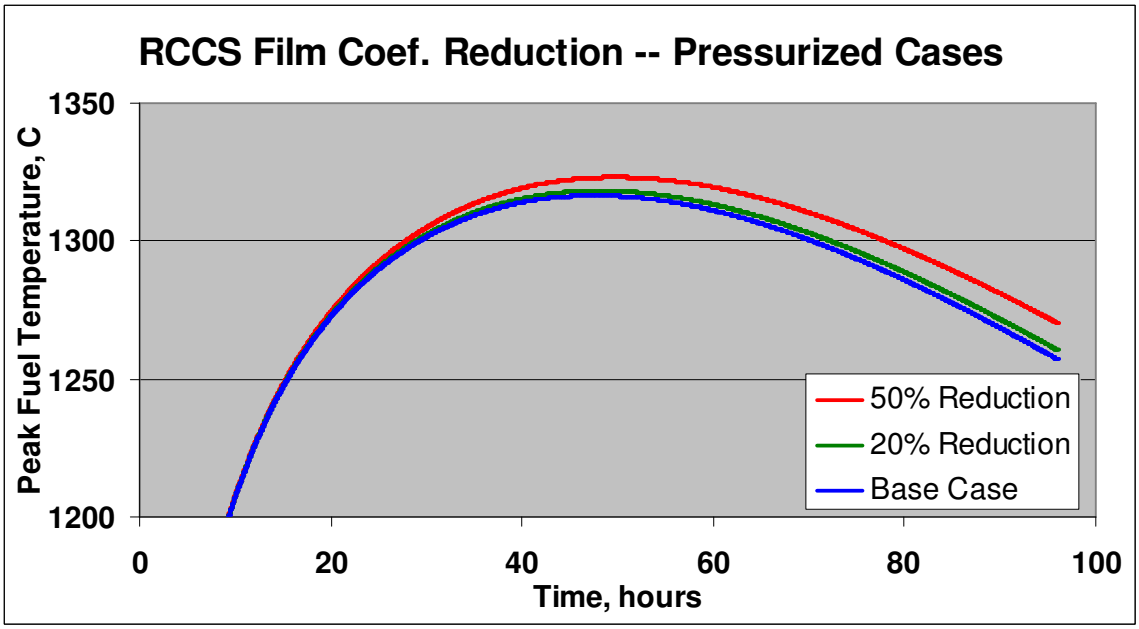

Figure 14. Effect of RCCS Film Coefficient on Peak Fuel Temperature for Pressurized Conduction Cooldown

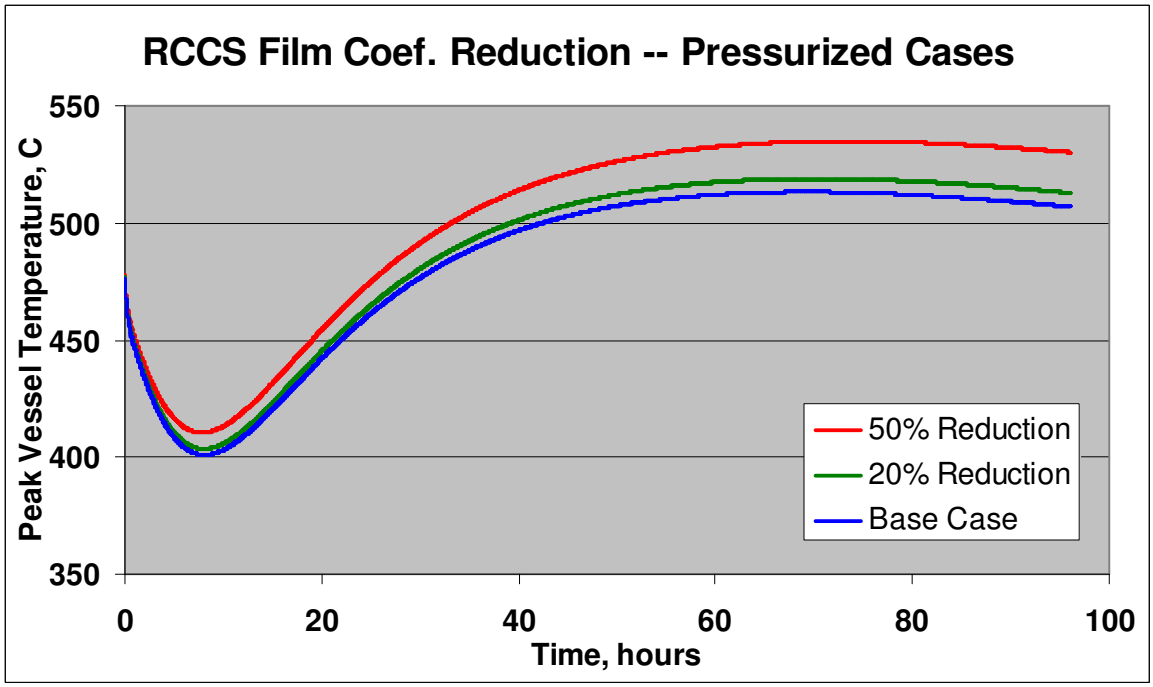

Figure 15. Effect of RCCS Film Coefficient on Peak Reactor Vessel Temperature for Pressurized Conduction Cooldown

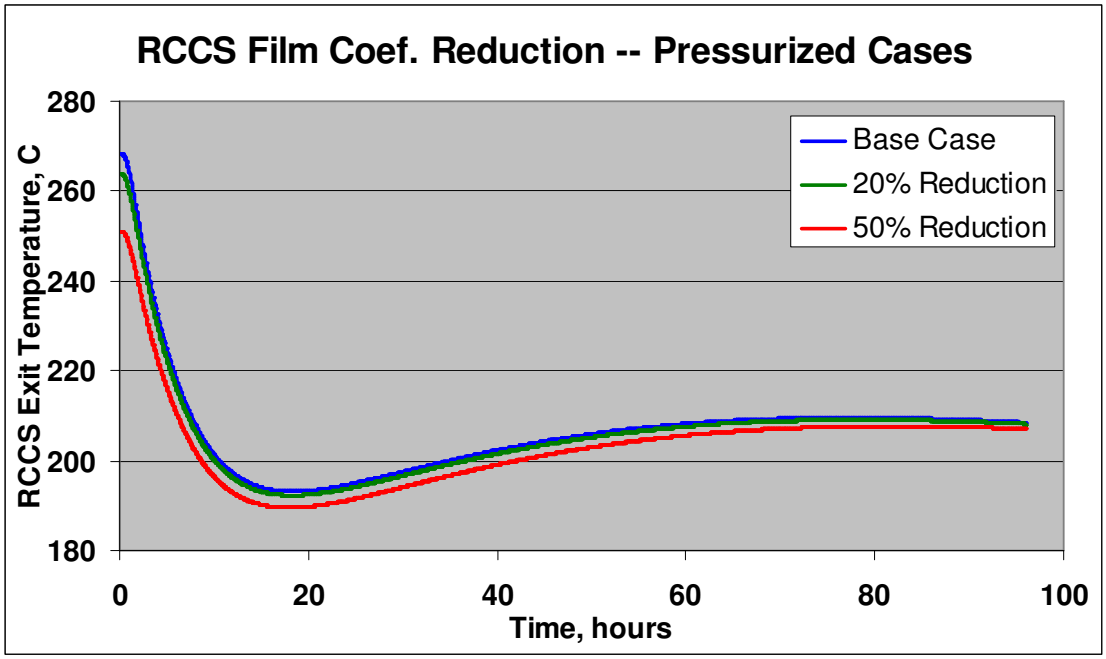

Figure 16. Effect of RCCS Film Coefficient on RCCS Exit Coolant Temperature for Pressurized Conduction Cooldown

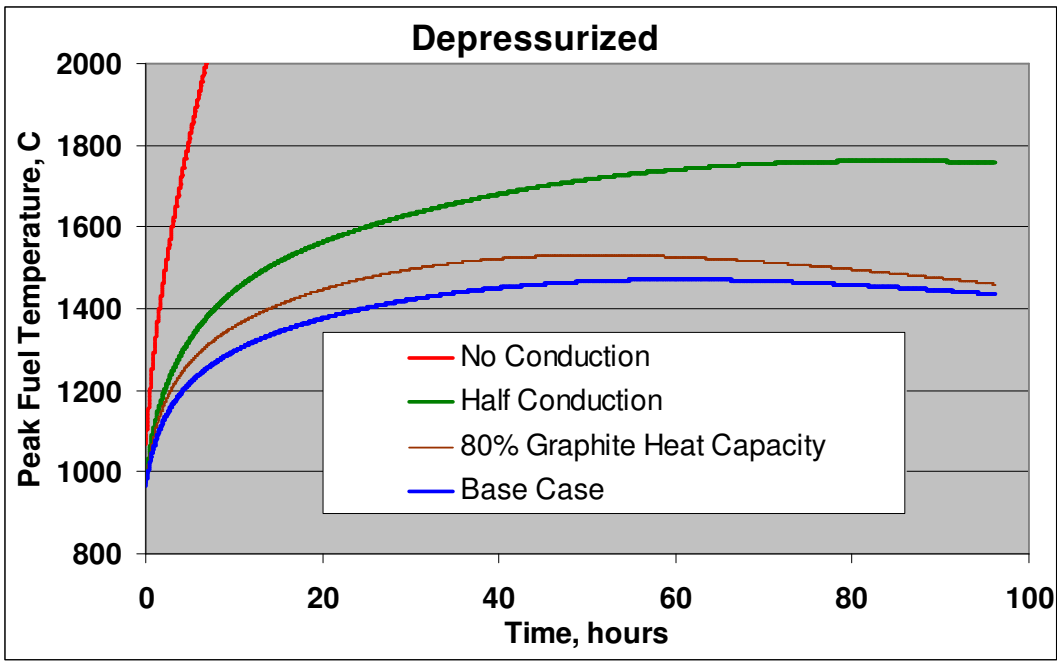

Figure 17. Effect of Core and Reflector Conductivity and Graphite Heat Capacity on Peak Fuel Temperature for Depressurized Conduction Cooldown

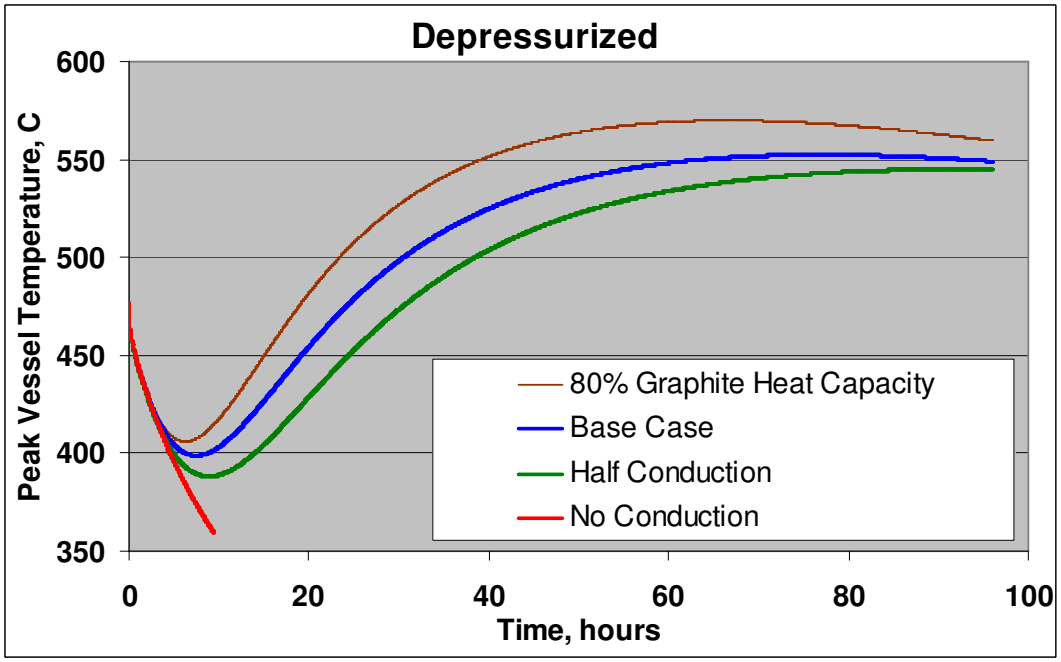

Figure 18. Effect of Core and Reflector Conductivity and Graphite Heat Capacity on Peak Reactor Vessel Temperature for Depressurized Conduction Cooldown

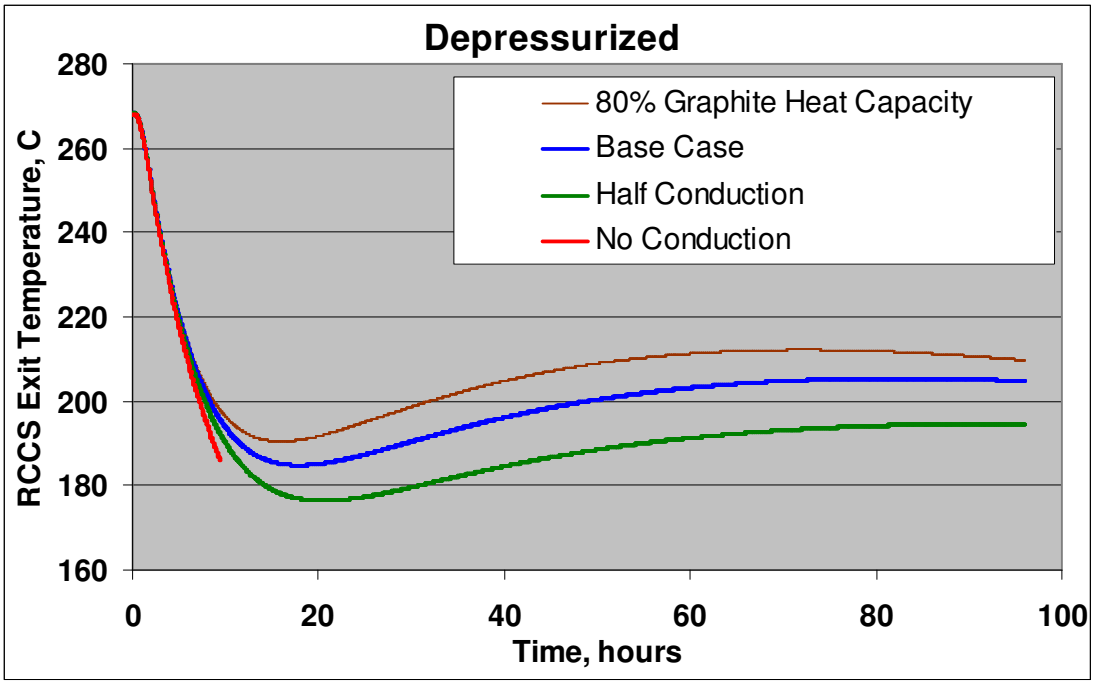

Figure 19. Effect of Core and Reflector Conductivity and Graphite Heat Capacity on RCCS Exit Coolant Temperature for Depressurized Conduction Cooldown

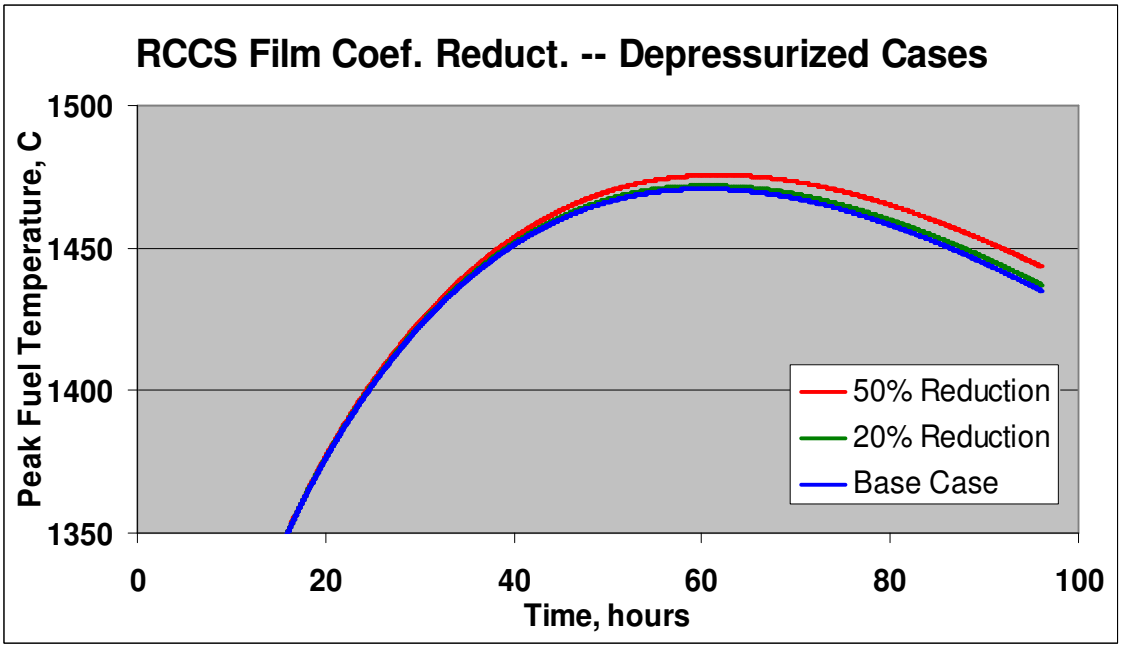

Figure 20. Effect of RCCS Film Coefficient on Peak Fuel Temperature for Depressurized Conduction Cooldown

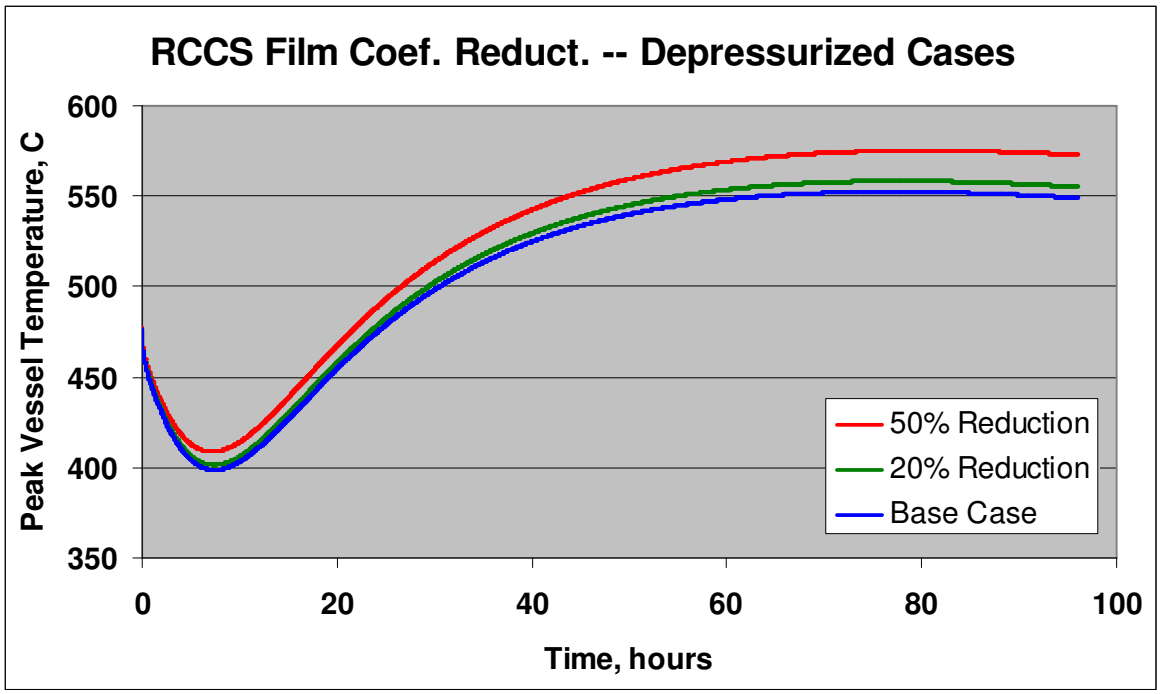

Figure 21. Effect of RCCS Film Coefficient on Peak Reactor Vessel Temperature for Depressurized Conduction Cooldown

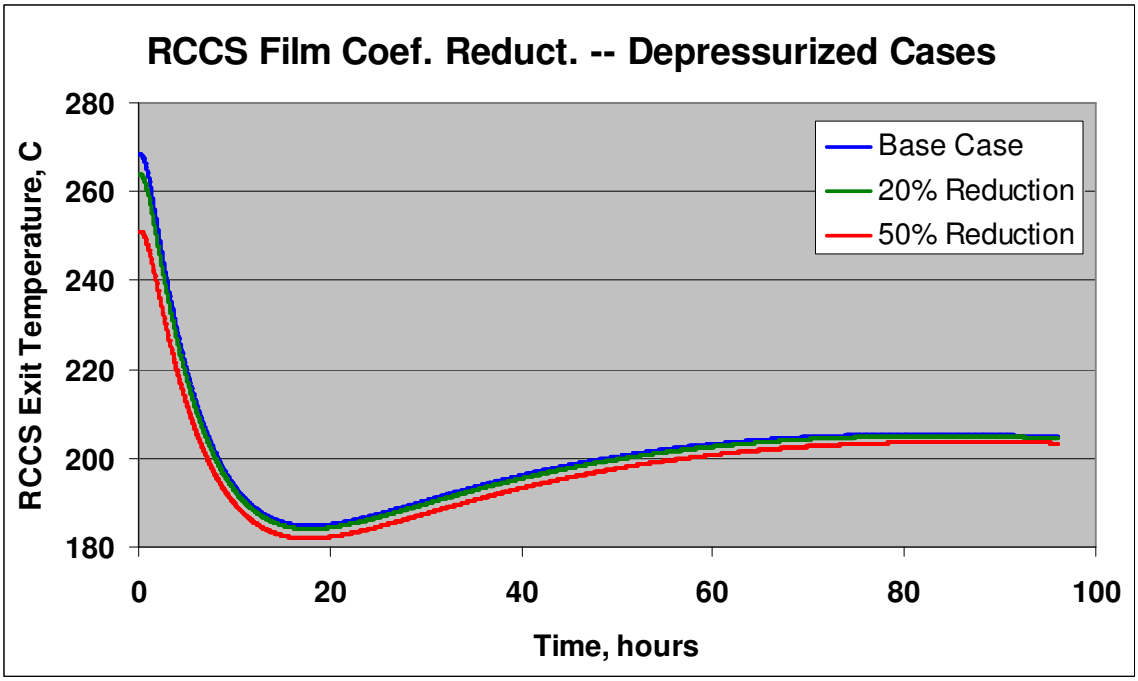

Figure 22. Effect of RCCS Film Coefficient on RCCS Exit Coolant Temperature for Depressurized Conduction Cooldown

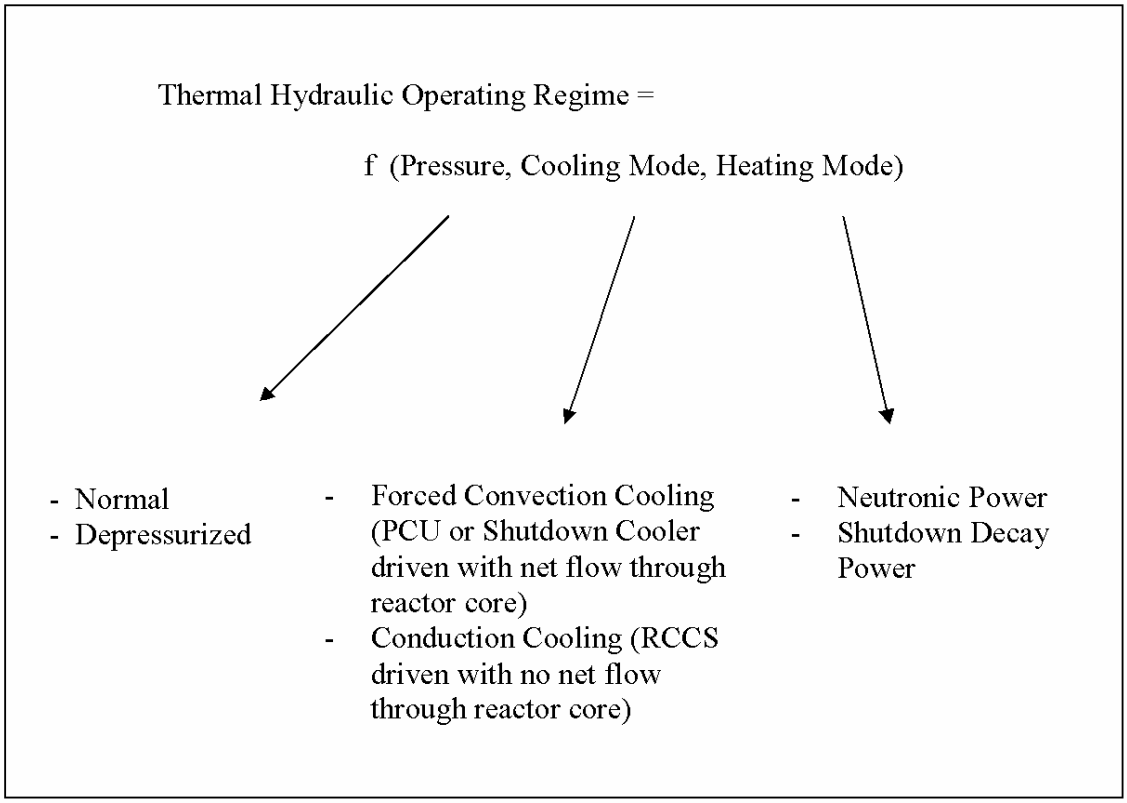

Figure 23. Factors Influencing Thermal-Hydraulic Operating Regime

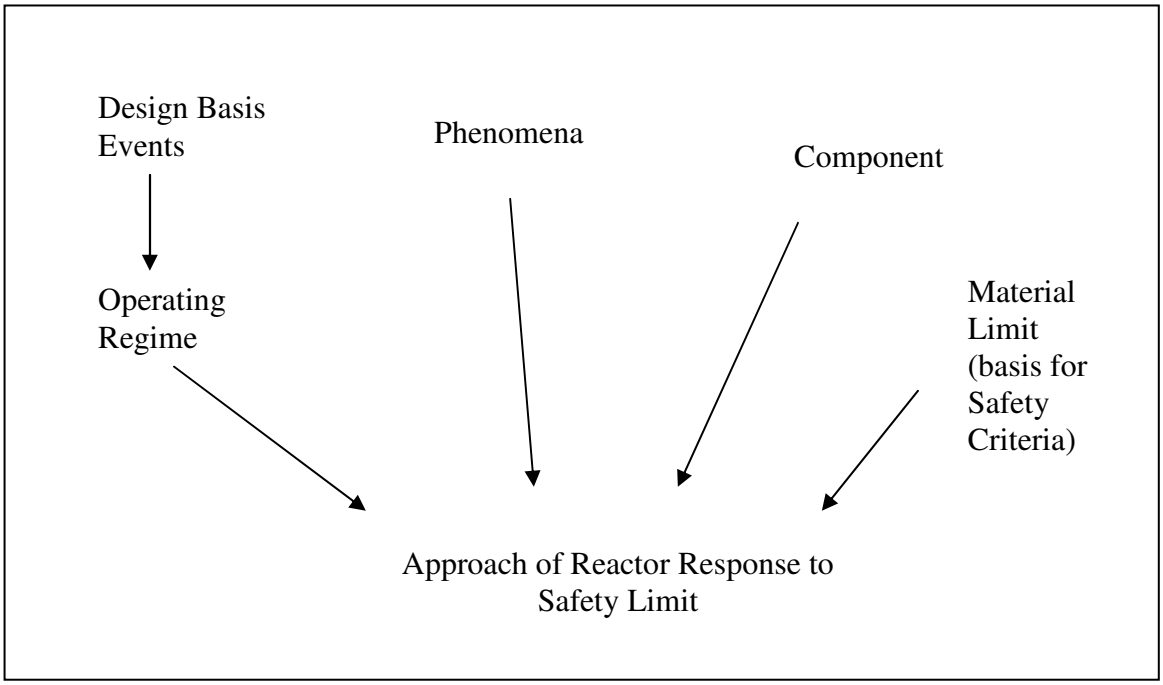

Figure 24. Factors Giving Rise to Safety Issues

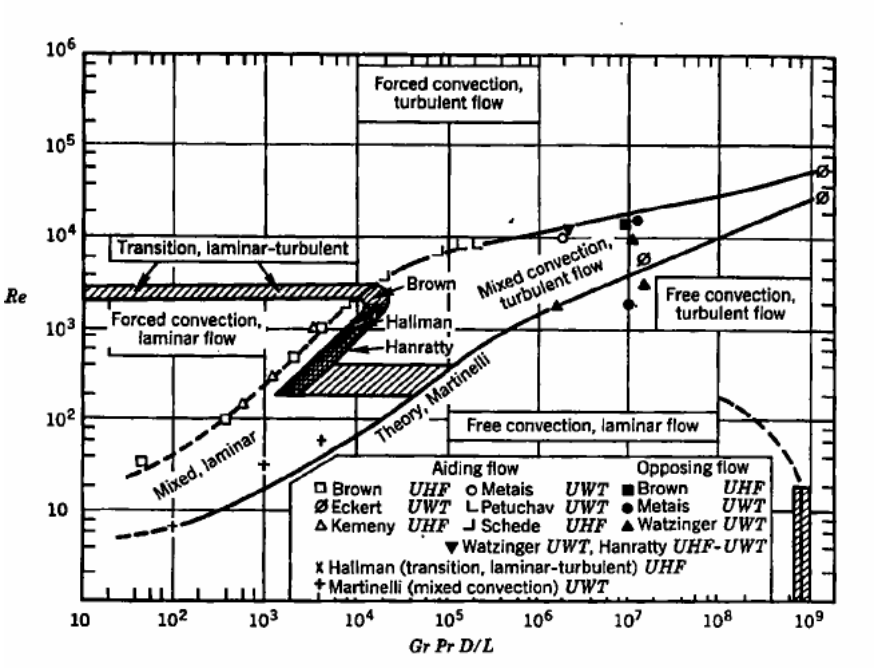

Figure 25. Map Identifying Mixed Convection Regime [12]

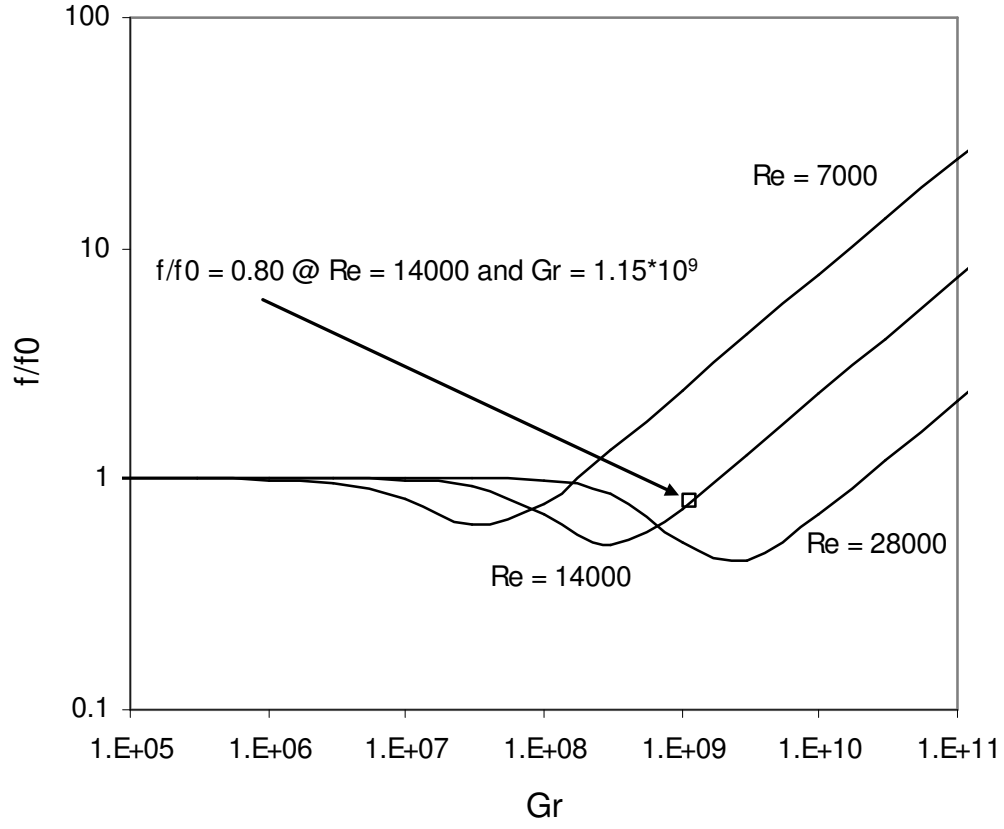

Figure 26. Ratio of Friction Factor in Vertical Upflow Heated Pipe to that in Unheated Pipe

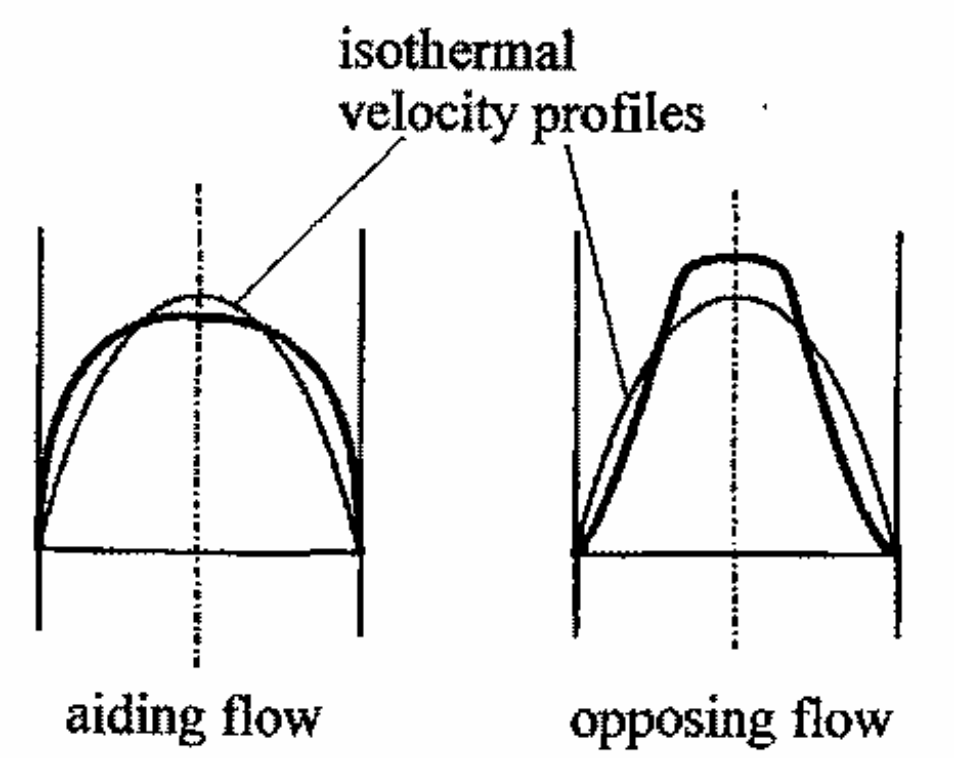

Figure 27. Velocity Profiles under Aiding and Opposing Turbulent Flow Conditions [11]

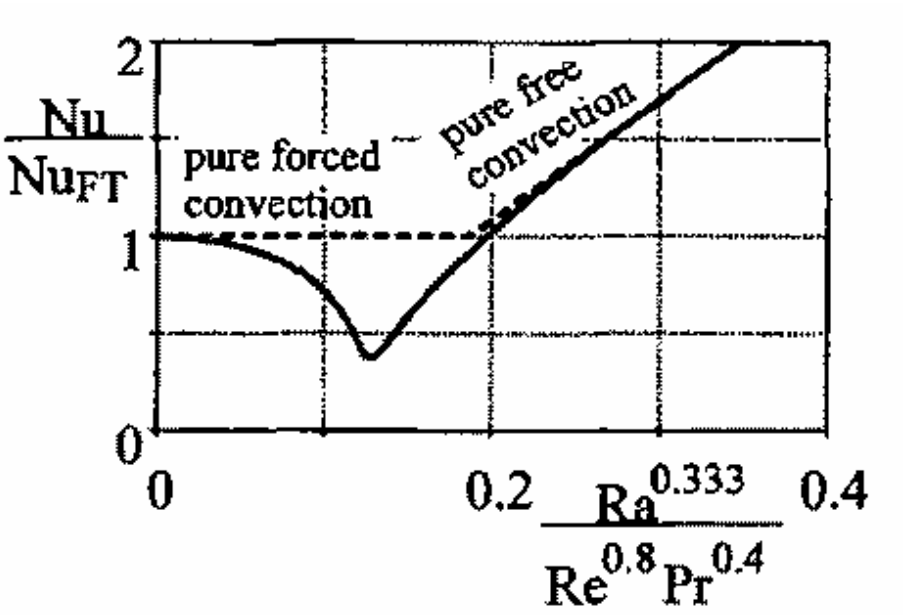

Figure 28. Heat Transfer for Aiding Mixed Convection [11]

Table 1
Peak Temperatures and RCCS Air Flow Rates
for the Pressurized Conduction Cooldown

Configuration	Peak Temperature, C		RCCS Air Flow, kg/s	
(Case)	Fuel	Vessel	Maximum*	Minimum
Base Case	1317	513	14.13	13.11
Half Conduction	1446	483	14.13	13.06
No Conduction	>2228	476?	14.13	<13.06
80% Graphite Heat Capacity	1370	529	14.13	13.21
80% RCCS Film Coefficient	1318	519	14.08	13.09
50% RCCS Film Coefficient	1323	535	13.94	13.01

*The initial value is the maximum value.

Table 2
Peak Temperatures and RCCS Air Flow Rates
for the Depressurized Conduction Cooldown

Configuration	Peak Temperature, C		RCCS Air Flow, kg/s	
(Case)	Fuel	Vessel	Maximum*	Minimum
Base Case	1471	552	14.13	12.98
Half Conduction	1762	545	14.13	12.79
No Conduction	>2227	476?	14.13	<12.97
80% Graphite Heat Capacity	1531	570	14.13	13.09
80% RCCS Film Coefficient	1472	558	14.08	12.95
50% RCCS Film Coefficient	1476	575	13.94	12.88

*The initial value is the maximum value.

Table 3 Relationship of Duty Cycle/Design Basis Events to Features of Asymptotic Steady-State Operating Regime

Values of Operating Regime Variables			Full Power Operation	Operational Transients	Refueling	Upsets													
						Protected							Unprotected						
						Loss of Generator Load	Reactivity Insertion	Loss of Cooling	Shaft Breakage	Loss of Coolant	Overcooling	Flow Blockage	Loss of Generator Load	Reactivity Insertion	Loss of Cooling	Shaft Breakage	Loss of Coolant	Overcooling	Flow Blockage
	Pressure	Normal Pressure	X	X		X	X	X	X		X	X	X	X	X	X		X	X
		Depressurized			X					X							X		
	Cooling	Forced Convection	X	X	X	X	X		X		X		X	X		X		X	
		Conduction						X		X		X			X		X		X
	Heating	Neutronic	X	X									X	X	X	X	X	X	X
		Decay Heat			X	X	X	X	X	X	X	X							

Table 4 Asymptotic Steady-State Operating Regimes and the Duty Cycle/Design Basis Events They Encompass. Ranked Generally in Order of Increasing Severity

Asymptotic Steady-State Operating Regime	Initiating Duty Cycle/Design Basis Events
OR1 - Normal Pressure/ Forced Convection Cooling/ Shutdown Decay Heat Generation	Loss of Generator Load - Protected Reactivity Insertion – Protected Shaft Breakage – Protected Overcooling - Protected
OR2 - Normal Pressure/ Forced Convection Cooling/ Neutronic Power	Full Power Operation. Operational Transients. Loss of Generator Load - Unprotected Reactivity Insertion – Unprotected Shaft Breakage – Unprotected Unprotected Overcooling - Unprotected
OR3 - Normal Pressure/ Conduction Cooling/ Shutdown Decay Heat	Loss of Cooling - Protected Flow Blockage - Protected
OR4 - Normal Pressure/ Conduction Cooling/ Neutronic Power	Loss of Cooling - Unprotected Flow Blockage - Unprotected
OR5 - Depressurized/ Forced Convection Cooling/ Shutdown Decay Heat	Refueling
OR6 - Depressurized/ Conduction Cooling/ Shutdown Decay Heat	Loss of Coolant - Protected
OR7 - Depressurized/ Conduction Cooling/ Neutronic Power	Loss of Coolant - Unprotected

Table 5 List of Design Basis Events Requiring Safety Analyses

Anticipated Operational Occurrences	1. Main loop transient with forced core cooling 2. Loss of main and shutdown cooling loops 3. Accidental withdrawal of a group of control rods followed by reactor shutdown 4. Small break LOCA (~1 in^2 area break)
Design Basis Accidents (only safety related systems can be used for recovery)	1. Loss of heat transport system and shutdown cooling 2. Loss of heat transport system without control rod trip 3. Accidental withdrawal of a group of control rods followed by reactor trip 4. Unintentional control rod withdrawal together with failure of heat transport systems and shutdown cooling system 5. Earthquake-initiated trip of heat transport system 6. LOCA event in conjunction with water ingress from failed shutdown cooling system 7. Large break LOCA 8. Small break LOCA

Table 6 VHTR Components

System	Components
Reactor Vessel	Inlet Plenum
	Riser
	Top Plenum and Components
	Core & Reflectors (Includes Bypass)
	Outlet Plenum and Components
Reactor Coolant Loops (to PCU and H_2 Process)	Hot/Cold Pipe
Power Conversion Unit (Direct Cycle)	Turbine
	Recuperator
	Precooler
	LP Compressor
	Intercooler
	HP Compressor
Hydrogen Process	H_2 Intermediate Heat Exchanger
RCCS	Reactor Cavity (Confinement)
	RCCS Tube (Air Duct)
	RCCS Piping and Chimney

Table 7 VHTR Phenomena

Phenomena	Issue	Associated Components
Flow Distribution	• Bypass flow • Non-uniform and asymmetric flow may result in local hot spot in core • Natural circulation inside core is one of core cooling mechanism during HPCC and LPCC • Natural circulation inside reactor cavity partly contributes to RCCS heat removal	Core/Reflector Plena Riser RCL Rx Cavity
Fluid Properties	• Accurate prediction of gas properties is a basic requirement for analyzing gas flow and heat transfer	Core/Reflector Plena Riser RCL RCCS
Pressure Drop	• Accurate representation of pressure drop is to ensure adequate design flow rate and flow distribution	Core/Reflector Plena Riser Loop RCCS PCU H_2 IHX
Convective Heat Transfer	• Accurate representation of heat transfer is to ensure adequate heat removal rate • Heat transfer regime tends to be in mixed or free convection heat transfer during accident conditions	Core/Reflector Plena Riser Loop RCCS PCU H_2 IHX
Radiation Heat Transfer	• Accurate representation of radiation heat transfer in a complex geometry is to ensure adequate heat removal from core to RCCS	Core/Reflector Riser RCCS
Contact Heat Transfer	• Accurate representation of contact heat transfer in a complex geometry is to ensure adequate heat removal from core to RCCS	Core/Reflector RCCS
Gas Conduction Heat Transfer	• Accurate representation of gas conduction is to ensure adequate heat removal from core to RCCS	Core/Reflector Rx cavity Riser
Thermal Mixing and Gas Species Stratification	• Thermal stratification in the plenums is a challenge to material integrity and core local hot spot • Species stratification and mixing	Plena Hot/Cold Piping
Material Properties of Fuel and Reflector	• Accurate representation of conductivity and specific heat of fuel and reflector is to ensure local temperature distribution. Effects of irradiation on the material properties are especially important in affecting the gap dimensions and consequently the bypass flow	Core/Reflector

Core Decay Heat	• Core power is the heat source that determines the consequent temperature transients	Core/Reflector
Reactivity Feedback	• Doppler feedback provides intrinsic safety features	Core/Reflector
Multi-Dimensional Heat Conduction	• Accurate prediction of local temperature distribution in a complex geometry is to ensure the local hot spot and reactivity feedback	Core/Reflector
Hot Plume	• Hot plume from core in the top plenum is a challeng e to vessel integrity	Top Plenum
Thermal Resistance/Heat Capacity of Shroud	• Thermal resistance and heat capacity of shroud in top plenum is to protect vessel overheat	Top Plenum
Core Configuration	• Gaps between blocks • Location of pebbles; pebble void fraction as a function of location and pebble trajectories	Core/Reflector
Jet Discharge	• Jet discharge into outlet plenum can induce spatial and temporal variations in temperature of the plenum wall, which may result in material fatigue • Momentum of impinging stream may damage insulation	Outlet Plenum
Thermal Striping	• High frequency temperature change by jet discharge can induce material fatigue	Outlet Plenum
Pipe/Insulator Conduction	• Accurate prediction of thermal resistance of pipe/ insulator is to ensure mechanical integrity of hot/ cold pipe	Hot/cold pipe
Critical Flow	• Accurate prediction of critical flow is to ensure depressurization of reactor vessel • The high velocities associated with the large-break may cause critical flow not only at the hot duct exit but also in some small area flow passages in the reactor vessel. The influence of the high flow rates on the redistribution of dust in the reactor vessel, the PCU, and into the reactor confinement should be considered.	Hot/cold pipe
Bulk CO Reaction (Homogeneous Chemical Reaction)	• Accurate prediction is to ensure species concentration and gas temperature	Core/Reflector Plena Riser
Graphite Oxidation	• Accurate prediction of graphite surface oxidation is to ensure peak fuel temperature by air-ingress	Core/Reflector
Molecular diffusion	• Accurate prediction of molecular diffusion in a complex geometry is to ensure on-set of bulk natural circulation and the reaction rate of bulk CO and graphite oxidation • Noise affects the diffusion process	Plena Riser Core/Reflector

Confinement Valve and Filter Characteristics	• The confinement relief valve and the filtering hardware and performance characteristics are important in establishing the valve lift interval, fluid discharge characteristics, and the fraction of dust that is retained in confinement	Reactor Cavity
Air Purge and Gas Species Distribution	• Accurate prediction of gas species distribution in reactor cavity is to define oxygen supply to reactor vessel	Reactor cavity
Dust from Core	• Graphite dust from the core is source term for fission product and aerosol transport in confinement	Reactor cavity
Conduction to Ground	• Conduction to ground is a final success path for core afterheat removal	Reactor cavity
Flow Mixing in Piping Plenums	• Flow mixing in RCCS plenums affects the flow distribution in RCCS	RCCS
Buoyancy Flow in Chimney	• Accurate prediction of buoyancy flow in chimney is to ensure RCCS heat removal rate	RCCS
Turbine Performance	• Accurate representation of turbine performance is to ensure system response during transients	PCU
Compressor Performance	• Accurate representation of compressor performance is to ensure system response during transients	PCU
Cooler Performance	• Accurate representation of heat transfer and pressure drop of coolers is to ensure system response during transients	PCU
Recuperator Performance	• Accurate representation of heat transfer and pressure drop of recuperator is to ensure system response during transients	PCU
Valve Performance	• Accurate representation of valve performance is to ensure system response during transients	PCU
Heat Conduction in Thick-Walled Structure	• Large spatial temperature gradient can lead to large thermal stress and component fatigue	PCU (turbine inlet)
Pressure Waves	• Pressure waves that move through the system will stem from: ■ PCU equipment malfunctions, e.g. compressor surges ■ A guillotine break of the hot duct or other lines in the system • Pressure waves may cause the dislodgement of dust in the system and may inadvertently cause an unexpected large differential pressure to exist in the system	PCU Reactor vessel and components Reactor cavity

Table 8 Inlet Plenum Composite PIRT*

Phenomena	HPCC		LPCC			LC	
	1	2	1	2	3	1	2
Flow Distribution	H,M		H,M			M,M	M,M
Heat Transfer (Forced Convection)	L,L		L,L			L,L	L,L
Heat Transfer (Mixed and Free Convection)					L,L		
Pressure Drop (Forced Convection)	L,L		L,L			L,L	L,L
Pressure Drop (Mixed and Free Convection)					L,L		
Thermal Mixing and Stratification		M,M		M,M	H,H		
Bulk CO Reaction				L,L	L,L		
Molecular Diffusion				M,M			
Pressure Waves							

* first entry is Prismatic Modular Reactor, second entry is Pebble Bed Reactor

Table 9 Riser Composite PIRT

Phenomena	HPCC		LPCC			LC	
	1	2	1	2	3	1	2
Flow Distribution	M,M		M,M	M,M		M,M	M,M
Heat Transfer (Forced Convection)	L,L		L,L			L,L	L,L
Heat Transfer (Mixed and Free Convection)					L,L		
Pressure Drop (Forced Convection)	H,M		M,M			H,M	H,M
Pressure Drop (Mixed and Free Convection)					L,L		
Radiation Heat Transfer		H,H		H,H	H,H		
Gas Conduction		M,M		M,,M	M,M		
Bulk CO Reaction				L,L	L,L		
Molecular Diffusion				H,H			
Pressure Waves							

Table 10 Top Plenum & Components Composite PIRT

Phenomena	HPCC		LPCC			LC	
	1	2	1	2	3	1	2
Flow Distribution	M,M	M,M	M,M	L,L	M,M	H,M	H,M
Heat Transfer (Forced Convection)	M,,M		M,M			L,L	L,L
Heat Transfer (Mixed and Free Convection)		M,M		L,L	M,M		
Pressure Drop (Forced Convection)	L,L		L,L			L,L	L,L
Pressure Drop (Mixed and Free Convection)		L,L			L,L		
Thermal Mixing and Stratification		H,M		L,L	H,H		
Hot Plumes		H,H		L,L	H,H		
Fluid Properties	L,L	M,M	L,L	L,L	L,L	M,M	M,M
Thermal Resistance/Heat Capacity of Shroud		H,H		M,M	M,M		
Bulk CO Reaction				L,L	L,L		
Molecular Diffusion				H,H			
Pressure Waves							

Table 11 Core and Reflector Composite PIRT

Phenomena	HPCC		LPCC			LC	
	1	2	1	2	3	1	2
Flow Distribution	H,H	H,H	H,H	H,H	H,H	H,H	H,H
Heat Transfer (Forced Convection)	H,H	L,L	H,H			H,H	H,H
Heat Transfer (Mixed and Free Convection)		H,H		L,L	M,M		
Pressure Drop (Forced Convection)	H,H	L,L	H,H			H,H	H,H
Pressure Drop (Mixed and Free Convection)		H,H		M,M	H,H		
Decay Heat (including Power Distribution)	H,H	H,H	H,H	H,H	H,H		
Reactivity Feedback						M,M	M,M
Fuel/Reflector Conductivity	M,M	H,H	M,M	H,H	H,H	M,M	M,M
Fuel/Reflector Specific Heat	H,H	H,H	M,M	H,H	H,H	M,M	M,M
Multi-D Heat Conduction Including Contact	H,M	H,M	H,M	H,M	H,M	H,M	H,M
Gas Conduction (Including Gaps)		H,H		H,H	M,M		
Radiation Heat Transfer				H,H	H,H		
Graphite Oxidation				M,M	H,H		
Bulk CO Reaction				M,M	H,H		
Molecular Diffusion				H,H			
Fluid Properties	H,H	H,H	H,H	H,H	H,H	H,H	H,H
Core Configuration	H,M	H,M	H,M	L,L	M,M	H,M	M,M
Pressure Waves							

Table 12 Outlet Plenum & Components Composite PIRT

Phenomena	HPCC		LPCC			LC	
	1	2	1	2	3	1	2
Flow Distribution	M,M	M,M	M,M	M,M	M,M	H,H	H,H
Heat Transfer (Forced Convection)	M,M		M,M	M,M	M,M	H,H	H,H
Heat Transfer (Mixed and Free Convection)		M,M		M,M	M,M		
Pressure Drop (Forced Convection)	L,L		L,L			M,M	M,M
Pressure Drop (Mixed and Free Convection)		M,M		L,L	M,M		
Thermal Mixing and Stratification		H,M		M,M	H,M		
Jet Discharge						H,H	H,H
Thermal Striping						H,H	H,H
Bulk CO Reaction				L,L	L,L		
Molecular Diffusion				H,H			
Fluid Properties	L,L	L,L	L,L	L,L	L,L	M,M	M,M
Pressure Waves							

Table 13 Hot/Cold Pipe Composite PIRT

Phenomena	HPCC		LPCC			LC	
	1	2	1	2	3	1	2
Heat Transfer (Forced Convection)	L,L		L,L			M,M	M,M
Heat Transfer (Mixed and Free Convection)					L,L	L,L	
Pressure Drop (Forced Convection)	L,L		L,L			L,M	L,M
Pressure Drop (Mixed and Free Convection)					L,L		
Pipe/Insulator Conduction							M,M
Critical Flow			L,L				
Pressure Waves							

Table 14 Reactor Cavity Composite PIRT

Phenomena	HPCC		LPCC			LC	
	1	2	1	2	3	1	2
Flow Distribution		L,L		L,L	L,L		
Heat Transfer (Mixed and Free Convection)		L,L		L,L	L,L		
Pressure Drop (Mixed and Free Convection)		L,L		L,L	L,L		
Radiation Heat Transfer		H,H		H,H	H,H		
Gas Conduction		L,L		L,L	L,L		
Conduction to Ground		L,L		L,L	L,L		
Dust from Core			M,H				
Air Purge and Gas Species Distribution			L,,M	M,M	M,M		
Confinement Valve and Filter Characteristics							
Pressure Waves							

Table 15 RCCS Air Duct Composite PIRT

Phenomena	HPCC		LPCC			LC	
	1	2	1	2	3	1	2
Heat Transfer (Forced Convection)		H,H		H,H	H,H		
Heat Transfer (Mixed and Free Convection)		H,H		H,H	H,H		
Pressure Drop (Forced Convection)		H,H		H,H	H,H		
Pressure Drop (Mixed and Free Convection)		H,H		H,H	H,H		
Radiation Heat Transfer		H,H		H,H	H,H		
Pressure Waves							

Table 16 RCCS Piping and Chimney Composite PIRT

Phenomena	HPCC		LPCC			LC	
	1	2	1	2	3	1	2
Heat Transfer (Mixed and Free Convection)		M,M		M,M	M,M		
Pressure Drop (Mixed and Free Convection)		H,H		H,H	H,H		
Flow Mixing in Piping Plenums		L,L		L,L	L,L		
Buoyancy Flow in Chimney		H,H		H,H	H,H		
Pressure Waves							

Table 17 Power Conversion Unit PIRT

Phenomena	HPCC		LPCC			LC	
	1	2	1	2	3	1	2
Turbine Performance						M,M	M,M
Turbine Valve Performance						H,H	
Heat Conduction in Thick-Walled Structure							M,M
Heat Transfer in Coolers						M,M	M,M
Pressure Drop in Coolers						M,M	M,M
Heat Transfer in Recuperator						M,M	M,M
Pressure Drop in Recuperator						M,M	M,M
Compressor Performance						M,M	M,M
Pressure Waves							

Table 18 Heat Transfer and Pressure Drop Dependence on Dimensionless Numbers for Laminar Flow between Vertical Parallel Plates

	Pressure Drop	Heat Transfer
Forced Convection	$f = \frac{6}{Re}$	$Nu = \frac{h y_0}{k} = \frac{\partial\left(\frac{T - T_m}{T_0 - T_m}\right)}{\partial\left(\frac{y}{y_0}\right)}$
Natural Convection	-	$v^* = \frac{v_x \rho C_p y_0}{k}$ $Gr = \frac{g \beta y_0^3 (T_1 - T_m)}{\nu}$ $y^* = \frac{y}{y_0}$ $Nu = \frac{h y_0}{k} = 1$

Table 19 Fuel Element Coolant Channel Dimensions and Full Power Thermal-Hydraulic Conditions

Parameter	Value
Reactor Power, Q (Mwt)	600
Reactor Mass Flowrate , W (kg/s)	320
Coolant Channel Diameter, D (m)	0.0159
Flow Fraction to Fuel Elements	0.8
Number of Fuel Element Columns, n_c	102
Number of Coolant Channels per Fuel Element, n_h	108
Length of Active Core Coolant Channel, L (m)	7.93
Average Fuel Element Coolant Channel Flowrate , w (kg/s)	0.023
Coolant Channel Wall Heat Flux, (Mw/m^2) $q'' = Q/(n_c n_h \pi DL)$	0.137

Table 20 Fuel Element Coolant Hydraulic Conditions as a Function of Operating Regime

Regime	Channel Normalized Flowrate	Channel Flowrate (kg/s)	Pressure (MPa)	Bulk Temperature (C)	Viscosity (μPa-s)	$Re = \frac{wD}{\mu A}$
Full Power	1.0	0.023	7.0	745	45	41,000
Pressurized with Shutdown Circulator	0.045*	0.0010	5.0	(807+341)/2= 574*	41	1,800
Depressurized with Shutdown Circulator	0.01*	0.00023	0.1	(1032+179)/2= 605*	42	410

* Based on Shutdown Cooling System performance given in [24].

Table 21 Fuel Element Coolant Thermal Conditions as a Function of Operating Regime

Regime	Normalized Power	Pressure (MPa)	Bulk Temperature (C/K)	Wall Heat Flux, q" (Mw/m^2)	Density, ρ (kg/m^3)	Coefficient of Volumetric Thermal Expansion, β (1/K)	Viscosity, μ (μPa-s)	Thermal Conductivity, k (W/m-K)	$Gr = \frac{g\rho^2 \beta q'' D^4}{k\mu^2}$
Full Power	1.0	7.0	745/1018	0.137 [a]	3.3	0.00098	45	0.37	$1.2x10^6$
Pressurized with Shutdown Circulator	0.059 [b]	5.0	574/847	0.0081	2.8	0.0012	41	0.32	89,000
Depressurized with Shutdown Circulator	0.024 [b]	0.1	605/878	0.0033	0.055	0.0011	42	0.33	12

. [a] From Table 19. [b] Based on Shutdown Cooling System performance given in [24].

Table 22 Dimensionless Numbers for Fuel Element Coolant as a Function of Operating Condition

	Re	Gr	Gr Pr D/L[a]
Full Power	41,000	1.2×10^6	$\sim 10^4$
Pressurized with Shutdown Circulator	1,800	89,000	$\sim 10^3$
Depressurized with Shutdown Circulator	410	12	~0.1

[a] D/L is ratio of hydraulic diameter to channel length and is taken as 0.01

Table 23 RCCS Duct Dimensions and Thermal-Hydraulic Conditions at Reactor Full Power

Parameter	Value
RCCS Power*, Q (Mwt)	3.3
RCCS Air Mass Flowrate *, W (kg/s)	14.3
Number of Ducts*, n	292
Average Duct Air Flowrate , w (kg/s)	0.049
Duct Dimensions*, a=horizontal width of heat transfer surface x b=horizontal depth (m)	0.05 x 0.25
Hydraulic Diameter, D (m)	0.083
Length of Active Core Region, L (m)	7.93
Duct Wall Heat Flux, (Mw/m^2) $q'' = Q/(naL)$	0.029

* from [24].

Table 24 RCCS Duct Coolant Hydraulic Conditions at Reactor Full Power

Duct Air Flowrate (kg/s)	Pressure (MPa)	Average Bulk Temperature (C)	Viscosity (μPa-s)	$Re = \frac{wD}{\mu A}$
0.049	0.1	(43+274)/2 =159	23	14,000

Table 25 RCCS Duct Coolant Thermal Conditions at Reactor Full Power

Pressure (MPa)	Average Bulk Temperature (C/K)	Wall Heat Flux, q" (Mw/m^2)	Density, ρ (kg/m^3)	Coefficient of Volumetric Thermal Expansion, β (1/K)	Viscosity, μ (μPa-s)	Thermal Conductivity, k (W/m-K)	$Gr = \frac{g\rho^2 \beta q'' D^4}{k\mu^2}$
0.1	159/432	0.029	0.83	0.0023	23	0.035	1.15×10^9

Table 26 Recommended Values for Empirical Constants in the High Reynolds Number k-ε Model.

C_μ	C_1	C_2	σ_K	σ_ε
0.09	1.44	1.92	1.0	1.3

Table 27 RCCS Experiments [15]

Benchmark Problem	I	II	III	IV	VI-a	VI-b
Gas		Helium	Nitrogen	Helium	Helium	Helium
Pressure, MPa	1.3×10^{-6}	0.73	1.1	0.47	0.96	0.98
Heat Input, Total, kW	13.14	28.79	93.93	77.54	2.58	7.99
Segment 1, kW	1.01	1.16	5.90	5.63	0	0
Segment 2, kW	2.31	3.11	16.05	19.60	0	0
Segment 3, kW	2.64	3.52	19.88	21.59	0	0
Segment 4, kW	2.46	5.10	22.24	22.70	0	0
Segment 5, kW	3.76	10.42	22.13	0	0	0
Segment 6, kW	0.96	5.49	7.72	8.00	2.58	7.99
Cooling Panel	Water	Water	Water	Water	Air	Air
Stand Pipes	No	No	No	With	With	With

Table D.1 Summary of Outlet Plenum Experiments

Experiment	Organization	Feature	Reference Numbers
1	JAERI HTTR Experiments	Without mixing promoter	17, 18
2	JAERI HTTR Experiments	With mixing promoter	19
3	JAERI HTTR Experiments	With mixing promoter	20
4	JAERI VHTR Experiments	2 concentric nozzles	21
5	Chinese HTR-10 Experiments	A few mixing promoter options	22
6	German HTR-Module Experiments	2 core bottom & mixing promoters options	23

Table D.2 Conditions of Outlet Plenum Experiments

Experiment	Fluid	Geometry	Scale	Temp., C	Pressure, MPa	Flow Rate, kg/s	Reynolds Number	Measured items
1	helium	Core bottom structure	1:1	400-1050	1.0-4.0	1.0-4.0		Temperatures of helium gas in hot plenum
2	helium	Core bottom structure	1:1	300-400	~2-4		~$1.8\text{-}4.7 \times 10^5$	Temperatures of helium gas in hot plenum
3	water	Core bottom structure	1:7	25-65	0.1		$0.4\text{-}1.0 \times 10^5$	Water temperatures in hot plenum
4	air	2 concentric nozzles		~20-50	0.1			Air temperatures of the mixing stream
5	air	Hot gas chamber, core bottom structure, & hot gas duct	1:1.5	20-90	0.1	Typ. 1.68 Max. 2.44	$1.4\text{-}5.8 \times 10^5$	Air flow rates, temperatures, and differential pressures
6	air	Core bottom structure	1:2.9	$\Delta T \leq 40$	0.1		$0.59\text{-}1.8 \times 10^6$	Air temperature, pressure, and velocity

Nuclear Engineering Division
Argonne National Laboratory
9700 South Cass Avenue, Bldg. 208
Argonne, IL 60439-4842

www.anl.gov

A U.S. Department of Energy laboratory managed by UChicago Argonne, LLC